DEVELOPMENT OF SHALE INHIBITORS FOR WATER-BASED FLUIDS: SYNTHESIS, AND EVALUATION STUDIES

BY

MUKAILA ABIODUN IBRAHIM

A Thesis Presented to the
DEANSHIP OF GRADUATE STUDIES

KING FAHD UNIVERSITY OF PETROLEUM & MINERALS
DHAHRAN, SAUDI ARABIA

In Partial Fulfillment of the
Requirements for the Degree of

MASTER OF SCIENCE
In

CHEMISTRY

DECEMBER 2019

KING FAHD UNIVERSITY OF PETROLEUM & MINERALS

DHAHRAN- 31261, SAUDI ARABIA

DEANSHIP OF GRADUATE STUDIES

This thesis, written by **MUKAILA ABIODUN IBRAHIM** under the direction of his thesis advisor and approved by his thesis committee, has been presented and accepted by the Dean of Graduate Studies, in partial fulfillment of the requirements for the degree of **MASTER OF SCIENCE IN CHEMISTRY**.

Dr. Tawfik A. Saleh
(Advisor)

Dr. Khalid R. Alhooshani
Department Chairman

Dr. Jameel R. Al-Thagfi
(Member)

Dr. Salam A. Zummo
Dean of Graduate Studies

Dr. Mohammed K. Al-Arfaj
(Member)

25/12/19

Date

Dedication

This thesis work is dedicated to Allah, and my entire family as well as my lovely wife whom strictly contributed to the success of this work through their untimely prayer.

ACKNOWLEDGMENTS

Many started the race, but few finished it. Life is a hurdle and it requires extra efforts and extreme hard work in order to feel among the successors. It is my pleasure to express my deep feelings pertaining to my success in this project.

First of all, I really appreciate the effort and support of my advisor, Dr. Tawfik A. Saleh for the exposure he has taken through in science. I appreciate him for his immense contribution from the start to the end of this work by his technical, scientific and financial supports as well as advice. Special thanks is also due to my committee members in persons of Dr. Jameel R. Al-Thagfi and Dr. Mohammed Khalid Al-Arfaj for their inspiring guidance and amiable support by giving professional touch to this work.

My sincere gratitude also goes to the chairman of the Chemistry department and his members of staffs including the faculties and technicians. The department instructors that I have encountered during my course work are recognized. I greatly appreciate the knowledge and scientific confidence they inculcated in me. The inputs of the technicians like Mr. Irshad, Mr. Hassan, Mr. Monsur and Mr. Abdl Rasheed is commended.

Lastly, I thank my family including my father, Mr. Ibrahim Olaitan Titilope, my mother Mrs. Ibrahim Tawakalt, my sister, Mrs. Halimat Ibrahim as well as my lovely wife; Mrs. Rasheedat Opeyemi Adebayo for her supports right from scratch till this moment. May Allah continue to assist them in their endeavors.

TABLE OF CONTENTS

LIST OF TABLES

LIST OF FIGURES

LIST OF ABBREVIATIONS

AA : Acrylic Acid

AA : Acrylic Acid

AA-AAm-C-Amyl : Acrylic Acid-Acrylamide-Amylcarbon Ester

AA-AAm-OD-C-Amyl : Acrylic Acid-Acrylamide-Octadecene-Amylcarbon

AAm : Acrylamide

AC : Activated Carbon

AC-D : Activated Carbon Modified Dendrimer

Amyl : Amyl Alcohol

API : America Petroleum Institute

APS : Ammonium Persulfate

AR : Anti-Swelling Ratio

AV : Apparent Viscosity

C-A : Allyl Activated Carbon

$CaCl_2$: Calcium Chloride

C-Amyl : Amyl Activated Carbon

$CaSO_4$: Gypsum

CEC : Cation Exchange Capacity

CMC : Carboxy Methyl Cellulose

DI water : Deionized Water

ECD : Equivalent Circulating Density

EDA : Ethylenediamine

EDA-G : Ethylenediamine-Modified Graphene

Ester

FTIR : Fourier-Transform Infrared

GBM : Gas-Base Mud

GGPA : Glucose Graft Copolyammonium

HMC : Hydroxymethyl Cellulose

HTCC : Chitosan Quaternary Ammonium Salt

HTHP : High Temperature High Pressure

IR : Infrared

KCl : Potassium Chloride

KPS : Potassium Persulfate

LTOBM : Low Toxicity Oil-Based Mud

MBCA	:	4, 4’-Methylenebis-Cyclohexanamine
MD	:	Mud Density
Na_2CO_3	:	Soda Ash
Na-Bt	:	Sodium Bentonite
NMR	:	Nuclear Magnetic Resonance
OBM	:	Oil Based Mud
OD	:	Octadecene
PAC	:	Polyanionic Cellulose
PAMAM	:	Poly(amidoamine)
PAMAM-OH	:	Hydroxyl-Terminated Polyamidoamine
PDADMAC	:	Polydiaminedimethyl Acrylamide
PEA	:	Polyetheramine
PEDA	:	Polyetherdiamine
PEI	:	Polyethyleneimine
PHPA	:	Partially Hydrolyzed Polyacrylamide
PHPG	:	Partially Hydrophobized Hyperbranched Polyglycerol
PV	:	Plastic Viscosity
PVA-g-DMAPMA	:	Poly (Vinyl Alcohol-g-Dimethyl Aminopropyl

		Methacrylamide
PVP	:	Polyvinylpyrrolidone
ROP	:	Rate of Penetration
SBM	:	Synthetic Based Mud
SDS	:	Sodium Dodecyl Sulfate
SEM	:	Scanning Electron Microscopy
TAE	:	Tallow Amine Ethoxylate
TGA	:	Thermal Gravimetric Analysis
TX-100	:	T-Octylphenoxyl Polyethoxy Ethanol
VeiBr	:	1-Vinyl-3-Ethylimidazolium Bromide
WBDFs	:	Water-Based Drilling Fluids
WBM	:	Water Based Mud
XRD	:	X-ray Diffractometry
YP	:	Yield Point
ZSCE	:	*Zizyphus Spina-Christi* Extract

ABSTRACT

Full Name : [MUKAILA ABIODUN IBRAHIM]
Thesis Title : [DEVELOPMENT OF SHALE INHIBITORS FOR WATER-BASED FLUIDS: SYNTHESIS, AND EVALUATION STUDIES]
Major Field : [CHEMISTRY]
Date of Degree : [DECEMBER, 2019]

In this work, we first report environmental benign and inexpensive water-soluble nanomaterial of activated carbon (AC) - polymer composites of partially aminated acrylic acid (C-g-AA-NH_2), hydrophobic acrylic acid-acrylamide-amylcarbon ester (AA-AAm-C-Amyl) and more hydrophobic acrylic acid-acrylamide-octadecene-amylcarbon ester (AA-AAm-OD-C-Amyl) as well as activated carbon dendrimer /polyvinylpyrrolidone (AC-D/PVP) as efficient inhibitors in water-based drilling fluid to prevent shale hydration problems in oil and gas well drilling. The prepared materials were characterized via various spectroscopic techniques including FTIR, NMR, and TGA. The prepared materials shale inhibition abilities were examined through anti-swelling ratio using sodium bentonite (Na-Bt) and degree of shale recovery of shale cuttings. The mechanisms of the inhibition were accomplished with SEM surface exploration of Na-Bt in contact with 2 wt% solution of each material. Results indicated that 2% of each entity drastically reduced water invasion into shale compared to KCl, the conventional inhibitor which its usage is being banned due to environmental nuisance. The efficiency of the composites is attributed to synergistic plugging property of the core-centered carbon nanoparticles that could plug the nanopores of the interlayer spacing of shale formation and the ionic, hydrogen boding or hydrophobic properties of the involved polymer of the composites as the case may be. This approach could significantly control fluid loss, reduce permeability and filtrate volume of drilling mud with the development of well-defined filter cake and thin film on the formation surface. The thermal analysis results also revealed that the materials could withstand high-temperature high pressure (HTHP) normally experience in well drilling. Thus, the composites could be a suitable replacement for KCl as save, cheap and efficient shale inhibitors in water-based mud for oil well drilling.

1. ملخص الرسالة

الاسم الكامل: مكيلا أبيودون إبراهيم

عنوان الرسالة: تطوير مثبطات مائية للحفريات الصخرية: طرق التحضير والتقييم

التخصص: الكيمياء

تاريخ الدرجة العلمية: ديسمبر 2019

في هذا البحث، تم تحضير مواد نانوية بيئية وغير مكلفة ذائبة في الماء من الكربون المنشط (AC) - مركبات بوليمر من حمض الأكريلك المغلف جزئياً (Cg-AA-NH2)، استرات حمض أكريلاميد أكريلاميد-أميل كاربون (AA-AAm-C-Amyl) وإستر أكريلاميد حمض أكريلاميد-أوكتاديسين- أميل الكاربون (AA-AAm-OD-C-Amyl) بالإضافة إلى dendrimer / polyvinylpyrrolidone الكربون المنشط (AC-D / PVP) لاستخدامها كمثبطات فعالة في سائل الحفر القائم على الماء لمنع مشاكل ترطيب الصخر الزيتي في حفر آبار النفط والغاز. تم توصيف المواد المعدة من خلال تقنيات طيفية مختلفة. تم فحص قدرات تثبيط المواد الصخرية المحضرة من خلال نسبة التضخم باستخدام البنتونيت الصوديوم (Na-Bt) ودرجة استخلاص الصخر الزيتي للقطع الصخري. أنجزت آليات التثبيط مع استكشاف خصائص الاسطح. أشارت النتائج إلى أن 2 ٪ من كل مادة قلل بشكل كبير من نفاذ المياه إلى الصخر الزيتي مقارنة مع كلوريد البوتاسيوم، المانع التقليدي الذي يحظر استخدامه بسبب العيوب المتعلقة بالبيئة. وتُعزى كفاءة المواد المركبة إلى خاصية التماسك للجسيمات النانوية الكربونية المركزية التي يمكن أن تقوم بتوصيل المسام النانوية في التباعد البيني لتكوين الصخر والخواص الأيونية أو الروابط الهيدروجينية أو الكارهة للماء للبوليمرات المحضرة. هذا النهج يمكن أن يتحكم بشكل كبير في فقدان السوائل، ويقلل من نفاذية وحجم الترشيح مع تكون غشاء رقيق على سطح الصخور. كشفت نتائج التحليل الحراري أيضًا أن المواد يمكن أن تصمد أمام الضغط العالي في درجات الحرارة العالية (HTHP) وهي الظروف التي تكون عادة في حفر الآبار. وبالتالي، يمكن أن تكون المواد المحضرة في هذه الدراسة بديلاً مناسبًا عن KCl كمثبطات صخرية منخفضة التكلفة وفعالة لحفر آبار النفط.

1. CHAPTER 1

INTRODUCTION

1.1 Background

Drilling fluids are good formulated inorganic and organic materials in a suitable solvent (water or oil) that are used in drilling industry to drill wells. The term is also used interchangeably as mud or drilling mud. The output effect of drilling muds is based on the condition of the well that is under drilling i.e. the well formation. [1]

Drilling fluid has many functions. Aside from cooling and cleaning effect on drilling bit, it helps in lubrication and transferring of drilling cuttings from downhole to the earth's surface. Based on the solvent component of mud formulation, they are classified into water-based mud (WBM), oil-based mud (OBM) and synthetic-based mud (SBM). [2], [3] The environmental concerns are associated with oil-based and synthetic-based muds that have limited their applications in drilling operations in oil and gas industries. Thus, water-based muds are the most widely uses for drilling wells due to their environment benign and low-cost. To meet the desired purpose of WBM for efficient drilling, various additives are usually incorporated in the fluid. An ideal WBM contains weighting agent (e.g. barite), viscosity control materials, emulsifier, flocculants and ultimately, a shale inhibitor. The most encountered formations in well drilling of petroleum deposit are shale accounting for about 70%. Approximately 90% of well drilling problems especially wellbore collapse or caving occurs in the shale formations due to it sensitivity to hydration when in contact with water causing loss of billions of dollars. [4], [5] Shales are phyllosilicate clays that contain minerals mixture of illite and smectite clays at varying proportions. Smectite is highly reactive towards water molecule by swelling and subsequently dispersed in drilling mud while illite is stable. [6] Thus, any shale formation that has a high amount of smectite to illite is susceptible to swelling and dispersion in drilling fluid. In view of the foregoing, shale inhibitors are usually added to WBM to minimize or eliminate shale hydration. Potassium Chloride (KCl) had been the generally used inhibitor to curb shale hydration in oil and gas industry. However, in recent times, KCl it uses to inhibit shale has decreased and even banned in some countries due to its high chloride ion that is having a great environmental impact on marine organisms.[7] For decades, researchers have been focusing on the development of cheap, efficient and sustainable shale inhibitors and have been in the forefront of oil and gas industries research. It is therefore imperative to explore some other materials with active and efficient chemistry to ameliorate the shale formation challenges during drilling of wells.

This research intended to design novel set of cheap and environmentally friendly nanopolymers and polymer composite. This be followed by exploring the characterization of the synthesized materials and test their viability for effective inhibition of shale hydration.

1.2 Statements of the problem

Shale hydration has been an inevitable and pressing challenging of oil and gas industries for decades. This menace has been specifically been tackled with a series of approaches including oil-based muds (OBMs) and synthetic-based muds (SBMs) which are threatening to the environment and highly expensive. Water-based muds (WBMs) with suitable shale inhibitor is considered more preferable due to its environmental benignity and economical potential especially in offshore shale drilling. Myriads of shale inhibitors have been explored by authors to cater for the retardation or complete eradication of shale hydration while drilling with WBMs due to the sensitivity of shale clay minerals with the free water in the WBMs. Most of these inhibitors face diverse challenges such as limited inhibiting ability; high cost, inability to withstand high-temperature high pressure (HTHP) normally encountered in a real application and ability to constitute an environmental nuisance.

Consequently, it becomes imperative to strategize, design and develop novel materials that could address the aforementioned challenges being faced by both conventional shale inhibitors like KCl and partially hydrolyzed polyacrylamide as well as others that have been examined by researchers in this regard.

1.3 Objectives of the study

The general objective of this research thesis project was to develop a new set of inexpensive, highly effective and nontoxic shale inhibitors that could be used as substitutes for the conventional KCl in the oil and gas industries. This would be achieved via the following specific objectives:

- To design activated carbon-based nanoparticles/polymer composites as inexpensive, effective and nontoxic shale inhibitors.
- To synthesize the activated carbon-based composite materials.
- To characterize the prepared materials using FTIR, NMR, SEM and other spectroscopic techniques. and

- To evaluate the materials as shale inhibitor in water-based drilling fluid using API standard methods.

1.4 Significance of the study

The essence of the activated carbon materials composite is due to its ease of functionalization and micro to nano size which could make it suitable for plugging the interspacing nanopores in the shale formation and it can proffer solution to the environmental hazard of KCl and the low inhibiting activity of most shale inhibitors.

1.5 Scheme of the research work

The research focus has three main schemes as presents below:

- Strategize, design and synthesize the activated carbon-based composite materials to be used as shale inhibitors through validated procedures.
- General characterization of the prepared materials using state-of-the-art spectroscopic and imaging techniques.
- Evaluation of the novelty of using the materials as shale inhibitor in water-based drilling fluid.

1.6 Scheme of research findings reporting

The thesis report is structured and arranged chronologically into five chapters to facilitate the reading and understanding as follows:

Chapter 1 described the problem of shale formation hydration, the essence of activated carbon composite, highlighted the general and specific objectives, followed by the statement of problem and significance of the study, as well as the scheme of the research findings and reporting.

Chapter 2 gave an overview about the literature of shale hydration mechanism and shale inhibition

Chapter 3 discussed comprehensively the design of novel partially aminated acrylic acid grafted activated carbon as an inexpensive shale hydration inhibitor.

Chapter 4 explained the preparation of amyl ester surface carbon-nanopolymer composite for sensitive shale drilling.

Chapter 5 described the efficient shale inhibition with activated carbon dendrimer/polyvinylpyrrolidone composite.

Chapter 6 summarized the conclusions obtained from the study.

2. CHAPTER 2

LITERATURE REVIEW

2.1 Well drilling challenges

Shales are generally defined as low-permeable phyllosilicate sedimentary rocks consisting of different clays with other minerals. Their permeability and porosity capacity depends on the proportion of clays and the minerals to one another. Thus, the formation could range from highly hydrated gumbo to a very hard brittle shale (Figure 2.1). [1], [2]

A sequence of difficulties is usually encountered during oil and gas as well as water wells drilling operations. These include wellbore instability (sloughing formations which could cause tight hole conditions, bridges, torque and drag, and fillings), shale swelling or hydration, formation damage, low rate of penetration, string corrosion and stickiness, the elevated temperature at the bit among others.[3], [4] For instance, if the hole is big, it becomes weak and difficult to stabilize, resulting in problems such as low annular velocities, poor hole cleaning, solids loading and poor formation evaluation (logging).[5-7]

About 90% of wellbore instability problems are associated with shale [8], [9]. Shale instability is initiated by the existence of clay minerals such as kaolinite, smectite, and montmorillonite as a result of their great affinity with the water [10], [11]. Nevertheless, clay mineral starts swelling after it interacts with the water and raising the wellbore instability like shale sloughing, tight hole, caving and reducing the efficacy of mud to lift

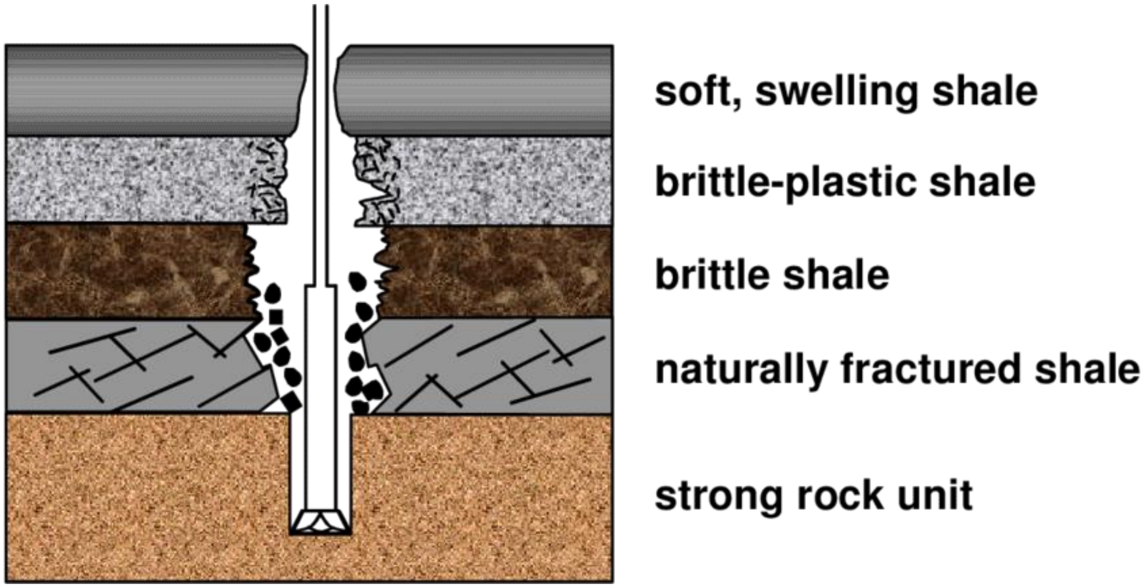

Figure 2.1: shale formation compostion and wellbore instability **[3]**

the drilled cuttings. [12] The clay swelling also decreases the rate of penetration because of the bit balling with a sticky clay. [13]

The mechanism of shale-water interaction may either be physical, mechanical or chemical. [14] The physical and mechanical means involve pore pressure due to osmotic pressure generated by differences in chemical potential during drilling. This results into pressure transmission from the drilling fluid hydraulic pressure to the shale causing instability. [15] Hence, the downhole (downstream) pressure decreases as the time goes on as a result of chemical potential changes. The water transport into shale may generally be in the form of osmotic (diffusion) or reverse osmosis (hydraulic pressure difference) or both. [16], [17] The chemical types of water movement into shale formation include chemical interactions, dispersion, and ion-exchange or adsorption. [18], [19]

Since shale is made up of octahedral clay sheets of aluminum central atoms or sometime with other metallic atoms like magnesium, calcium, etc. sandwiched between two tetrahedral sheets with silicon center, it reacts with water molecule and its other ionic composition due to aluminum affinity for water and chemical potential difference respectively. [20] This led to weakening of electrostatic or van der Waal's forces between the clay silicate layer and dispersion. [6] Pressure difference between the shale pore and the drilling fluid as well as the chemical potential between the pore liquid and mud fluid possess significant forces that causes unstable wellbore (Figure 2.2). [21] For instance in a brittle shale, formations fracture could be distorted and penetrated the network of the fractures by overbalance mud. This could lubricate surface of the fractures and consequently leads to wellbore and pore pressure equilibration, and finally shale failure. [22]

In shales, mud weight is usually enough to balance formation stress, as wells are usually stable. With water-based mud, chemical differences could cause interactions between mud and shale that lead to softening of rock. Highly fractured, dry, brittle shales could also be extremely unstable leading to mechanical problems (Figure 2.3). [7], [23], [24]

2.2 Drilling Fluid

Drilling fluids also called drilling muds or muds are the type of fluids (mainly liquids or sometimes gases) that are used in holes drilling operation in oil and gas industry. These are also used in water borehole drilling purposes. The major function of drilling fluid is to maintain downhole pressure in the well. Other important roles of muds are:

- Transporting of drilling cutting from wellbore to the surface.
- Cleaning, lubrication and cooling of drilling shaft and bit.
- Stabilization of well falling.
- Prevents the invasion of formation fluids (water, gas and oil).
- Sealing of formation pore throats and cracks by forming thin filter cake layer with low permeability.
- Permits the analysis of cuttings and automatic logging of well status.

2.3 Types of drilling fluid

Drilling muds are used to control hydrostatic pressure in the drilling operation, to transport cuttings from subsurface through the annulus to surface and to cool and clean the bit in the hard-geological layer during long time drill. However, all these could be attained through excellent rheology. [25] The three types of drilling muds that are used in drilling industries

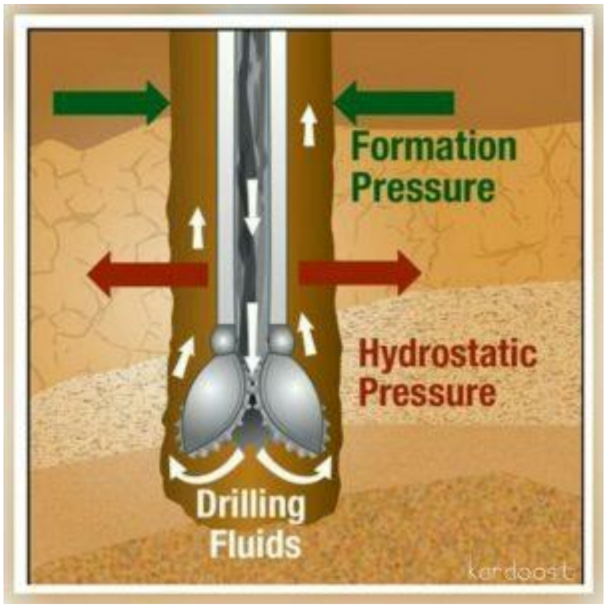

Figure 2.2: Pressure difference influence on formation stability. [26]

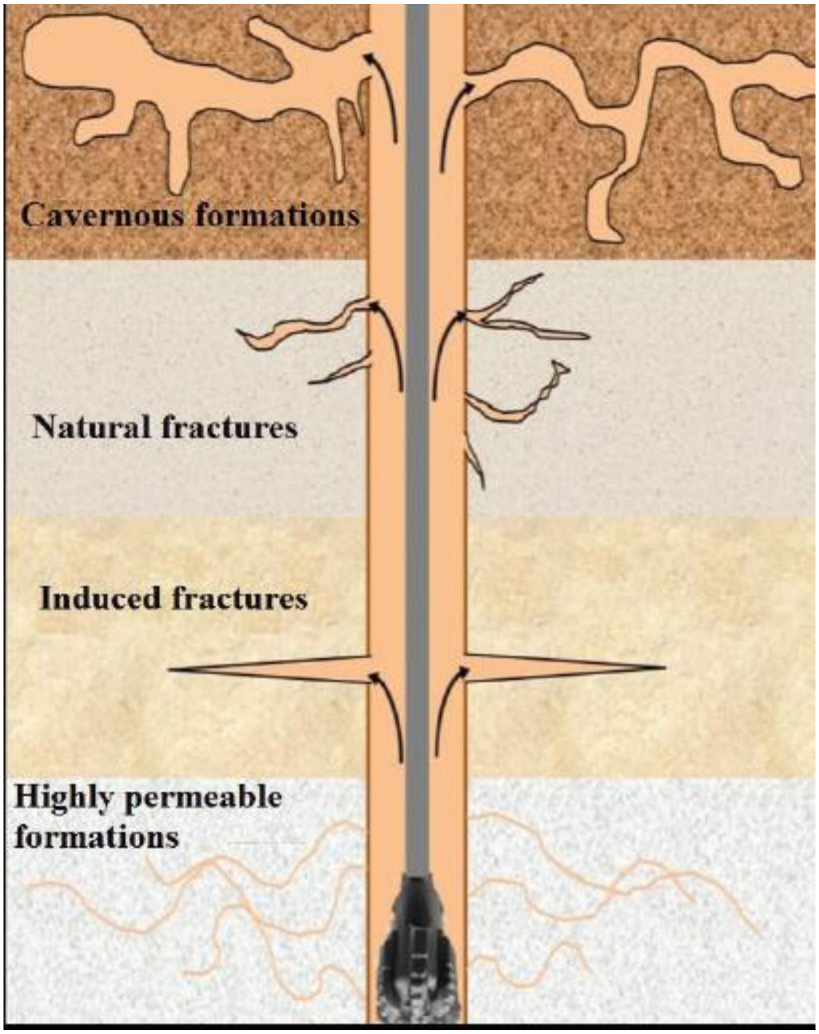

Figure 2.3: Lost circulation modes [27]

are water-based mud (WBM), oil-based mud (OBM) and synthetic-based mud (SBM). [1], [28]

The WBM majorly contains bentonite and other chemicals additive such as barite (as weight material), thickener (such as xanthan gum, glycol, polyanionic cellulose (PAC), starch, guar gum), calcium carbonate, caustic soda, soda ash, and shale inhibitor. [29], [30] Almost 80% of the mud is made up of water while the rest 20% are additives. About 80% of wells drilling in the oil and gas industries are achieved using WBM due to its environmental friendliness, easy geotechnical analysis and less cost. [11] However, WBM is susceptible to a large amount of shale hydration because of great interaction between water in the mud and shale formation composition of the drilling well as a result of chemical differences, hence, leading to wellbore instability. [31]

On the other hand, oil-based mud (OBM) and synthetic-based mud (SBM) are made up of 95% petroleum oil, water, salts and other materials. They are thermally stable less or not affected by bacterial actions and prevention of corrosion to drilling equipment. The muds also have excellent shale inhibition, easy cleaning, lubricity properties, lengthy storage ability and reusable, although, relatively expensive compared to WBM. [32], [33] The OBM contains oil continuous phase and dispersive water phase in combination with wetting and gelling agents and emulsifiers. The oil component may be diesel, fuel oil, kerosene and other forms of crude or mineral oils while the water part may be freshwater or sodium or calcium chloride solution. OBM and SBM reduced the shale swelling due to less water in the composition which makes them suitable for drilling in highly water-sensitive shales zone. [34] In addition, they could withstand high-temperature deep drill that usually leads to dehydration of WBM and prevents stickiness and balling of the bit.

Conversely, their utilization in wells drilling is limited due to their environmental toxicity capacity of when used and cuttings disposal, high cost, poor formation logging during drilling and sometimes constitute damage of formation. [35]

Water-based drilling fluids (WBDFs) are and are environmentally friendly. [36] Their performances outweigh that of the OBM and SBM systems which makes them be widely used in oil-well drillings. They are preferred because of their excellent equivalent circulating density (ECD) management, environment friendliness, better rate of penetration, low cost and toxicity and have no influence on well logging. [35], [37], [38] However, their use is associated with instability challenges such as cuttings degradation, fluid loss, bit balling, stuck pipe and so on resulting from shale interaction of water-sensitive Shales with water in the mud which causes swelling and dispersion of shale. [39] Hence, shale inhibitors (ranging from former inorganic salts to polymers and recently nanoparticles) are usually added to WBM for elimination or minimization of the shale hydration. [29], [40]

The other type of fluid that is uncommonly used is gas-base mud (GBM), which **involves** the use of air or nitrogen gas as fluid. It is basically utilized in drilling fragile and fractured formations where using WBM, OBM and SBM is a challenge. It has excellent drilling performance, limit formation damage, fasten drilling period and appealing cost.

2.4 Additives for drilling

The main component of drilling mud is bentonite which gives it the thixotropic trait and wide range of additives are also added to provide it with essential rheological properties to accomplish well stability and best drilling operation. Such characteristics include plastic viscosity (PV), mud density (MD), yield point (YP), apparent viscosity (AV), lubricity, mud filtrate loss volume as well as gel strength. In addition, this must be combined with proper mud formulation to provide chemical properties that will promote shale inhibition. [28], [41]

Bentonite helps in the suspension of mud weight material; improves cleaning capacity of mud; provides viscosity; enhances hole stability, and helps in the reduction of fluid loss and water seepage into permeable formations by forming thin filter cake with low permeability. [42], [43] Some common additives in drilling fluids include density control additives, viscosity additives, shale inhibitors, lubricants, flocculants, fluid loss additives (to control loss of drilling fluids into permeable formations) and so on. Extra care is necessary to select additives and their proportion in the mud to obtain the best rheological properties (viscosity and density) and other important parameters such as tolerable pH, less corrosivity, thermal stability, and low stickiness. [44] Typical drilling fluids additives are discussed in the following paragraphs.

2.4.1 Additives for viscosity control

Clay like bentonite; thickeners such as xanthan gum (flowzan), starch, glycol, guar gum, carboxymethylcellulose and polyanionic cellulose (PAC) are the common viscosity additives. They are very vital to achieving the required rheology to support cutting transportation during drilling. However, the reduction of viscosity is accomplished using flocculants. Some of the flocculation additives include brine, potassium chloride, calcium chloride ($CaCl_2$), acrylates, gypsum ($CaSO_4$), soda ash (Na_2CO_3), sodium bicarbonate, tetrasodium pyrophosphate, polyphosphates, and lignosulfates. [45–48]

2.4.2 Density control and filtration control additives

A weighting or density agents (such as barite, hematite, calcium carbonate, dolomite, magnetite, iron oxide) are added to increase the overall density of the drilling fluid. So, sufficient bottom-hole pressure can be maintained thereby preventing any formation damage and facilitates withdrawing of the dry pipe. [49] The pressure by the density material must be enough to form a filter cake on the wall of the hole. Adequate mud density also increases buoyant effect on cuttings carrying capacity. However, excessive mud density may result to overbalance, reduce penetration rate induced fracture and high cost. [50]

2.4.3 Filtration and rheology (viscosity) control additives

These are used to reduce fluid loss of drilling fluid in different mud (either WBM or OBM) and high-temperature drilling conditions. [51] An example of these additives is carboxy methylcellulose (CMC), low and high viscosity PAC, bentonite, guar gum, xanthan gum, hydroxyethyl cellulose (HMC) and modified starch in WBM, while gilsonite (asphalt bitumen) and organophilic lignite in OBM. [21], [52] Partially hydrolyzed polyacrylamide (PHPA) may also act as filtration control material aside from its primary shale encapsulation and thickening (viscosifier) function in drilling mud. [8], [48], [53] Poor flow performance of fluid may result to loss of circulation, reduction in penetration, filling of a hole by cuttings and enlargement well.

The WBM filtration control additives roles include hole stabilization and fluid loss minimization predominantly adsorption of water into permeable formations. Gilsonite supports shale formations stabilization, reduces API, high pressure and high temperature

(HPHT) fluid loss, and also aid in thermal and emulsion stability and enhance the suspension properties of oil-based fluid systems. [15]

2.4.4 Other additives

Other additives being used in drilling fluid are an emulsifier, defoamer, wetting agents and fluid loss control additives. Emulsify agents are anionic, cationic or neutral chemicals that enable a homogenous mixture of two immiscible liquids. Surfactants, soaps, detergents and organic acids are common emulsifiers in WBM while amine-based compounds and fatty acids are used in OBM. [54] These additives may help in emulsion stability, improve the thermal stability of mud, enhance viscosity and contribute to filtration control. [55]

Defoamers are chemicals to reduce foaming in mud especially the one for a highly saline environment like brackish and saturated salt water. Other popular additives are the thinning agents which allow the modification of viscosity and the solids content of the fluid. They are used to reduce the thickness to improve fluid permeability. [1], [56] An example of such additives is lignosulphonate and lignite. Lubricants and anti-scaling or anti-spotting agents are also widely used as additives in drilling. Their functions are to reduce friction, drag as well as torque in the drilling operation. Stuck pipe free oils, drill detergents, and lube are important substances for lubricity and anti-scaling in muds. [57] Polymer addition to bentonite is within the range of 0.1 to 2% which is based on the polymer and its influence on the ultimate fluid composition. [30]

2.5 Shale clay minerals composition

Shale is made up of crystalline octahedral clay sheets of aluminum ion (Al^{3+}) or sodium ion (Na^{+}) central atoms or sometime with other metallic atoms like magnesium, calcium among others sandwiched between two tetrahedral sheets with silicon center (Figure 2.4). [58] It reacts with water molecule and its other ionic composition due to Na^{+} and Al^{3+} affinity for water and chemical potential differences respectively. This leads to the weakening of electrostatic or van der Waal's forces between the clay silicate layer and dispersion of clay particles in drilling fluid. [54]

The largest content of shale are clay minerals (around 60%) which make them shale swelling determinants. Clays are phyllosilicates of crystalline aluminosilicate sheets with negative charge faces due to component different which are held together with Vander Waal forces. [59] Clay has diverse mineral constituents at various proportions. The type that are germane to shale includes smectite (montmorillonite), chlorite, illite, and kaolinite. The characteristics of these minerals are highlighted in Table 1 as well as their SEM images in Figure 2.5. As presented in Table 1, kaolinite, chlorite and illite do not undergo swelling in fluid pertinent to their low cation exchange capacity (absorptivity) and surface area. Though, they sometimes undergo dispersion in mud and sloughing by hydration. The absence of water in the inter-lattice of illite having sandwiched aluminum and/or iron or magnesium octahedral layer makes it non-reactive with water in WBM. The high CEC of smectite, on the other hand, accounts for its high sensitivity to water and consequent swelling which had been reported by several authors. [60] Smectite is usually found majorly in shale as a single component (such as montmorillonite or hectorite) or in

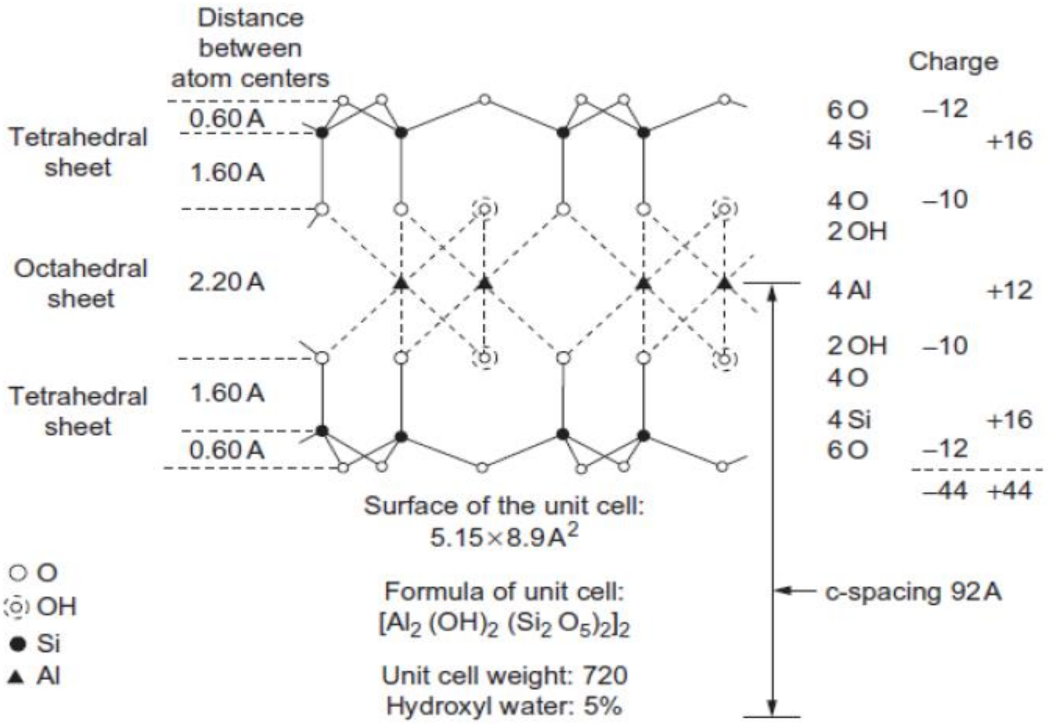

Figure 2.4 : Schematic representation of arrangement of atomic composition of clay minerals in three layer unit cell. [59]

Table 2.1: Clay minerals properties

Clay mineral	**Formula**	**Structure**	**CEC**	**Surface area (m^2/g)**
Smectite	$(0.5Ca.Na)_{0.7}(Al.Mg.Fe)_4[(Si.Al)_8O_{20}].nH_2O$	wrinkled or wavy layers	80-150	700
Kaolinite	$Al_4[Si_4O_{10}](OH)_8$	Packed layers	1-10	20
Illite	$[K_{1-1.5}Al_4[Si_{7-6.5}Al_{1-1.5}O_{20}]\ (OH)_4]$	Long granule with irregular shape	10-40	100
Chlorite	$[Mg.Al.Fe]_{12}[(Si.Al)_8O_{20}](OH)_{16}$	Platelet	<10	100

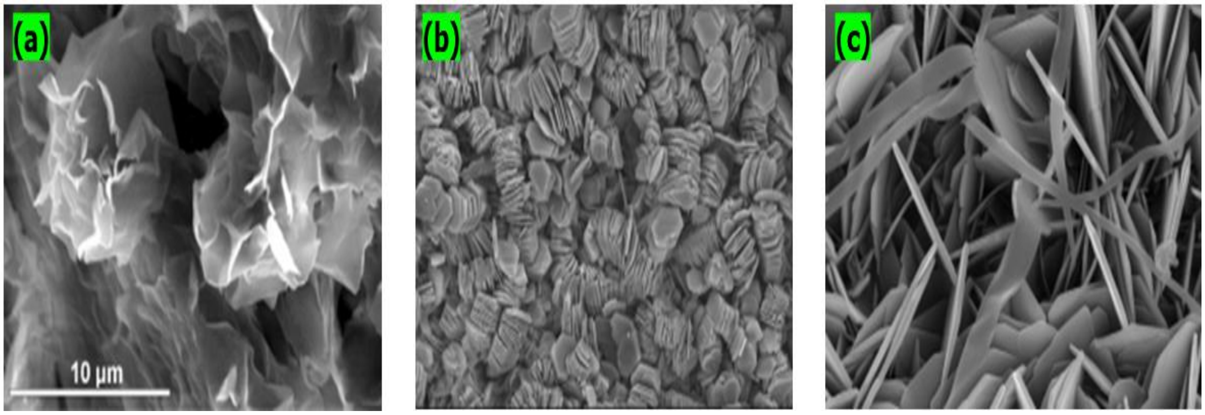

Figure 2.5: The SEM image of (a) smectite (b) kaolinite (c) illite and chlorite [61]

combined form with either chlorite or illite. The great swelling tendency of smectite makes it the point of focus in designing inhibitors for shale drilling assigned to the high amount of sodium content. [62]

2.6 Shale hydration (instability)

Shale formation has been established to behave like a semipermeable membrane. Due to the high affinity of shale clay minerals for water, it usually undergoes rapid swelling and dispersion when being drilled with water-based mud (Figure 2.6). Shale hydration or swelling mechanism have been studied by various researchers. Drilling fluid salinity (of WBM), activity, the drilling temperature, the type of cation sandwich in clay sheet as well as the pressure between the fluid and the formation have been identified as determinant factors of shale hydration. [47], [57] This has been generally proposed to involve the synergetic effect of water chemistry and mechanical processes. The water chemistry lead to *osmotic* hydration while the mechanical results to *crystalline* swelling.[16], [45] Both create stress and strain in the shale formation which lead to instability during well drilling. Forms of water contact with shale include pore free water, surface hydration, water adsorbed by capillary as well as infiltration capillary water. [63] However, few of these are associated to shale swelling.

2.6.1 Osmotic swelling

Osmotic hydration is the migration or diffusion of water molecules into formation which premise on concentration gradient which generates osmotic pressure within clay structure in shale as shown in Figure 2.7. [64]

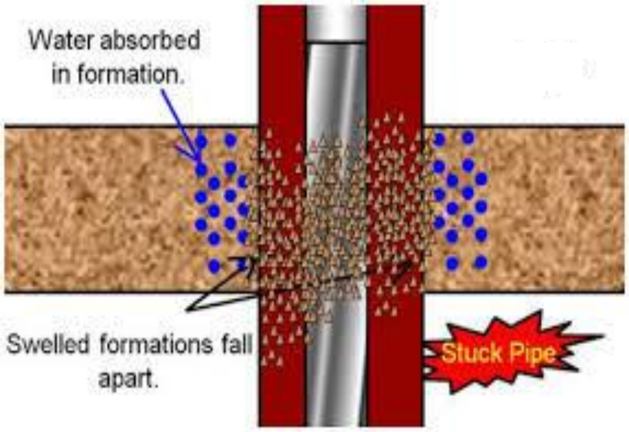

Figure 2.6: Well collapse due to shale minerals swelling [65]

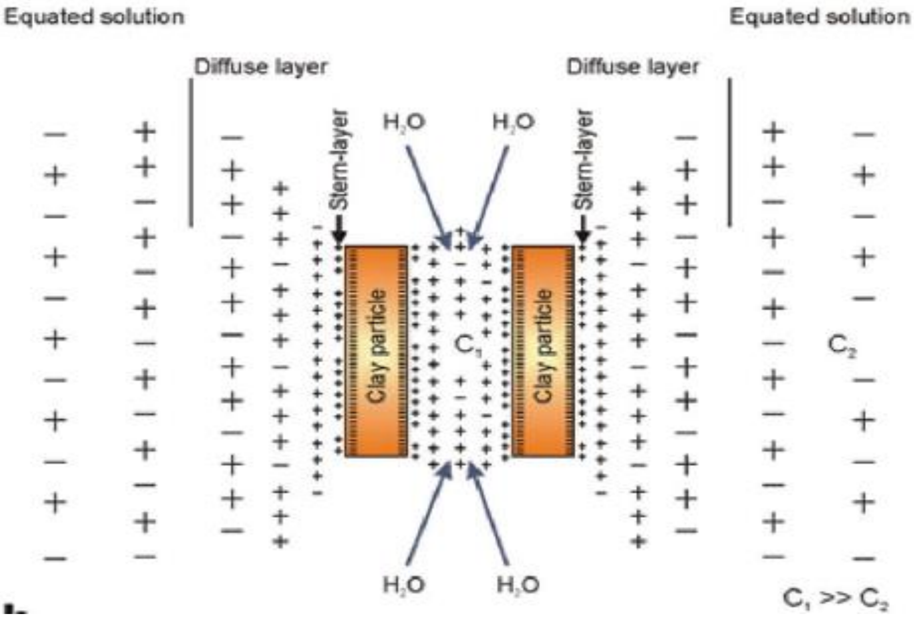

Figure 2.7: Mechanism of osmotic swelling in shale [17]

The chemical activity and hydraulic pressure coupled effect determine the volume of water that enters the shale. The equivalent pore pressure between drilling fluid and the shale formation changes which would consequently affect the stabilization of the formation. [66] The flow of water between formation and mud may be through ion exchange, convection, diffusion, reaction, injection and adsorption. [67]

2.6.2 Crystalline swelling

Crystalline swelling may also be referred to as surface hydration. It exists in the formation drilling with a high content of brine or cations with more than one valence such as calcium. Formation of inter-layer cation hydrates (Figure 2.8) due to water adsorption energy occurs at the interface resulting into increase in layer spacing. [12], [14] The rate of swelling depends on the cation exchange capacity (CEC), size and kind of the sandwiched cations in the clay. Montmorillonite which is the major sensitive component of shale that causes instability exists in sodium and potassium forms as in sodium bentonite (Na-Bt) and calcium bentonite (Ca-Bt). When more of sodium ion (Na^+) are present between two layers of silicate sheets, there is irregular and non-directional water arrangement at clay interlayer based on reduction in an attractive force between the clay layer. [24], [68] The Na-Bt react aggressively with water due to sodium high reactivity with the water molecules. In contrast, when the exchangeable cation of montmorillonite is hydrogen ion (H^+), calcium ion (Ca^{2+}) or magnesium ion (Mg^{2+}), a lesser regular and directional arrangement of water molecules on clay surface occur consequent upon high attractive force of the interlayer by extremely great charge density on the cations. This makes Ca-Bt less reactive to hydration and swelling. [13]

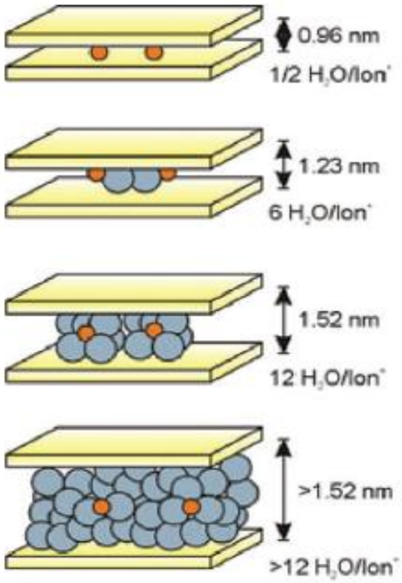

Figure 2.8: Mechanism of crystalline swelling in shale [17]

2.7 Shale hydration inhibition

The rise in need for shale inhibitor is still important in the oil and gas industry till today particularly with the exploration of deep-water deposits and shale gas. The Minimization of free water in water-based mud (WBM) interaction with clay mineral is key to addressing wellbore instability. Inhibitors are materials or chemicals added to water-based drilling fluids to hinder hydration, swelling and degradation of shales and clays. [29], [69] WBMs are preferred to oil-based and synthetic-based muds in the case of the environment, reservoir analysis, ECD management in control of pressure, the rate of penetration and safety. [70] Nevertheless, shale will swell as a result of hydration, dispersed or disintegrated and lead to well instability and mechanical problem without good shale inhibitor. [71], [72] A series of materials have been designed to address the issue of swelling of shale including inorganic salts and inert materials (macro-, micro- and nano-materials) [73], organic molecules (such as esters and amines) [74] and polymers. Many drilling fluid additives have been used to either change mud density or its chemical properties to enhance WBM functionality in drilling, especially for shale inhibition. Additives are either dissolved or suspended in the drilling fluid to increase its density in order to control pressure formation and to combat the effect of sloughing or heaving shales that may be encountered. [27] In principle, the negative charges on shale particles are either stabilized by a positive ion of the salts by intercalation in shale matrix and/or shale stabilization due to the formation of hydrogen bond between clay particles and atoms with lone pair atom (N or O) on the polymers or other materials used as inhibitors. [75–77]

2.7.1 Inhibition mechanism

The mode of action of the shale inhibitors have been proposed to include hydrogen bond formation with clay surface, ion exchange, sealing of clay surface by thin-layer film, alteration of surface reactivity with water and plugging of pore throats and flaws in formation. [17], [78], [79] Thin layer film formation by polymer molecules on clay surface helps to prevent or reduce ion exchange in the mud with that of the fluid of shale formation by moderating the mud activity. Physical properties of formation like permeability, fluid activity and porosity are also preserved by this means. [80], [81]

2.7.2 Types of inhibitors

Various chemical inhibitors have been examined in addressing the interaction between water in mud and shales formation, Table 2. Conventional shale inhibitors include inorganic salts of potassium, calcium, zinc and ammonium (KCl, $CaCl_2$, NH_4Cl, $ZnCl_2$) [54], silicates (sodium and potassium) [82], asphalt and modified gilsonite [30], high molecular weight polymers (polyacrylamide, polyvinylpyrrolidone, copolymers) [83], [84], low molecular weight polymers (polyglycol, polypropyleneoxides) [77], [85] and natural polymers (starch and cellulose) [46], [86], [87]. Other inhibitors that have been reported include polymer of quaternary amines and their salts [88], [89], ionic and amino acid polymers, glycols, ionic liquids, surfactants [35], [90] and recently nanomaterials and their composites.

Traditionally, KCl and potassium salt of partially hydrolyzed polyacrylamide (PHPA) using KCl are used to lessen the shale swelling difficulties. PHPA may also react with bentonite in low-solid mud, linking its particles together to improve fluid rheology with no consequences of solid laden increment. [11] The KCl mud efficiency is worthy for shale swelling inhibitions at high concentrations, however, it has negative impacts on fluid rheology and environment, and may result in loss of filtration. [91]

Besides, polymers like acrylamide and PHPA are acceptable heat insulators that can be utilized for inhibition by coating shale surfaces and sealing microfractures with a thin film that retards disintegration and dispersion. This polymer is more effective with the addition of KCl but it does not tolerate the downhole conditions of high-pressure and high temperature (HPHT). [92] Amines and imine polymers including their composites of with quaternary ammonium salt and/or other polymers have been reported to be functional inhibitors in literature. [93]

2.7.3 Nanomaterial as shale inhibitors

Currently, the technical challenges are being faced by gas and oil ad sectors for preparing drilling muds to increase rheological property and shale inhibition to address nanopore throat in shale and withstand high-temperature conditions experienced in the downhole. Rheological properties of the WBM are significant in drilling operation which also serve as an indication of active inhibition of shale. Conventional WBMs contain shale stabilizers and inhibitors as heat insulators, macro or microsize and cannot plug nano-pores of shales. [94] Thus, water enters the wellbore resulting in high mud filtrate volume and clay swelling. Expansion and distribution of micro-cracks in hard brittle shale have also shown some concerns in drilling. [95] To deter this, easy formation of filter cake on wellbore by trapping of nanoparticles in pore or micro-cracks to limit filtrate volume by sealing which leads to enhancement of formation stability. [94]

Table 2.2: Categories of recent chemical compounds that have been investigated as inhibitors in the water-based drilling fluid

General categories of inhibitors	**Specific inhibitor**	**Performance comparison**	**Advantage**	**Disadvantage**	**Mechanism**	**Reference**
Amines/amides/imines compounds and polymers	Poly (acrylamide-dimethyldially ammonium chloride/poly (vinyl alcohol)	-	Effective inhibition of shale hydration	Bad odor and cannot withstand high temperature	Electrostatic interaction and hydrogen bonding	[93]
	Polyethyleneimine	-	-	Degrade at high temperature.	hydrogen bond between -OH on shale particle and amino group on inhibitor	[9]
	Polyamidoamine dendrimers	KCl and Polyetherdiamine (PEDA)	Superior inhibition than conventional KCl and PEDA	Degrade at high temperature.	Hydrogen bonding	[19]
	4, 4’-methylenebis-cyclohexanamine (MBCA)	Polyetherdiamine (PEDA)	MBCA is more effective as inhibitor and physical plug of micropores and can withstand high temperature (up to 220^{o}C) than PEDA	-	Hydrogen bonding	[96]

Specific inhibitor	Performance comparison	Advantage	Disadvantage	Mechanism	Reference
Polyetherdiamine (PEDA)	Na and K formate	Efficient inhibition than formate salt	Cannot withstand HTHP	Hydrogen bonding	[63]
Melamine quaternary ammonium salt	-	Excellent inhibition	Toxic and noncompatible with anionic additives	Electrostatic interaction and hydrogen bond	[88]
Hydroxyl-terminated polyamidoamine (PAMAM-OH) dendrimers	-	PAMAM-OH retarded shale hydration more effective when combined with KCl	Inhibition maybe minimized at high temperature	Hydrogen bond	[97]
KCl modified partially hydrophobized hyperbranched polyglycerol (PHPG)	Unmodified HPG and commercial PEG400 and polydiaminedimethyl acrylamide (PDADMAC)	KCl-HPG has superior inhibition than ordinary HPG, PEG400 and PDADMAC.	HPG may undergo degradation at high temperature	Complex formation between HPG and K^+	[40]

Specific inhibitor	Performance comparison	Advantage	Disadvantage	Mechanism	Reference
Polyetheramine (PEA) and poly (vinyl alcohol-g-dimethyl aminopropyl methacrylamide (PVA-g-DMAPMA)	-	Inhibitive characteristic is not affected at high temperature	Expensive	Hydrogen bonding	[31]
Polyethyleneimine (PEI)	Chitosan quaternary ammonium salt (HTCC)	PEI is more active inhibitor than HTCC due to positive ion form between water and PEI.	-	PEI nitrogen protonation in water leading to hydrogen bond	[37]
Polyampholyte	-	Inhibit shale swelling effectively	Toxic at high concentration and degrade at relatively high temperature	Ionic interaction and hydrogen bonding	[98]
Tallow amine ethoxylate (TAE)	KCl	TAE possesses inhibition compete with that of KCl and it is compatible with other fluid additives	-	Hydrogen bonding	[75]
Ethylenediamine-methylacrylate	-	It has good inhibitor property.	-	Hydrogen bonding	[99]

General categories of inhibitors	Specific inhibitor	Performance comparison	Advantage	Disadvantage	Mechanism	Reference
Gelatin	Gelatin	KCl, PEA, polydimethyldiallyl ammonium chloride (PDMDAAC)	It is biodegradable and has better inhibition than KCl, PEA and PDMDAAC and nontoxic	It may degrade at elevated temperature and requires high quantity in application	Hydrogen bonding	[100]
Graphene	Ethylenediamine-modified graphene (EDA-G)	KCl, polyether amino, and chitosan quaternary ammonium salt (HTCC)	Perform better than KCl and polyether amino but has similar inhibition capacity as HTCC	-	Physical sealing and chemical inhibiting through hydrogen bond formation	[7]
Ionic liquid	Monomer and homopolymer of 1-vinyl-3-ethylimidazolium bromide (VeiBr)	KCl and HTCC	Effective at low concentration (0.05wt% of VeiBr better than 5wt% KCl but has same functionality as 2wt% PEA). Active at high temperature up to 300°C.	It might not be compatible with some additives.	Physical plugging and chemically inhibition by hydrogen bonding	[101]

General categories of inhibitors	Specific inhibitor	Performance comparison	Advantage	Disadvantage	Mechanism	Reference
Natural polymer	Chitosan quaternary ammonium salt (HTCC)	Polyether amino (PEA)	Inhibits shale better than PEA even at high temperature, environmental friendly and biodegradable	It is not compatible with some additives, toxic and pH-dependent	Electrostatic interaction and hydrogen bond	[35]
	Zizyphus spina-christi extract (ZSCE) surfactant	KCl and polyamine	ZSCE has better performance than KCl and the polyamine and it is ecofriendly	Activity may reduce at elevated temperature	Electrostatic interaction and hydrogen bonding	[102]
	Triterpenoid saponin from *Glycyrrhizin* extract of *Glycyrrhiza glabra*	KCl and t-octylphenoxyl polyethoxy ethanol (TX-100)	Biodegradable and environmental friendly and inhibit shale hydration than KCl and TX-100	Degradation may occur at extreme temperature and which would lead to reduction in inhibition	Encapsulation of clay particles by thin film and hydrogen bonding	[103]
	Glucose graft copolyammonium (GGPA)	-	GGPA inhibits water absorption into bentonite efficiently at 0.5 wt% and could withstand temperature around 0-300°C	Might not be compatible with some additives	Adsorption to clay surface through ion exchange, surface hindrance to water affinity and hydrogen bond	[39]

Due to low permeability of shale, formation of filter cake via filtration loss on the wall of wellbore is usually difficult. Thus, gradual transfer of equilibrate pressure between mud and pore pressure occurs in the absence of a potential barrier that results into transient pore pressure and instability. [104] In the presence of microcracks during drilling, the filter cake can easily be formed with the cracks playing a major role in filtration loss with less permeation through the material bulk pore throats. Moreover, migration of particle to plug pore throat which actively reduces permeation into the formation experiences at a suitable drilling fluid flow rate. [56]

Nanomaterials or nanocomposites have been found to be suitable for effective plugging of microfractures and pore throats due to their ability to reduce fluid loss into cracks and pores of the formation. [105] They, therefore, prevent equilibration between wellbore and pore pressure that could result into formation failure and consequent collapse. The effective dispersity of nanomaterials in drilling fluids due to their extremely small sizes enhances their performance to inhibit shale hydration. [106], [107] Nanoparticles mud systems have been identified to tackle these challenges. They could enhance fluid rheology as well as encourage shale inhibition, lubricity, and filtration of WBM. Reports have also shown them to aid mud sealing capacity as plugs for nanopores and micro-fractures in shale drilling, cheap and inexpensive. [94], [108], [109] Nanoparticles could form tough and dense mud cake which may significantly reduce fluid loss. [110]

Literarily, nanoparticles are nanomaterials (1-100nm size) with the superior surface area and can impact excellent fluid properties at minute concentration. [111] They have a distinctive size and hydro-dynamism with the ability to react with formations in inhibiting shale. [112]

Nanosilica [113]–[115], nanopolymers [94], multi-walled carbon nanotube [11], graphene nanoplatelet [7], [116], [117], laponite [51], [118], polymer-silica nanoparticles composite [92], [119], [120] among others are typical example of nanomaterials that have been tested as shale inhibitors in water-based drilling fluids with distinguished performance relative to common inhibitors.

2.7.4 Shale inhibition characterization

Characterization of shale is very important in drilling industry to understand its interaction with drilling fluid components. According to America petroleum institute (API) methodology, physical and chemical techniques are being used to explore clay swelling, mechanical and physico-chemical parameters, shale inhibition mechanism. [121] One or more of the methods that are being used to achieve the purpose are as follows.

X-ray diffraction and fluorescence test is used to evaluate composition of drilling fluid shale mineral, swelling and crystallization.

Cation exchange capacity (CEC) test is an established technique for shale reactivity examination by determining the amount of exchangeable cation in the clay.

Linear swelling test uses linear displacement response when clay is in contact with drilling fluid to assess the swelling of shale.

Porosity test is used to evaluate the size of pore throat in the clay grains mineral through injection of mercury.

Gravity swelling test is used to examine ability of mud to drill formation by exploring its interaction of with shale.

Capillary suction test is a technique for filter cake filtration capacity as well as salt interaction with the clay.

Thermal gravimetric analysis (TGA) **test** is a method being used for evaluation of thermal stability of drilling fluid and forms of water in clay layers.

Shale dispersion test is a method being used to review the shale inhibition ability of a fluid by measure the swelling and dispersion percentage of shale cuttings at a condition similitude to that of wellbore.

Anti-swelling test is like the shale dispersion and linear swelling test. It helps to measure the capability of the mud to suppress shale swelling and dispersion.

Rheology evaluation is highly significant in the assessment of drilling fluid performance. The viscosity (plastic and apparent viscosity), yield point and thixotropic character of clay colloid in mud is normally achieved to fathom fluid performance. The basic rheological parameters that are normally study include apparent viscosity, plastic viscosity and yield point.

Apparent Viscosity (AV) this is a one-point viscosity measurement to know if the fluid is in line with the acceptable viscosity. It is measured by averaging the shearing viscosity of the fluid at 600 rpm using the formula.

$$\mathbf{AV} = \frac{\theta_{600}}{2} \qquad \mathbf{2.1}$$

Plastic viscosity (PV) is a measure of the extend and effect of solid materials such as weighting additives on the plasticity of the fluid. This could be accomplished as follows.

$$\mathbf{PV = \theta_{600} + \theta_{300}} \qquad \mathbf{2.2}$$

Yield point (YP) allows the measurement of the overall viscosity and density of the mud. It depends on the concentration and properties of solid portion of drilling fluid. Thus, excessive viscosity and density of mud will lead to high YP. This is basically calculated using the formula below.

$$\mathbf{YP = \frac{(2\theta_{300} + \theta_{600})}{2}} \qquad \mathbf{2.3}$$

3. CHAPTER 3

NOVEL PARTIALLY AMINATED ACRYLIC ACID GRAFTED ACTIVATED CARBON AS AN INEXPENSIVE SHALE HYDRATION INHIBITOR

3.1 Introduction

Drilling fluid is generally used in oil and gas wells and even in water boreholes drillings. About 70% of wellbore instability problems are associated to shale hydration. [122] Shale instability is caused by the presence of clay minerals such kaolinite, smectite, and montmorillonite as a result of their great affinity for water. [8], [53], [117]

When clay minerals interact with water, they swell and raise the wellbore instability problems such as shale sloughing, tight hole, caving and reduce efficiency of mud to lift the drilled cuttings. [4] Clay swelling also reduces the rate of penetration (ROP) due to bit balling with sticky clay. The three types of drilling muds that are used in drilling industries are water-based mud (WBM), oil-based mud (OBM) and synthetic-based mud (SBM, also called low toxicity oil-based mud, LTOBM). [1], [17]. The use of OBM and SBM in wells drilling are limited due to their environmental toxicity, high cost, poor formation logging during drilling and sometimes constitute damage of formation. [4] [123] About 80% of wells drilling in oil and gas industries are achieved using WBM due to its environmental friend liness, easy geotechnical analysis and less cost. [117] However, its use is associated with instability challenges resulting from the interaction of water-sensitive Shales with active water molecules in the mud which causes swelling and dispersion of shale, and thus results into loss of billions of dollars through wellbore collapse. [1] [124] Hence, shale inhibitors are usually added to WBM for elimination or minimization of the shale hydration by serving as water molecule hindering-component to preserve shale during drilling purpose. [4] [123] Conventional shale inhibitors include inorganic salts of potassium, calcium and ammonium (KCl, $CaCl_2$, NH_4Cl), asphalt, modified gilsonite [48], [54] and polyacrylamide (PAM) and partially hydrolyzed polyacrylamide (HPAM) [125], [126]. Other that have been studied by researchers include polymers of amine, imines, quaternary amines and their salts [127], [128], modified glucose [4] [123], ionic and amino acids polymers [129], ionic liquids [17] [130], and surfactants (ionic and nonionic) [131]–[135]. KCl mud performance is excellent for shale swelling inhibition but at high concentration, it has negative impacts on fluid rheology, and ultimately affects the environment [17], [123] [130–132], [136]. Amines and imine polymers including their composites with quaternary ammonium salt and/or other polymers have been reported to be functional inhibitors in many research works. [124] [137] Most of these substances have one or more drawbacks to reduce clay hydration including toxicity, degradation at elevated temperature, incompatibility with other fluid additives, pH dependent, high concentration requirement, expensive and offensive odor. [138] Nanoparticles and nanopolymers mud systems have been identified to tackle these challenges. They could enhance fluid rheology [117] [54] [139] as well as encouraging shale inhibition, lubricity and efficient filtration of WBM [140]. Reports has also shown them to aid mud sealing capacity as plugs for nanopores and micro-fractures in shale drilling, and inexpensive. [125], [126], [141], [142]

Attentions have is being giving to the consideration of nanomaterials to inhibit shale in drilling mud due to their unique essence to plug tiny pores and fractures in shale formations to grossly reduce both mechanic and chemical (hydration) damage of the wellbore. Among such materials that have been explored are graphene and functionalized graphene [117], [138], [143–145], silica and nanosilica composites [79], [92], [114], [146]–[148], nano polymers [149], [150], and laponite [51] among others are typical example of nanomaterials that have been tested as shale inhibitors in water-based drilling fluids with distinguished performance relative to common inhibitors.

In this work, we designed a novel partially aminated cheap activated carbon-based grafted acrylic acid polymer denoted as C-g-AA-NH_2 and investigated its ability to inhibit shale hydration. The presence of nanosized carbon particles in the material contributed to its effectiveness in inhibiting water interaction with shale and its excellent temperature tolerance. This finding may serve as an economical replacement for the conventional KCl being used as mud component to inhibit hydration of shale in oil and gas industry.

3.2 Experimental

3.2.1 Materials

All the chemicals used were analytical grade. The 6-10 mesh shale cuttings used for recovering measurement was donated by Aramco, while the activated carbon as prepared from waste tires through carbonization. Sodium bentonite (Na-Bt) and potassium persulfate (KPS) were supplied by Sigma-Aldrich, USA. Ethylenediamine (EDA), allyl chloride and acrylic acid (AA) were purchased from Fluka AG, Chemische Fabrik, Switzerland. Hydrochloric acid, sodium hydroxide, hydrogen peroxide and ethanol were obtained from BDH Chemicals, England.

3.2.2 Synthesis of allyl activated carbon (C-A)

A certain amount of activated carbon was first treated 37% HNO_3 by fluxing for 6 h. This was then filtered, washed with excess DI water to remove residual acid and finally dried at 105 ^oC for 24 h in the oven to obtain a powder which was further grounded into fine particles. A 5 g fraction of treated carbon-containing carboxylic functionalities was reacted with 31 g allyl chloride in the presence of 100 ml (0.45 M) sodium hydroxide at 60 ^{o}C for 8 h. The product was then filtered, washed with excess deionized water and ethanol, and finally dried at 60 ^{o}C for 12 h to get allyl terminated carbon (C-A) as shown in Figure 1a.

3.2.3 Preparation of C-g-AA-NH_2

The C-g-AA-NH_2 was prepared via a free radical polymerization. [149] Exactly 1.5 g C-A and 16 g AA were charges into a three-necked flask containing 100 ml DI water equipped with a magnetic stirrer, condenser and a nitrogen gas inlet. The solution was purged with nitrogen gas for 10 min to remove dissolved oxygen, the flow rate was then reduced and maintained throughout the reaction period. Solution of 0.5 g KPS in 10 ml DI water was introduced gradually to initiate polymerization. After reacted for 3 h at 60 ^{o}C, 6.7 g EDA in 200 ml ethanol was added and stirred vigorously at room temperature for 24 h. The viscous C-g-AA-NH_2 (Figure 3.1b) was precipitated in acetone and dried in a vacuum for 12 h.

3.3 Characterization

3.3.1 Fourier transform infrared spectra (FTIR) and proton NMR

Thermo Scientific Nicolet iS10 FTIR spectrophotometer was used to obtain the IR spectrum of C-g-AA-NH_2. A 2.5 cm KBr pellet containing 5 wt% of the sample was made and the IR spectrum was then carried out at room temperature and scanned between 4000−500 cm^{-1} wavenumber range with 4 cm^{-1} resolution and 16 scans. The proton NMR

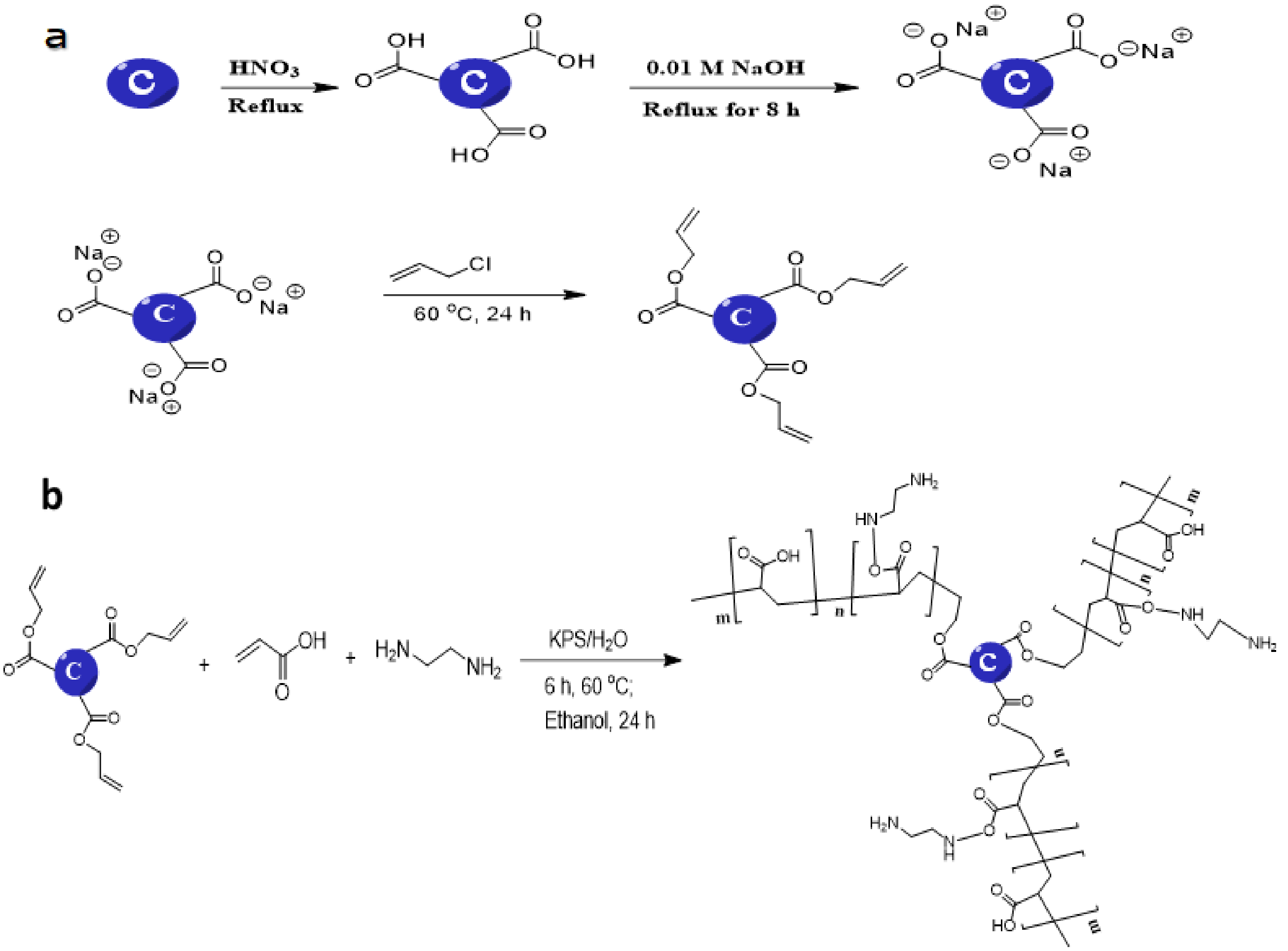

Figure 3.1 : (a) Synthesis of C-A. (b) Preparation of C-g-AA-NH_2

(^{1}HNMR) was established with 400 MHz Brucker AV III 400 spectrometer using D_2O as a solvent.

3.3.2 Scanning Electron Microscope (SEM) and Thermogravimetric Analysis (TGA)

The morphology of the shale sample and Na-Bt were observed under Scanning electron microscope (SEM) before and after the inhibition test. The thermogravimetric analysis (TGA) was obtained in a TGA analyzer (TA Instruments SDT-Q600 Simultaneous TGA / DSC, USA) within 25 – 700 ^{o}C range temperature under nitrogen atmosphere.

3.4 Inhibition testing

3.4.1 Anti-swelling test

The anti-swelling ratio (AR) was measured. [150] Bentonite (1 g) was dispersed in 20 ml of 2 wt% composite solution and left for 2 h. The mixture was then centrifuged at 1500 rpm and the change in the bentonite volume by calculating AR based on equation 3.1.

$$AR = \frac{V_W - V_P}{V_W - V_O} \qquad \textbf{3.1}$$

where V_W and V_P are bentonite change in volume in distilled water and in the polymer solution, respectively, while V_O is it volume in kerosene.

3.4.2 Immersion Test for shale inhibition

In this method, the previously grounded shale sample that has been sieved via 100 mesh was dried at 105 ^{o}C for 4 h. The 10 g fine shale particles will then be compressed into a disc pellet of 5 cm under 10 MPa in a hydraulic presser for 5 mins. This was followed by submersion into 20 ml of 10 wt% KCl solution, deionized water, and 2 wt% of the prepared inhibitor respectively. The submerged samples were then be observed after 16 h. [130]

3.4.3 Shale Recovery Test

Shale recovery test was conducted on shale samples in the solution of each inhibitors. Briefly, crushed shale sample in the range of 6−10 mesh sizes were utilized for this test. About 50 g of this shale was added into 350 mL of each inhibitor's solution in 500 ml vessel. This was then hot-rolled in hot-roller oven for 16 h at 150 °C. Upon completion, the mixture was cooled to room temperature, filtered, washed with DI water, and dried at 105 °C for 24 h in a vacuum oven. The dried shale remains were then sieved through 40-mesh sieve. The sieve retained shale was weighed and recorded to be M_1 which was used to calculate recovery as shown in equation 3.2. [138]

$$\text{Recovery} = \frac{M_1}{50} \text{ X } 100\ \% \qquad \textbf{3.2}$$

3.5 Results and discussion

3.5.1 Preparation of C-g-AA-NH$_2$

Free radical polymerization was used to graft polymer molecules of the surface of the activated carbon nanoparticles to form the partially aminated C-g-AA-NH$_2$ depicted in Figure 3.1b. The mole ratio of AA to DEA is 2:1 in order to obtained average amination. The blue core center in the structure of C-g-AA-NH$_2$ is the carbon nanoparticle on which the partially aminated acrylic acid is grafted. Infrared analysis was conducted on the prepared materials to confirm successful synthesis. As it can be seen in Figure 3.2, IR spectral of C-A and C-g-AA-NH_2 show vibrational bands indicating the type of bond present in their structure. For C-A spectrum, the 3403 cm^{-1} stretching band is due to C-H of alkene ($C=CH_2$) while the peaks extending from 1710 cm^{-1} to 1650 cm^{-1} and 1598 cm^{-1} are due to carbon-carbon double bond (C=C) and carbonyl (C=O) respectively. The spectrum of C-g-AA-NH_2 shows characteristic feature of hydroxyl group (-OH) and amino group (-NH_2) hydrogen stretching bands with overlapping peaks at 3374 cm^{-1} and 3292 cm^{-1}. The band at 2882 cm^{-1} and 1645 cm^{-1} are due to amide hydrogen and C=O stretching; the one at 1405 cm^{-1} is due to C-O stretching; and the peak at 1548 cm^{-1} and 1305 cm^{-1} could be ascribed to -N-O-C band.

Figure 3.3 shows the ^{1}HNMR spectrum of C-g-AA- NH_2 to further corroborate the IR result that the material synthesis was achieved. The characteristic peak between 1.5 and 2 ppm is due to -CH_2- proton. The -NH_2 proton is absent due to the interaction of D_2O, but -CH- proton shows between 2.0 and 2.5ppm. The peak of 3.5-4.0 ppm indicates the proton of -CH_2-N-. The broad peak around 4.0-4.5 ppm could be ascribed to -NH-O-, CH-C=O peak

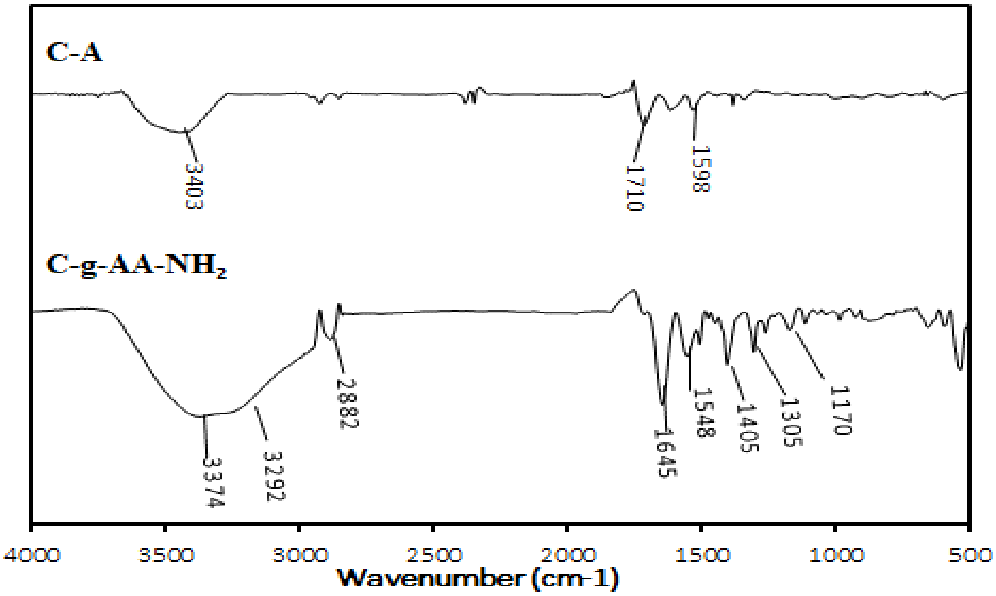

Figure 3.2: FTIR spectral of C-A and C-g-AA-NH2

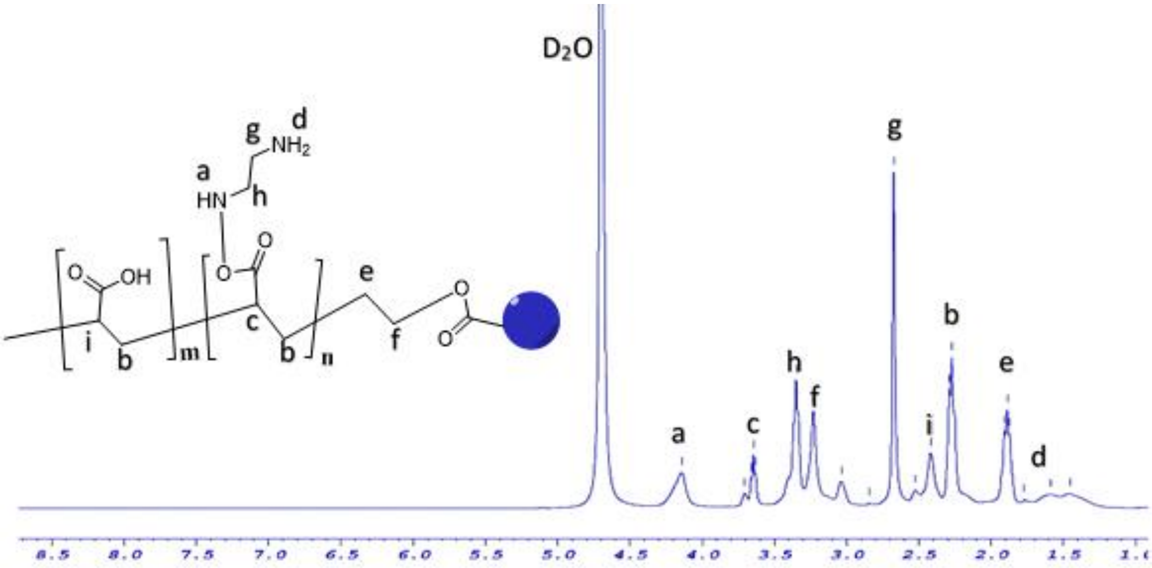

Figure 3.3: ^{1}HNMR spectra of C-g-AA-NH_2

is around 2.4 ppm and the huge peak at around 4.8 ppm is associated with the solvent. The FTIR and ^{1}HNMR outcomes revealed that the proposed compound was successfully prepared.

3.5.2 The TGA result of C-g-AA-NH_2

The high temperature tolerance of shale inhibitor is key to their excellent performance to minimize shale hydration during drilling processes as a result of high temperature usually encountered in downhole. [138] The thermogravimetric analysis showing the degradation of C-g-AA-NH_2 with increase in temperature is presented in Figure 3.4. The material demonstrated a good thermal stability toward. As the temperature increases from 25 ^oC to about 250 ^oC, the weight of C-g-AA-NH_2 descended gradually accounting for about 30% weight loss. This could be ascribed to the liberation of intercalated moisture in the material's structure. [150] The steady declining of the curve at the middle around 250 ^oC – 480 ^oC is due to the degradation of the grafted polymer component on the surface of the carbon nanoparticles resulted in the loss of almost 45% of the material's weight. The last almost constant tailing part of the curve above 480 ^oC signifies the carbonization of the residual material. This result discloses the possibility of using C-g-AA-NH_2 to protect shale-water interaction at high temperature-high pressure normally experienced in wellbore drilling.

3.5.3 Mechanism of action of C-g-AA-NH_2 as an inhibitor

In order to explain the inhibition mechanism of C-g-AA-NH_2, the surface of bentonite before and after in contact with it was inspected. It is apparent in Figure 3.5 that the 2 wt% C-g-AA-NH_2 aqueous solution forms a thin film on the surface of Na-Bt based on the hydrogen bond formation between the clay surface and the -OH, -NH- and $-NH_2$ grafted polymeric part (Figure 3.6). [136], [151] Meanwhile, the core centered carbon nanoparticles also participated in the protection of water invasion by plugging nanopores. The presence of ester group at the surface of the core-centered carbon nanoparticle further resists water intrusion into the clay premising on its hydrophobic nature. [144]

3.5.4 Inhibition experiments

3.5.5 Anti-swelling ability of C-g-AA-NH_2

The anti-selling potential of 2 wt% C-g-AA-NH_2 was examined, and its performance was compared with that of KCl (10 wt%) which is the common shale inhibitor for drilling operation in oil and gas industries. The anti-swelling capacity of C-g-AA-NH_2 was discerned relatively to 10 wt% KCl as can be seen in Figure 3.7a. The swelling of Na-Bt was greatly retarded in the presence of 2 wt% C-g-AA-NH_2 accounting for an anti-swelling ratio of 80.3% compared to 10 wt% KCl which is approximately 55.4%. Thus, C-g-AA-NH_2 could effectively minimize shale hydration because it demonstrated an outstanding inhibitive trait towards Na-Bt clay which has similar properties of smectite component of shale formations.

3.5.6 Shale recovery experiment

The shale recovery test was undertaken to check the effect of C-g-AA-NH_2 on the dispersion of real shale in drilling fluid at a condition similar to the one usually experience in a normal downhole of a wellbore. Recovery test is highly crucial in order to evaluate the strength of any material or compound that can be used to tackle aggressive interaction of

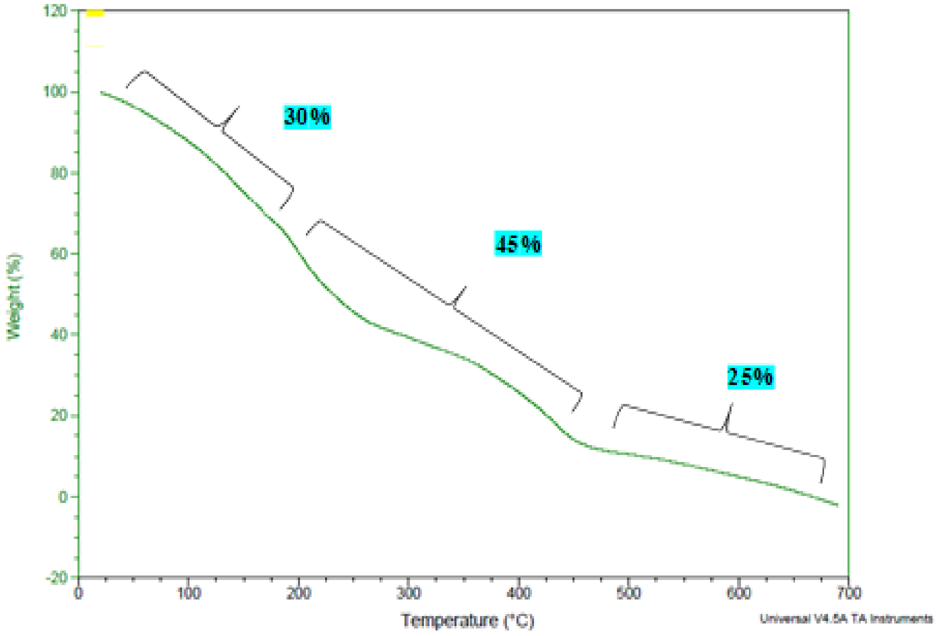

Figure 3.4: Thermal stability analysis of C-g-AA-NH_2

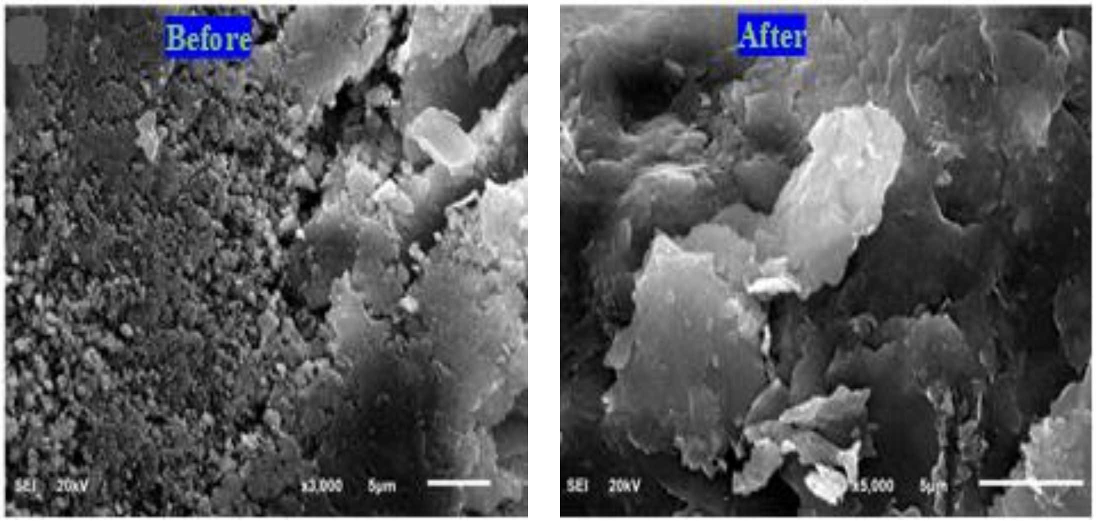

Figure 3.5: SEM image of Na-Bt before and after interaction with 2 wt% C-g-AA NH_2 for 24 h

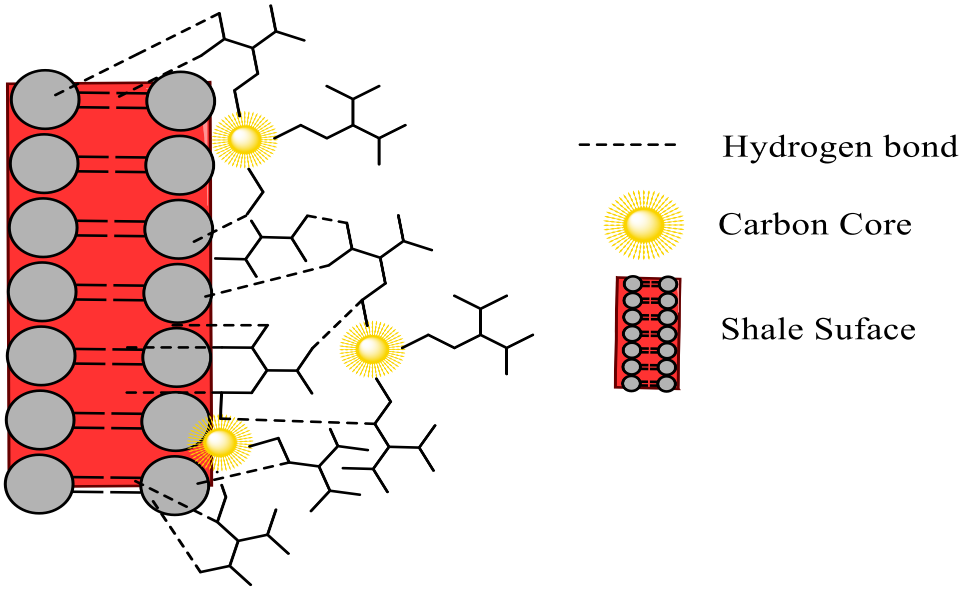

Figure 3.6: Mechanism of action of C-g-AA-NH$_2$

active water in mud with shale. The percentage recovery recorded for the shale in water of the prepared material was compared with that of KCl and pure water. The outcome of 10 wt% KCl and 2 wt% C-g-AA-NH_2 are represented in Figure 3.7b.

It was realized that 2 wt% C-g-AA-NH_2 gave a brilliant number of 91.04 % recovery compared to KCl solution with just 63.04%. The value of the recovery in pure water was 35.1% revealing that the shale sample has significant hydration and swelling action in water. The performance of the C-g-AA-NH_2 is better compared to some previous studies such as 89% reported for copolymer acrylamide sulfonate [37] and 85% for laponite nanoparticles [38].

3.5.7 Immersion test

The nature of Na-Bt pellet immersed in different 2 wt% C-g-AA-NH_2, water and 10 wt% KCl at early the stage and after 24 h were examined. At the end of the experiment, there was a slight change in the size and volume of Na-Bt in 2 wt% C-g-AA-NH_2 solution. However, the Na-Bt underwent a serious increment in its volume in water via rapid swelling interaction with water molecule which makes it to dispersed widely in the fluid. On the other hand, there was a dispersion of Na-Bt in the 10 wt% KCl but less rise in the volume of the dispersed pellet due to substitution of aluminum ions which is very reactive with water molecules with potassium ions which tend to bring the clay together. Therefore, 2 wt% C-g-AA-NH_2 has a tremendous capacity to efficiently abrogate shale hydration.

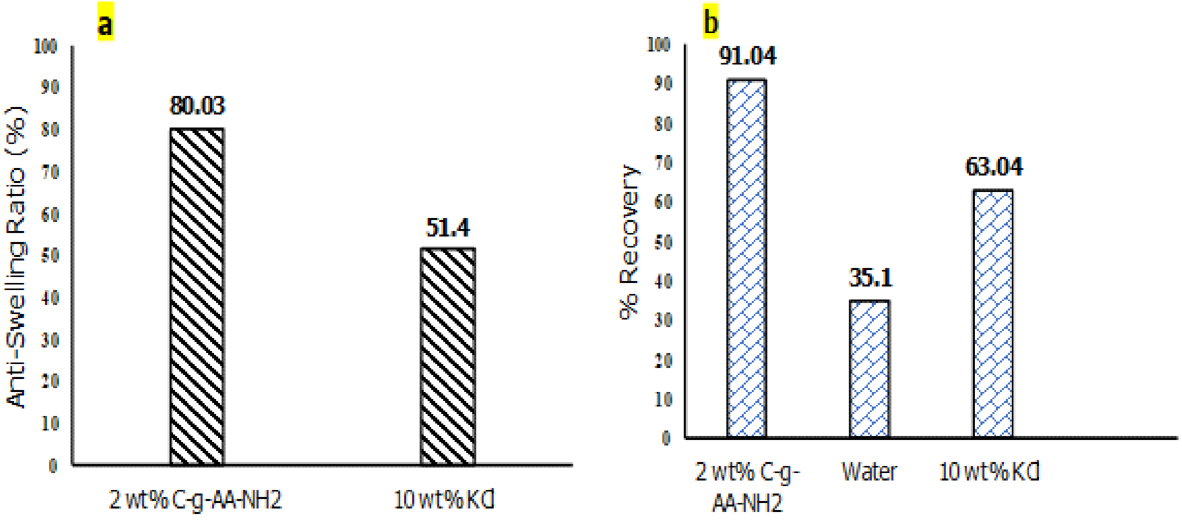

Figure 3.7: (a) Anti-swelling ratio of inhibitors and (b) Percentage shale fragments recovery.

4. CHAPTER 4

AMYL ESTER SURFACE CARBON-NANOPOLYMER COMPOSITE FOR SENSITIVE SHALE DRILLING

4.1 Introduction

Contemporary research on inhibiting shale hydration majorly focuses on controlling fluid loss through the special fabrication of shale inhibitors. [142], [152] Excessive fluid loss into shale formations have been the major cause of failure of wellbore due to high filtrate volume infiltration into formations from the mud formulation. [153–155]

When free water in mud gets in contact with clay minerals especially smectite which has high reactivity and extreme swelling character in an aqueous medium, it aggressively absorbs water and dispersed in fluid in question. [18], [156] Thus, creating mechanical imbalance leading to loss of wellbore by collapsing and elevation of the general oil and gas exploitation cost. [71], [157], [158] To tackle this menace, an adequate effort through preparation and/or formulation of drilling fluid to mitigate shale formation swelling and sloughing is key. [159] Water-based mud (WBM) has taken over the place of Oil-based mud (OBM) and Synthetic-based mud (SBM) in the oil and gas drillings. [160], [161] Though OBM and SBM provide merits like good lubricity and bit cooling and perform excellently in drilling shale regions of wells, they show poor logging ability, impact the environment negatively and highly expensive. [162] The WBM, on the other hand, is safe, cheap and easy in logging data during drilling operation. Nevertheless, it requires the incorporation of a suitable inhibitor to preserve shale minerals from reaching water molecules in the formulated fluid. [163]

Water-soluble polymeric materials are well known for their clean traits due to the presence of little or no volatile organic compounds in their solution. This property makes both natural and synthetic polymers to be integrated in diverse formulations in industries such as pharmaceuticals, foods, oil and gas etc. [164] Appreciable numbers of polymers have been applied in different fields as emulsifiers, dispersants, bio-stimuli materials, gel, film agents, foam/emulsion stabilizers/destabilizers, rheology modifiers, thickeners, binders, antimicrobial ingredients among others. [165] Application of polymers as shale inhibitor is not exempted due to their ability to form thin films on shale surface, control filtration volume and help in adjusting fluid rheology to suit shale formation drilling. [118] Different water-soluble synthetic homo- and co-polymers have been tested and applied as shale inhibitors. [166] Among them that have been widely studied as potential shale inhibitors are the polyesters, polyacrylonitrile ammonium salt; polyacrylic acids and its metals polyacrylates, polyacrylamide and its copolymers [107], [167], polyglycols, Zwitterionic polymers, cationic polymers [164], polyammonium [168] etc.

The advent of nanomaterials has led researchers toward their use in various applications. They have been proved to be capable of providing solutions shale formations damage because of their feasibility to block the nano-fractures and nano-pores in the formation. [111], [169], [170] Nanosized starch [87], silica nanoparticles [110] as well as their composite [92], [164], [171], aluminum nanoparticles [172] and transition metal nanoparticles [173] have been recently established as potential plugging agents of pore throats in shale.

Carbon is one of the major abundant elements on earth. It occurs naturally as coal or graphite and with other elements such as organic molecules. Graphene oxide [138] and functionalized graphene [144] are some of the carbon-based nanomaterials that have been recently tested as viable shale inhibitors. Conversely, the scale-up of graphene for this purpose may be quite challenging due to the high cost requires in its largescale production.

Activated carbon (AC) is also a kind of nanocarbon that have a large surface area, high porosity and high surface reactivity which makes it useful as adsorption material for both organic and inorganic pollutants. [174], [175] The activity of AC even gets improved when it surface is modified with various molecules or atoms (such as heteroatoms). [176] It is very cheap to prepare, easily available, economically viable and can be generated from various precursor sources including biowastes [177–183], fossil fuels [184], [185], polymers (natural and synthetic) [186], [187] and oil and gas waste (like asphaltene) [188]. The quality and the performance of activated carbon (AC) mainly depends on the precursor used for its preparation. Other applications of activated carbons (ACs) include decolorization, catalysis, purification, separation and deodorization. [189 –197] Inorganic nanoparticles are associated with aggregation in aqueous media which affects their ability to plug pores in shale. [190] So, combining the plugging ability of AC nanoparticle with hydrophobic and/or hydrophilic characteristics of polymers will be a great idea to disperse them for effective and efficient shale inhibition. Herein we designed polymer- amyl ester modified AC composites that could be an excellent mud component to inhibit shale hydration in oil and gas drilling operation. Both the more hydrophobic acrylic acid co acrylamide co octadecene with amyl functionalized activated carbon (AA-AAm-OD-C-Amyl) and partially hydrophilic hydrophobic acrylic acid co acrylamide with amyl functionalized activated carbon (AA-AAm-C-Amyl) polymer composites showed outstanding performance in retarding the interaction of free water molecules in drilling fluid. Their mode of action could be premised on the synergetic effort of the polymer molecule and the plugging ability of nanosized activated carbon with pores that could allow the penetration of polymer film as well as the physical interaction due to Van der Wal force of the hydrophobic backbone of polymer with the amyl chain of the activated carbon amyl ester.

4.2 Experimental

4.2.1 Materials

Shale cuttings for the recovery test was provided by Aramco. The activated carbon functionalized for the preparation of the composite was obtained from waste tires. Sodium bentonite (Na-Bt) and ammonium persulfate (APS) were provided by Sigma-Aldrich, USA. Octadecene, acrylamide (AAm), acrylic acid (AA), sodium sulfite, sodium dodecyl sulfate (SDS) and amyl alcohol (Amyl) were supplied by Fluka AG, Chemische Fabrik, Switzerland. Nitric acid and sodium hydroxide were obtained from BDH Chemicals, England. All the chemicals utilized are of analytical grades.

4.2.2 Amyl esterification of activated carbon

Around 2 g of activated carbon pretreated with under reflux with 37% HNO_3 for about 6 h. The obtained product was then filtered, washed with deionized water to remove excess acid until neutral pH was observed, dried for 24 h at 105 ^{o}C in oven and pulverized into fine powder. Into 250 ml round bottom flask was transferred 500 mg of treated activated carbon. This was followed by the introduction of 50 ml amyl alcohol and 1 drop of 98% sulfuric acid as catalyst. The mixture-containing flask was transferred into an oil bath and equipped with magnetic stirrer. After reacted for at 105 ^{o}C 6 h with the flask opened in the fume hood in order to get rid of water molecules as by-product, the amyl ester activated carbon was retrieved by filtration. This was then washed with deionized water and dried at 60 ^{o}C for 12 h to obtain amyl ester modified activated carbon (C-Amyl) as presented in Figure 4.1a.

4.2.3 Synthesis of polymer- C-Amyl composite

Two polymer-C-Amyl composites were prepared through free radical polymerization technique according to the method described in a patent. [198] Acrylic acid co acrylamide co octadecene with amyl functionalized activated carbon (AA-AAm-OD-C-Amyl) and hydrophilic hydrophobic acrylic acid co acrylamide with amyl functionalized activated carbon (AA-AAm-C-Amyl) were prepared. The first polymer composite (AA-AAm-OD-C-Amyl) is more hydrophobic than the second (AA-AAm-C-Amyl) in order to justify the plugging essence of C-Amyl. In the experiment, two three-neck flasks containing a magnetic stirrer were placed in separate oil baths. Thereafter, 1.0 g C-Amyl was introduced with 100 ml of deionized water to each flask and subjected to rigorous mechanical stirring for 30 min. This was followed by simultaneous addition of 2.5 g of AA and 2.47 g AAm to the first flask indicating equimolar of the two monomers for AA-AAm-C-Amyl. On the other hand, 8.9 g of OD, 1.25 g AA and 1.24 g of AAm were added the same time.

min to get rid of the dissolve oxygen in the mixtures at room temperature. The free radical polymerization was initiate finally by the introduction of 0.04 g ammonium persulfate (APS), and 0.01 g sodium sulfite as co-initiator. The temperature of the systems was increased to 60 ^{o}C and reacted for 6 h to complete the polymer composite synthesis. After completion of the reactions, the composites were precipitated in ethanol. The precipitated materials were then retrieved by filtration and dried for 10 h under vacuum (Figure 4.1b).

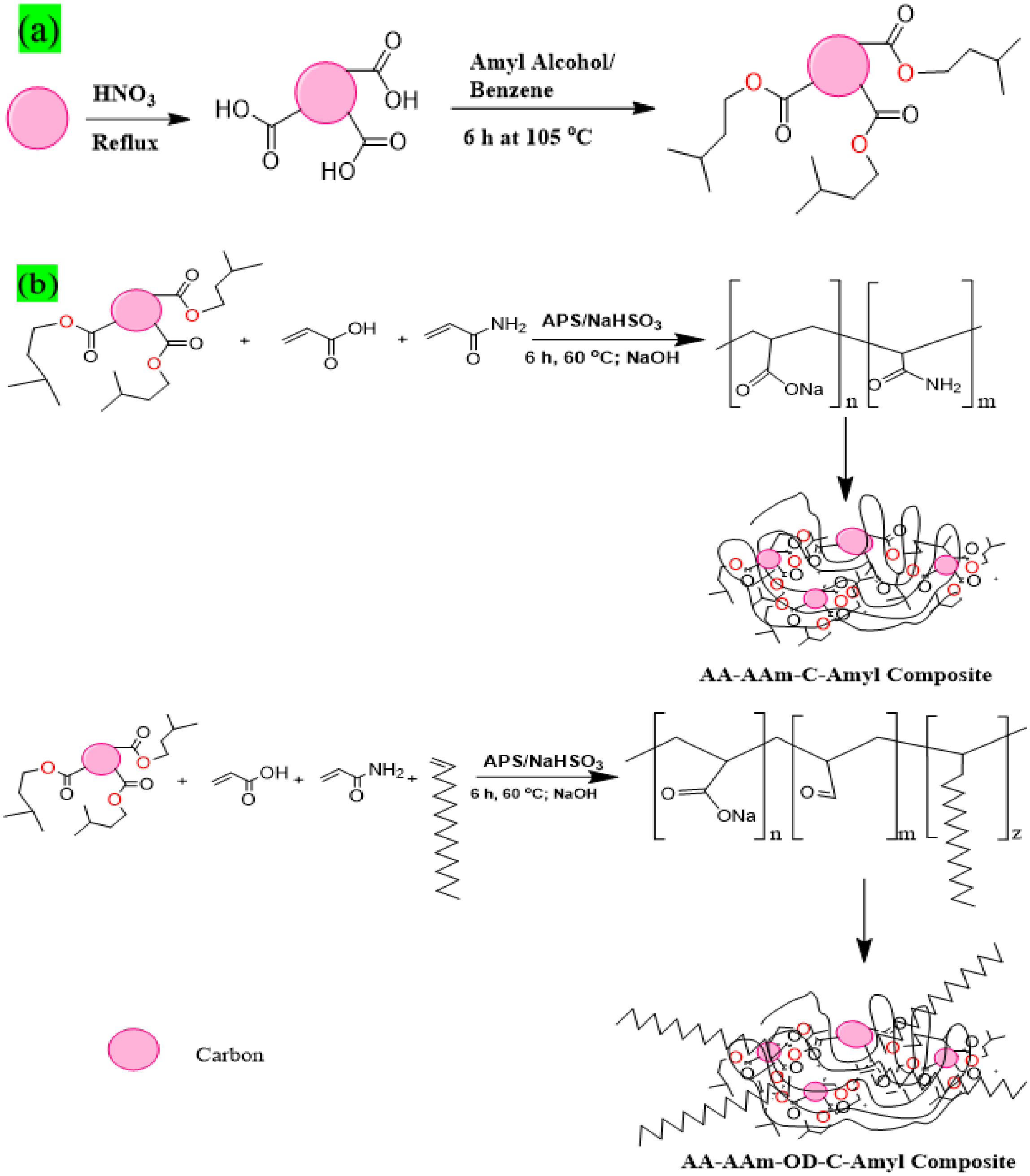

Figure 4.1: Preparation of (a) C-Amyl and (b) AA-AAm-OD-C-Amyl and AA AAm-C-Amyl composites.

4.2.4 Fourier transform infrared spectra (FTIR) and proton NMR measurements

Thermo Scientific Nicolet iS10 FTIR spectrophotometer was used to determine the IR spectrum of AA-AAm-C-Amyl, AA-AAm-OD-C-Amyl as well as the monomers and the C-Amyl. For AA-AAm-C-Amyl, AA-AAm-OD-C-Amyl and C-Amyl, potassium bromide pellets of 2.5 cm diameter containing 5 wt% of the sample was made and the IR spectrum was then carried out at room temperature. The samples were scanned between 4000−500 cm^{-1} wavenumber range with 4 cm^{-1} resolution and 16 scans. Moreover, the FTIR analysis was support with proton NMR (^{1}HNMR) to reflect the successful preparation of the products. This was achieved with 400 MHz Brucker AV III 400 spectrometer using D_2O as a solvent.

4.2.5 Scanning Electron Microscope (SEM) and Thermogravimetric Analysis (TGA)

The morphology of the shale samples before and after they got in contact with Na-Bt were observe under a Scanning electron microscope (SEM) FESEM/FIB/GIS (Tescan Lyra-3). The thermogravimetric analysis (TGA) was obtained in a TGA analyzer (TA Instruments SDT-Q600 Simultaneous TGA / DSC, USA) within 25 – 700 ^{o}C range temperature under nitrogen atmosphere.

4.3 Inhibition testing

4.3.1 Anti-swelling ratio evaluation

The anti-swelling ratio (AR) was measured. [150] This was accomplished in accordance with the China's Natural Gas Industry Standard SY/T 5971-94 for measuring clay stabilization in drilling fluids. Around 1 g of Na-Bt was dispersed in 20 ml of 2 wt% composites solution and left for 2 h. The mixture was then centrifuged at 1500 rpm until the fluid phase is clearly separated from the clay particles and the change in the bentonite volume by calculating AR based on equation 4.1.

$$AR = \frac{V_W - V_P}{V_W - V_O} \qquad \textbf{4.1}$$

where V_W and V_P are bentonite change in volume in distilled water and in the polymer solution, respectively, while V_O is it volume in kerosene.

4.3.2 Shale inhibition ability by immersion examination

The immersion study was carried out on Na-Bt in the presence of the two prepared materials. The results were compared with swelling of the Na-Bt in both water and potassium chloride (KCl) to prove the efficacy of the materials to inhibit shale. In this study, Na-Bt powder of was first dried at 105 ^{o}C for 4 h to eliminate the adsorbed moisture. This was then weighed into 10 g portions that were compressed into a pellet discs of 5 cm under 10 MPa in a hydraulic presser for 5 mins. Afterward, the pellets were then submerged into 20 ml of deionized water, 10 wt% KCl solution, and 2 wt% of the prepared inhibitors. The immersed samples were then be observed after 16 h.

4.3.3 Shale cuttings dispersion test

Shale recovery test was conducted on shale samples in the solution of each inhibitors. Briefly, crushed shale sample in the range of 6−10 mesh sizes were utilized for this test. About 50 g of this shale was added into 350 mL of each inhibitor's solution in 500 ml vessel. This was then hot-rolled in hot-roller oven for 16 h at 150 °C. Upon completion, the mixture was cooled to room temperature, filtered, washed with DI water, and dried at 105 °C for 4 h in a vacuum oven. The dried shale remains were then sieved through 40-mesh sieve. The sieve retained shale was weighed and recorded to be M_1 which was used to calculate recovery as shown in equation 4.2 [18].

$$\text{Recovery} = \frac{M_1}{50} \text{ X } 100\ \% \qquad \textbf{4.2}$$

4.4 Results and discussion

4.4.1 Synthesis of polymer- C-Amyl composite

The composites were formed through free radical polymerization as presented in Figure 4.1b. The mole ratio of the monomers in the composites are 0.5: 0.5 for AA and AAm in AA-AAm-C-Amyl, and 0.25: 0.25:0.5 for AA, AAm and OD in AA-AAm-OD-C-Amyl respectively.

The FTIR spectrum of the composites and monomers are shown in Figure 4.2 a and b. As shown in Figure 4.2a for the C-Amyl spectrum, the peak at 2921 cm^{-1} is due to C-H stretch of the amyl chain. The peak at 1721 cm^{-1} is due to ester carbonyl (C=O) stretching vibration, while the peaks at 1572 cm^{-1} and 1214 cm^{-1} are characteristic features of C-H bending and C-O-C vibrations respectively. The AAm spectrum has two peaks, 3421 cm^{-1} and an extending shoulder at 3194 cm^{-1} which can be ascribed to hydrogen vibrational stretching of N-H. It also has two peaks at 1672 cm^{-1} and 1605 cm^{-1} (shoulder band) indicating C=O vibration of amide (N-C=O) and C=C of alkene respectively. The C-H bending vibration appears at 1428 cm^{-1} and 960 cm^{-1}. Also, for AA-Na, the C-H stretching band is seen at 2920 cm^{-1} as well as the C-H bending vibration at 1407 cm^{-1}. The peak at 1703 could be attributed to C=O stretching vibration of AA will the C-O-Na band surfaces at around 1163 cm^{-1}. The spectrum of AAm in AA-AAm-C-Amyl composite shows an amine vibration peak ($-NH_2$) at within 3407 cm^{-1} which broadens to around 2950 cm^{-1} indicating C-H stretching band which is not clear. The broad peak at 1640 cm^{-1} maybe as a result of C=O stretching overlap of C-Amyl, AA and AAm while the broad peak at 747 cm^{-1} is allotted to C-H bending vibrations of all the three components of the composite which their hydrogen may be interacting with one another. With regard to AA-AAm-OD-C-Amyl (Figure 4.2b), the peak of N-H stretching come up at 3357 cm^{-1} which is overlapping with C-H stretching of methylene around 2950 cm^{-1}. The vibrational bands at 1641 cm^{-1} and 540 cm^{-1} could be related to C=O of C-Amyl, acrylic acid and acrylamide, and C-H bending of OD. In the two composites, there are no absorption peaks around 1620–1680 cm^{-1} pertaining to C=C bond. Therefore, the FTIR reflects the successful polymerization of the monomers in both composites.

The ^{1}HNMR spectral of AA-AAm-C-Amyl and AA-AAm-OD-C-Amyl composites are presented in Figure 4.3 a and b. These were checked to support the FTIR results to validate

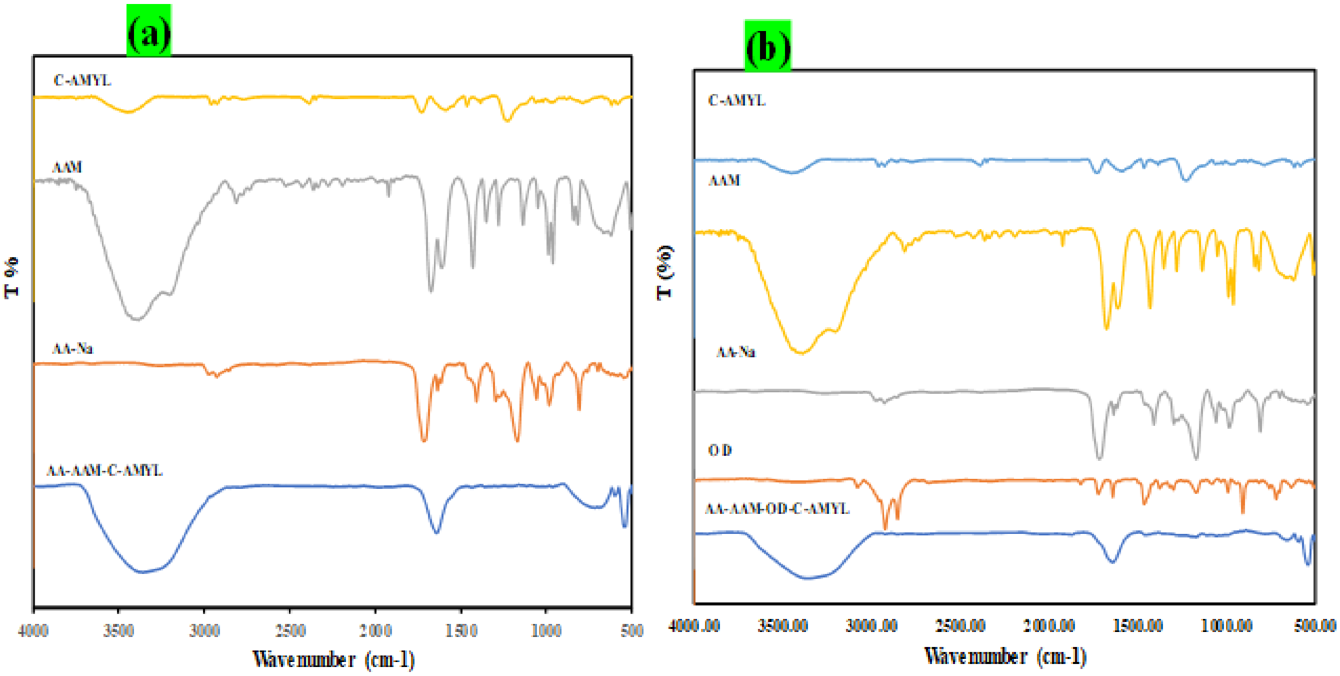

Figure 4.2: FTIR spectral of (a) AA-AAm-C-Amyl composite compared to its components, (b) AA-AAm-OD-C-Amyl composite relative to each single component that makes it.

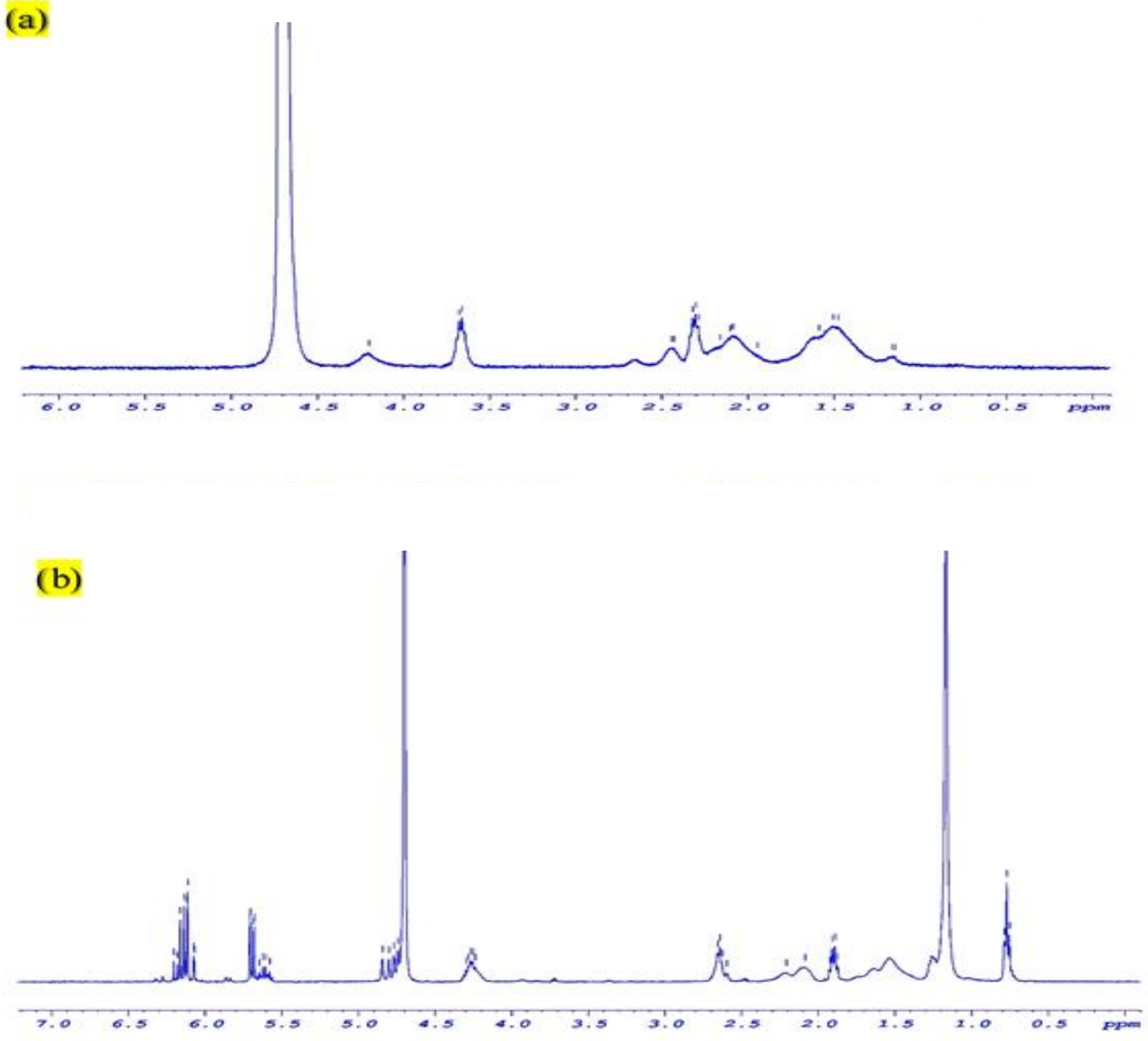

Figure 4.3: ^{1}HNMR spectral of (a) AA-AAm-C-Amyl composite (b) AA-AAm OD-C-Amyl composite

the successful preparation of the materials. As is can be observed in Figure 4.3a for the ^{1}HNMR of AA-AAm-C-Amyl, the characteristic peaks of 1.16-1.25 ppm and 1.51-1.58 are due to -CH_2- and -CH_3 protons of amyl chain. The chemical shift of 2.08 ppm is attributed to the shielded proton in -CH_2-CH-C=O-NH_2 of acrylamide while the peaks between 2.30-2.44 ppm indicate the shielded proton in -CH_2-HC-C=O-ONa of acrylic acid. The peaks at 3.66-3.67 ppm and the one at 4.201 are associated with deshielded protons in -CH_2-HC-C=O-ONa and -CH_2-CH-C=O-NH_2. The intense peak at around 4.68 ppm shows the deshielded peak of the C-Amyl ester proton. For AA-AAm-OD-C-Amyl (Figure 4.3b) however, the highly shielded peaks at around 0.75 ppm, 1.164 ppm and 1.87 ppm are features of OD. The shielded peak of -CH_2-CH-C=O-NH_2 and -CH_2-HC-C=O-ONa appear at 2.21 ppm and 2.63 ppm respectively. The peak at 4.84 ppm maybe connected to D_2O molecule. The chemical shifts showing at 4.24 ppm, 5.58 ppm and 6.07 ppm correspond to the deshielded protons of -CH_2-CH-C=O-NH_2, -CH_2-HC-C=O-ONa and C-amyl ester. The proton peaks of -NH_2 are missing in both spectral as a result of substitution with D_2O.

4.4.2 The TGA results

The high-temperature tolerance of shale inhibitor is key to their excellent performance to minimize shale hydration during drilling processes as a result of high temperatures usually experience in wellbore. [169] The thermogravimetric analysis showing the degradation of AA-AAm-C-Amyl and AA-AAm-OD-C-Amyl as the temperature rises are displayed in Figure 4.4a and b. The material shows excellent thermal stability. In AA-AAm-C-Amyl of Figure 4.4a, about 20 % weight loss was experienced as the temperature rises to 250 ^oC from room temperature. The decrease in the quantity of the material at this stage could be ascribed to the vaporization of structural water molecules. [150] A further decreasing gradually in the percentage of the remaining material accounting for about 40% reduction up to a temperature of 480 ^{o}C. The polymer component started undergoing degradation at this stage. The last part of the graph showing the further decomposition of the composite above 480 ^{o}C to around 620 ^{o}C upon which there is no discern weight diminish of the material until 700 ^{o}C is reached. This is a step of the degradation history when the material undergoes carbonation to form a carbon residue. Approximately 25 % residue was still present indicating that the AA-AAm copolymer contributed to the mass of the activated carbon center of the C-Amyl.

In contrast, in the TGA graphical representation of AA-AAm-OD-C-Amyl (Figure 4.4b), a steady declination of the material's weight was observed between room temperature and 220 ^{o}C. This may also be response of moisture evaporation from the material with almost 30% loss in weight. Above this temperature to about 380 ^{o}C, drastically weight loss is clearly shown as a result of rapid depolymerization and decomposition responsible for above around 30% reduction in the material content. The depolymerize remnants went through carbonization above this temperature until it reaches 520 ^{o}C with almost 30% declination over which there is no further obvious weight retardation. The leftover at the end of the analysis is 10% pointing that vaporization of molecules of some of the polymer molecule occurred which is smaller than that of AA-AAm-C-Amyl. This could be as a result of OD fragmentation at high temperature into small molecular weight volatile organic compound that can easily liberated.

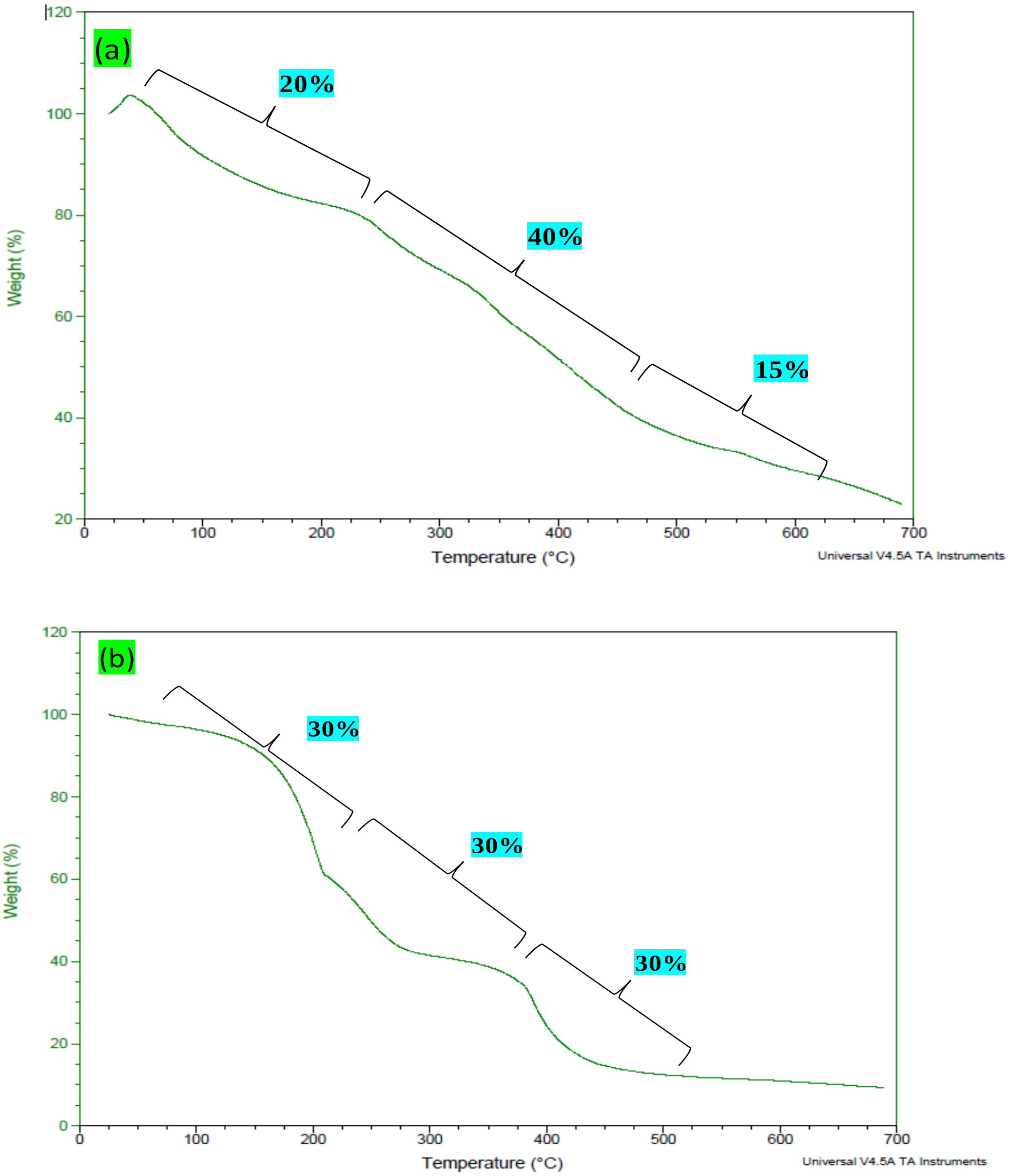

Figure 4.4: Thermal stability analysis of (a) AA-AAm-C-Amyl and (b) AA-AAm OD-C-Amyl

4.5 Inhibition experiments

4.5.1 Anti-swelling characteristics of AA-AAm-C-Amyl and AA-AAm-OD-C-Amyl

The anti-selling ability of 2 wt% AA-AAm-C-Amyl and AA-AAm-OD-C-Amyl were evaluated and compared with that of 10 wt% KCl which is the most commonly used shale inhibitor in oil and gas industries for drilling shale formations. The result of the anti-swelling are shown in Figure 4.5a. It is clear that Na-Bt is made-up of 80% or more montmorillonite of which makes it to react and swells rapidly when it interacts with water. The swelling of Na-Bt was greatly reduced in the presence of 2 wt% of both AA-AAm-C-Amyl and AA-AAm-OD-C-Amyl. The best result was recorded in AA-AAm-C-Amyl corresponding to about 95.2% anti-swelling ratio. This was followed by AA-AAm-OD-C-Amyl showing anti-swelling ability of 93.7% and the 10 wt% of KCl gave the list value of 55.4%. Thus, C-g-AA-NH_2 could effectively minimize shale hydration because it demonstrated an outstanding inhibitive trait towards Na-Bt clay which have similar properties of smectite component of shale formations.

4.5.2 Shale recovery experiment

The shale recovery examination was carried out in the 2 wt% of the composite’s solution. This is vital to doublecheck their efficiency to prevent untimely hydration and dispersion of shale cuttings during drilling operations. The results of the recovery test are shown in Figure 4.5b.

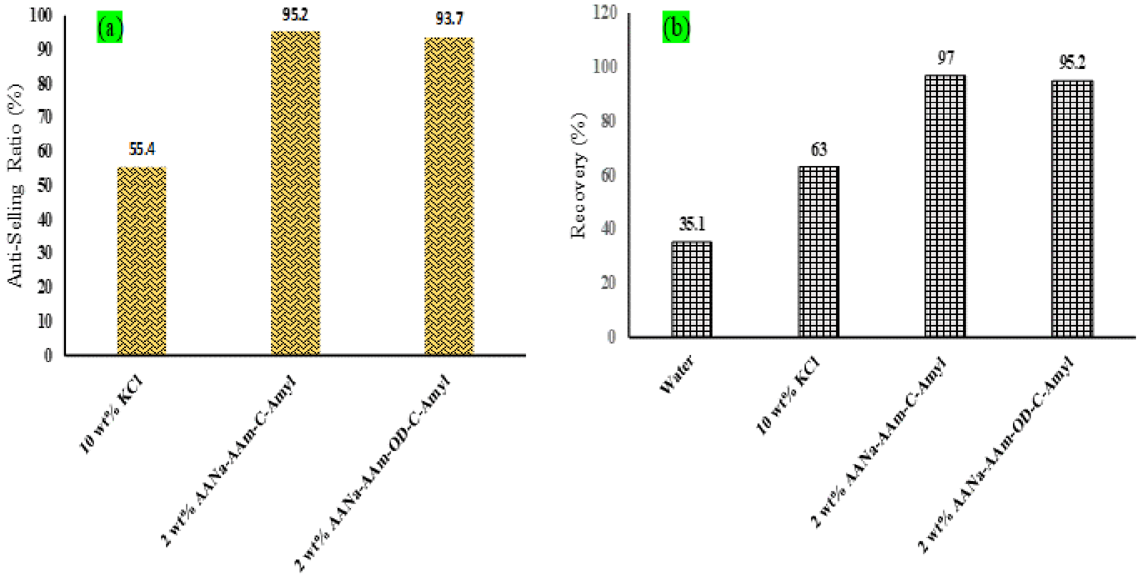

Figure 4.5: (a) Anti-swelling ratio and (b) Shale recovery test result of AA AAm-C-Amyl and AA-AAm-OD-C-Amyl composites

The percentage recovery noted for the shale in the aqueous solution of the prepared materials were compared with that of KCl and pure water. The value of obtained in pure water was 35.1% demonstrating significant hydration and dispersion of shale in water. The 10 wt% KCl gave 63.0 % but the 2 wt% AA-AAm-C-Amyl and AA-AAm-OD-C-Amyl show higher values of 97.0 % and 95.2% respectively. This result indicates that AA-AAm-C-Amyl and AA-AAm-OD-C-Amyl could greatly hinder shale hydration and dispersion during drilling even when used in the real fluid formulations. This further correlates the outcomes of the anti-swelling measurement that could enhance the stability of wellbore.

4.5.3 Immersion test

Immersion test has been a reliable method for decades usually use in the oil and gas industry to explore the inhibition strength of shale inhibitors using Na-Bt. The state of Na-Bt pellet was observed in water, 10 wt% KCl and the 2 wt% solution of the synthesized components. The status of Na-Bt at few minutes after insertion into and after 24 h of introduction in the media were observed. The Na-Bt in deionized water suffered more hasty swelling than KCl and composites solution due to the extreme infiltration of water molecules. However, in 10 wt% KCl, Na-Bt dispersed with little swelling due to substitution of sodium ions with potassium ions that help in the aggregation of the clay particles together. In contrast, the Na-Bt pellets in AA-AAm-C-Amyl and AA-AAm-OD-C-Amyl did not experience an obvious collapse in their shape reflecting the essence of the prepared materials to strongly tackle the problem of shale hydration.

4.5.4 Mechanism of composites inhibition

It is important to discuss the mechanism of inhibition of AA-AAm-C-Amyl and AA-AAm-OD-C-Amyl composites to prove their capability to address shale clay hydration. The surface of the Na-Bt pellets after the immersion tests were investigated with SEM. Figure 4.6 represents the SEM image of the plain Na-Bt surface and when exposed to the composite's solution. The plain Na-Bt has a rough surface and pores as shown in Figure 4.6a. The coarse and pores surface of the Na-Bt were plugged by forming a thin film relating to adsorption of C-Amyl/polymer composite upon exposure to 2 wt% of AA-AAm-C-Amyl and AA-AAm-OD-C-Amyl solution (Figure 4.6 b and c)

Since activated carbon (AC) generally have a high surface area, it could firmly adsorb polymer matrix with on its surface. In addition, with the presence of amyl ester on the surface of AC, the amyl chain could interact with the polymer backbone to form a more hydrophobic shell on the modified parts of AC. [127] The high surface energy and surface area of the exposed AC part could facilitate it adhesion to clay surface to plug the micropores. [199] On the other hand, the myl tail tends to form a hydrophobic film with the polymer chain in both AA-AAm-C-Amyl and AA-AAm-OD-C-Amyl which repels the approach of water molecules toward the shale surface. One should assume that the AA-AAm-OD-C-Amyl should give the best result due the presence of the long chain of hydrophobic OD, however, the two-polymer component makes similar contribution of forming a thin film covering AC and shale. The better result of AA-AAm-C-Amyl in the immersion and the shale recovery test maybe relied to hydrogen bond formation potential higher due to more acrylic acid and acrylamide groups than that of AA-AAm-OD-C-Amyl. To this end, AA-AAm-C-Amyl and AA-AAm-OD-C-Amyl have the tendency to be used as active shale inhibitors in drilling and minimizing the capillary effect in water-based mud. This further justifying the potency of AC as an excellent plugging agent for shale micropores and cracks.

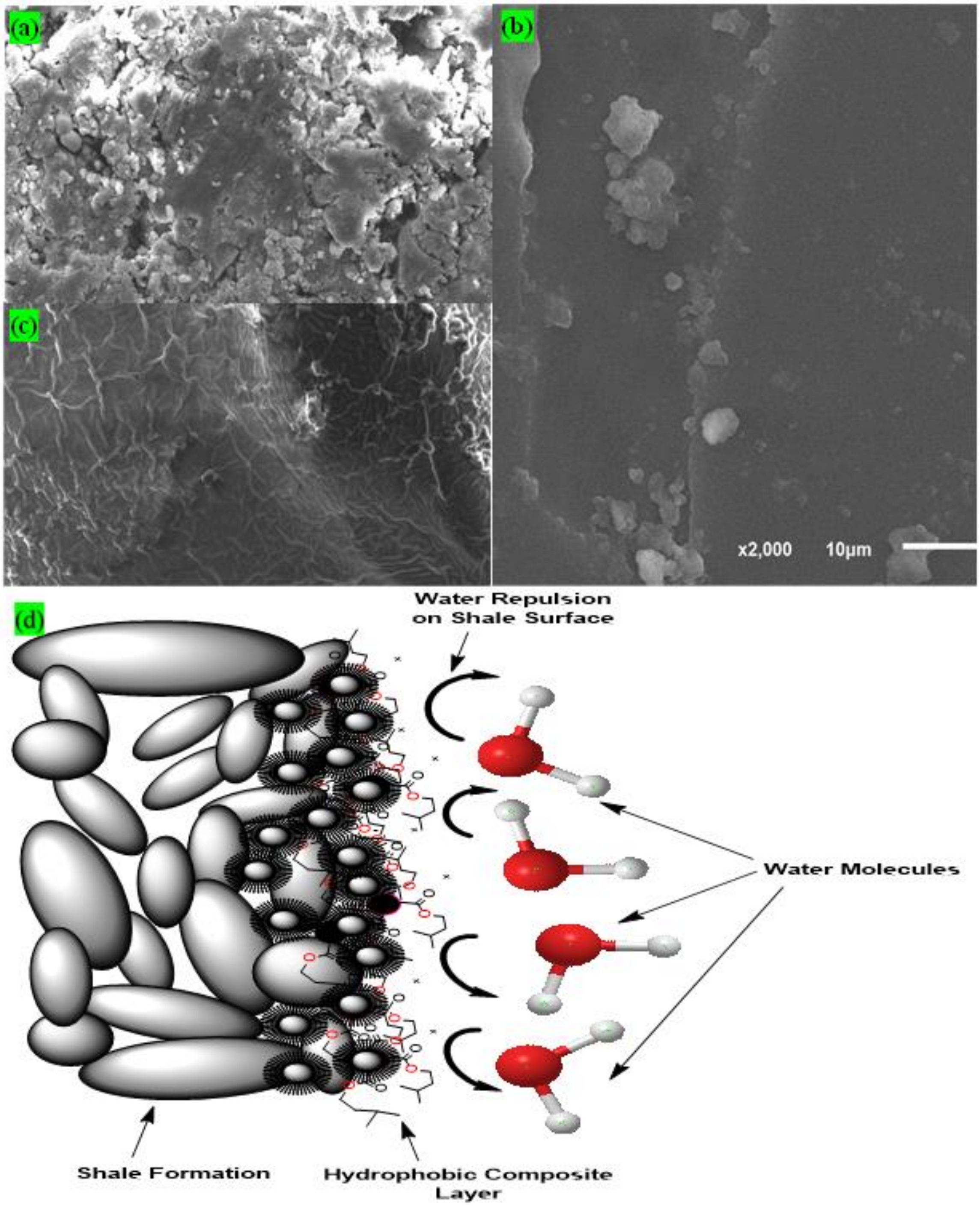

Figure 4.6: The SEM image of (a) plain Na-Bt, and Na-Bt immersed in (b) 2 wt% AA-AAm-C-Amyl and (c) AA-AAm-OD-C-Amyl after 24 h.

5. CHAPTER 5

EFFICIENT SHALE INHIBITION WITH ACTIVATED CARBON DENDRIMER/POLYVINYLPYRROLIDONE COMPOSITE

5.1 Introduction

The rising the demand for oil and gas led to the search for other sources including shale gas exploration and exploitation. [160], [200] In order to reach and tap the oil and gas deposit in any geological housing the reserve, drilling of a suitable well is required. Drilling fluids of different solvent (oil or water) based is necessary for the drilling to lubricate and clean the drilling bit, transport drilling cutting from downhole to the surface, maintain pressure or prevent pressure loss in the borehole, prevent fluid loss into shale formation and ultimately address the problem of shale swelling. [3–5] Though oil-based muds (OBMs) and synthetic-based muds (SBMs) have exceptional performance such as great lubricity, high temperature tolerance and excellent rheological properties compared to the water-based muds (WBMs). [32], [166] Nevertheless, OBMs are threatening to the environment which has limited their application in drilling process except in case where their use is unavoidable particularly in deep sea sensitive shale drilling. [52], [201] WBMs had been great substitute for OBMs because of their economical and eco-friendliness advantage. Sequence of problems are being faced by formation being drilled by WBMs as a result of water interaction. These include high drag with torque, bit balling, cuttings dispersion, caving, sloughing, stuck pile, wellbore collapse, reduced drilling rate and circulation loss. [13], [77], [202] The overall outcome is the excessive costs of oil well drilling operations. [30]

Amine based polymer and oligomers such as dendrimers, hydrocarbon diamines, lipophilic amine polymers, amino acids, polyamines, polyethoxylated amines among others have been utilized as effective shale inhibition. The activeness of these molecules is conversely affected by pH variation. They tend to undergo deprotonation as the pH increases which is a major property of amine-terminated compounds. Since the conventional mud formulation pH in oil and gas drilling is usually around 8.4, the activities of amine-based clay minerals inhibitors inevitable hindered.

Activated carbon (AC) is a nanocarbon with a large surface area and porosity. [174] Functionalization of AC surface has also been proofed to enhance its application [176]. Aside from being inexpensive, it is highly abundance and could be generated from wide range of sources including wastes [177], [181], [183] and polymers[186], [199]. Its application ranges from adsorption to catalysis. [191], [194] When modified dendrimer, AC activity gets improved having high hydrodynamic volume in solution which improves its interaction with various functional groups through hydrogen bond formation. [203–205] Polyvinylpyrrolidone (PVP) is an amphiphilic biocompatible water-soluble polymer which is widely use in various industrial applications such as cosmetics and even in drug delivery and as food additives. [206], [207] The cyclic hydrophilic amide ring and the hydrophobic methylene/methine polymer backbone provides it with the amphiphilic property. [208] Incorporation of PVP in dendrimer have been found to been useful in drug delivery. [209] In this work we prepared a dendrimer functionalized AC denoted as AC-D and PVP composite to explore its shale inhibition power. The matrix performed brilliantly in retarding water interaction with shale minerals. This could be linked to the relatively high hydrogen bond density that could be formed between the dendrimer, the PVP and the clay surface to form a preventive film towards water; the plugging potential of AC and the hydrophobic character of the PVP polymer chain.

5.2 Materials and method

5.2.1 Materials

The AC was prepared from waste tyre via a method in our previous work. Ethylenediamine, ethanol and methyl methacrylate were purchased from Fluka Chemical, Swithzerland. Vinylpyrolidone, Azobisisobutyronitrile (AIBN) and methanol were supply by Sigma Aldrich, USA. Nitric acid was provided by BDH Chemical, UK. All chemicals were used as received.

5.2.2 Synthesis of the AC-D

The surface functionalization of the AC with second generation dendrimer was accomplished in line with the standard method with slight modification. [210], [211] This is a divergent poly(amidoamine) (PAMAM) synthesis method involving two-step. The first step involves the generation of ester terminals (AC-COOH) on the AC surface (Figure 5.1) while the second result to the conversion of the ester surface to dendrimer generations (Figure 5.2). Typically, 500 mg of AC-COOH was put in a round bottom flask containing 150 ml methanol and sonicated for 15 min for adequate dispersion of the material. The flask was then transferred to an oil bath, equipped with a nitrogen atmosphere and stirred with a magnetic stirrer. EDA (5 g) was added to the AC suspension gradually over a period of 30 min and stirred for 24 h. The resulting product was then filtered, dried and re-dispersed in methanol. Methyl methacrylate of 37 g was gradually added to the mixture, stirred at 0 °C for 30 min and allow to go back to room temperature upon which it was further stirred for 24 h. The final product was retrieved, washed with ethanol and dried at 40 °C for 12 h. The PAMAM stages were repeated until dendrimer generation was gotten.

5.2.3 The AC-D/polyvinylpyrrolidone composite

This was carryout by free radical polymerization. [212] The AC-D (25 mg) was dispersed in 100 ml ethanol and subjected to rigorous stirring in three-necked flask incorporated in an oil bath. This was followed by the addition of 10 g of PVP and purged by nitrogen for 15 min to eliminate dissolved oxygen. The reaction was initiated by adding 1.5 g AIBN dissolved in 5 ml ethanol and allowed to run at 60 ^{o}C for 15 h. The product obtained was precipitated in cold ethyl acetate under stirring. The precipitated was recovered and dried for 24 h at 60 ^{o}C.

5.2.4 Fourier transform infrared spectra (FTIR) and proton NMR measurements

Thermo Scientific Nicolet iS10 FTIR spectrophotometer was used to determine the IR spectrum of AC-D and AC-D/PVP composite. The potassium bromide pellets of 2.5 cm diameter containing 5 wt% of the sample was made and the IR spectrum was then carried out at room temperature. The samples were scanned between 4000−500 cm^{-1} wavenumber range with 4 cm^{-1} resolution and 16 scans. Moreover, the FTIR analysis was support with proton NMR (^{1}HNMR) to reflect the successful preparation of the products. This was achieved with 400 MHz Brucker AV III 400 spectrometer using D_2O as a solvent.

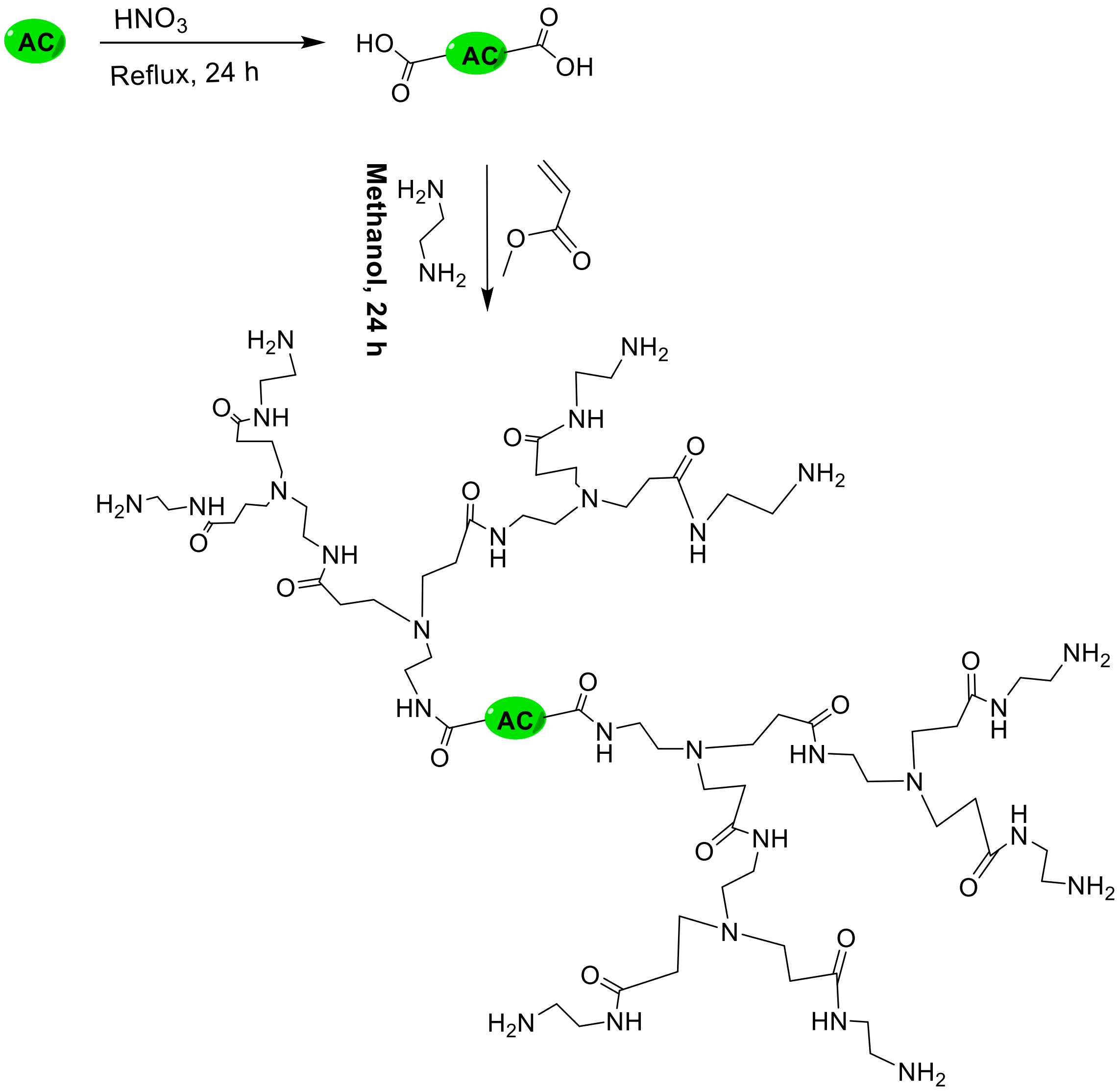

Figure 5.1: Synthesis of the AC-D

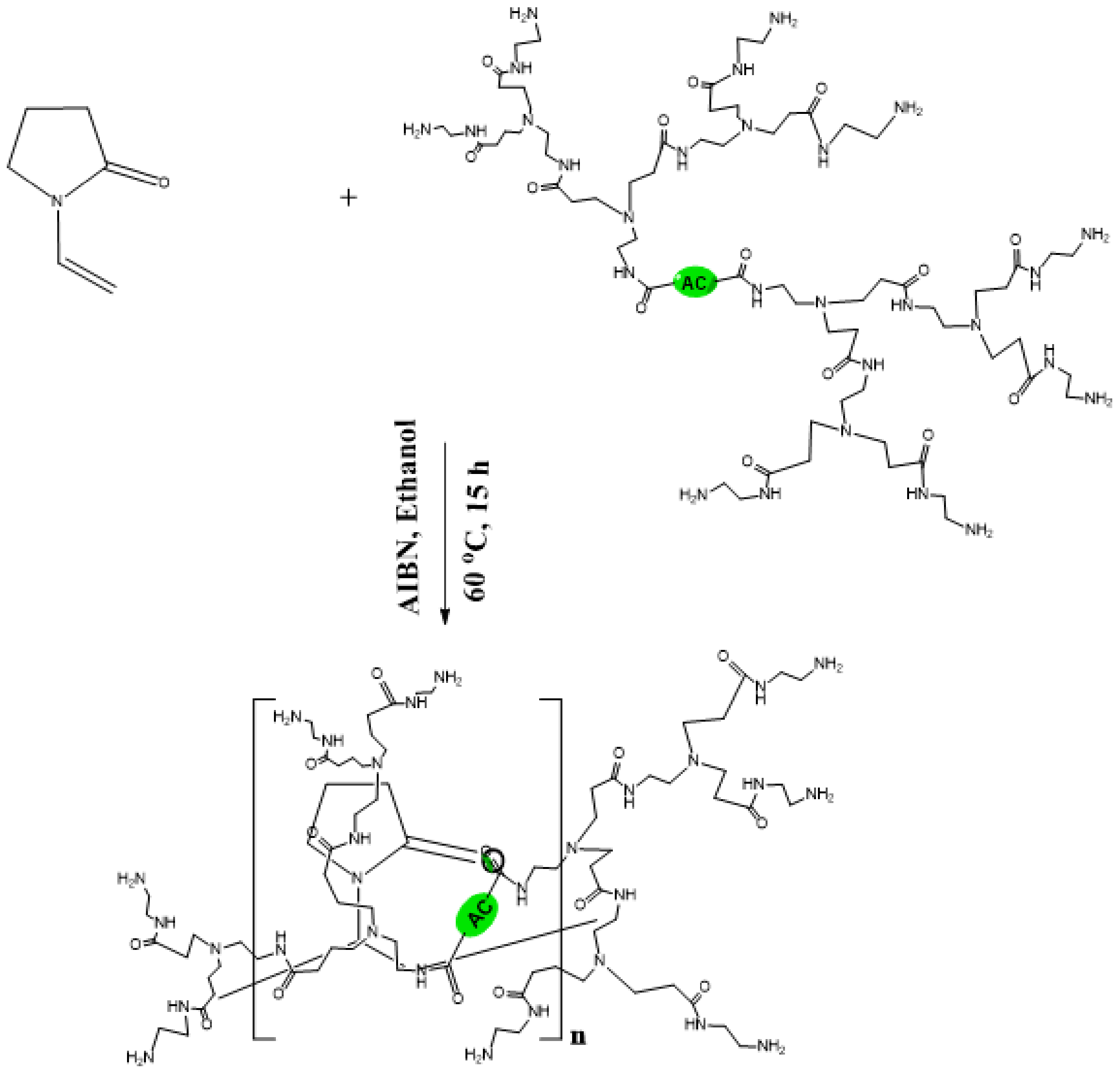

Figure 5.2: AC-D/polyvinylpyrrolidone composite

5.2.5 Scanning Electron Microscope (SEM) and Thermogravimetric Analysis (TGA)

The morphology of the shale samples before and after they got in contact with Na-Bt were observe under Scanning electron microscope (SEM) FESEM/FIB/GIS (Tescan Lyra-3). The thermogravimetric analysis (TGA) was obtained in a TGA analyzer (TA Instruments SDT-Q600 Simultaneous TGA / DSC, USA) within 25 – 700 ^{o}C range temperature under nitrogen atmosphere.

5.3 Inhibition testing

5.3.1 Anti-swelling ratio evaluation

The anti-swelling ratio (AR) was measured. [150] This was carried out in accordance with the China's Natural Gas Industry Standard SY/T 5971-94 for measuring clay stabilization in drilling fluids. Around 1 g of Na-Bt was dispersed in 20 ml of the composite solution and left for 2 h. The mixture was then centrifuged at 1500 rpm until the fluid phase is clearly separated from the clay particles, and the change in the bentonite volume by calculating AR based on equation 5.1.

$$AR = \frac{V_W - V_P}{V_W - V_O} \qquad \textbf{5.1}$$

where V_W and V_P are bentonite change in volume in distilled water and in the polymer solution, respectively, while V_O is it volume in kerosene.

5.3.2 Shale inhibition ability by immersion examination

The immersion study was carried out on Na-Bt in the presence of the two prepared materials. The results were compared with swelling of the Na-Bt in both water and potassium chloride (KCl) to prove the efficacy of the materials to inhibit shale. In this study, Na-Bt powder of was first dried at 105 ^{o}C for 4 h to eliminate the adsorbed moisture. This was then weighed into 10 g portions that were compressed into a pellet discs of 5 cm under 10 MPa in a hydraulic presser for 5 mins. Afterward, the pellets were then submerged into 20 ml of deionized water, 10 wt% KCl solution, and 2 wt% of the prepared inhibitors. The immersed samples were then be observed after 16 h.

5.3.3 Shale cuttings dispersion test

Shale recovery test was conducted on shale samples in the solution of each inhibitor. Briefly, crushed shale sample in the range of 6−10 mesh sizes were utilized for this test. About 50 g of this shale was added into 350 mL of 2 wt% solution of inhibitor in 500 ml vessel. This was then hot-rolled in hot-roller oven for 16 h at 150 °C. Upon completion, the mixture was cooled to room temperature, filtered, washed with DI water, and dried at 105 °C for 4 h in a vacuum oven. The dried shale remains were then sieved through 40-mesh sieve. The sieve retained shale was weighed and recorded to be M_1 which was used to calculate recovery as shown in equation 5.2 [51].

$$\text{Recovery} = \frac{M_1}{50} \text{ X } 100\ \% \qquad \mathbf{5.2}$$

5.4 Results and discussion

5.4.1 The AC-D/polyvinylpyrrolidone composite

The composite activated carbon-dendrimer/polyvinylpyrrolidone (AC-D/PVP) was achieved via free radical polymerization. The successful preparation of the material was explored with FTIR.

The FTIR spectrum of the composites and the AC-D are shown in Figure 5.3. The absorption peaks suggest the characteristic of the bond present in the structure of the two entities. It is clear that peaks in both AC-D and AC-D/PVP at around 3426 cm^{-1} is associated to N-H stretching. The broad nature of AC-D/PVP around this region may be due to residual water molecule O-H vibration stretching mode. For AC-D/PVP, the peak at 1633 cm^{-1} is due to C=O stretch of the pyrrolidone group. The peak at around 1465 cm^{-1} is as a result of CH_2 bending of the polymer chain backbone while the one at 1289 cm^{-1} is may be ascribed to C-N stretching vibration. Pertaining to AC-D, the peak at 2920 cm^{-1} is a characteristic feature of C-H stretching. The C=O stretching appeared at 1720 cm^{-1} and the peaks at 1008 cm^{-1} and 1196 cm^{-1} are properties of C-N stretching vibration of the dendrimer. The FTIR spectral reveal the production of the intended composite composites.

Figure 5.4 shows the ^{1}HNMR spectrum of the composites. This study was undertaken to further complement the result of the IR spectrum generated. The single peak at 4.65 ppm indicates the presence of water which might be from the solvent or residual water molecule in the material. A chemical shift of 3.5 ppm is the peak of H on the polymer backbone

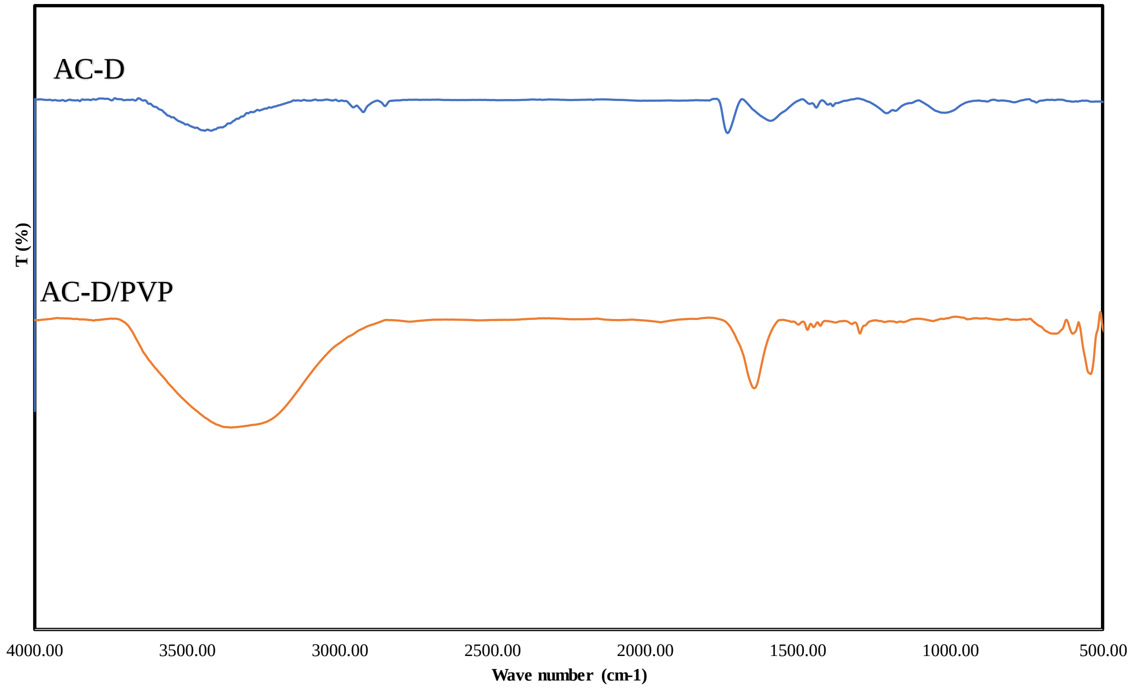

Figure 5.3: The FTIR spectral of AC-D against AD-C/PVP composite.

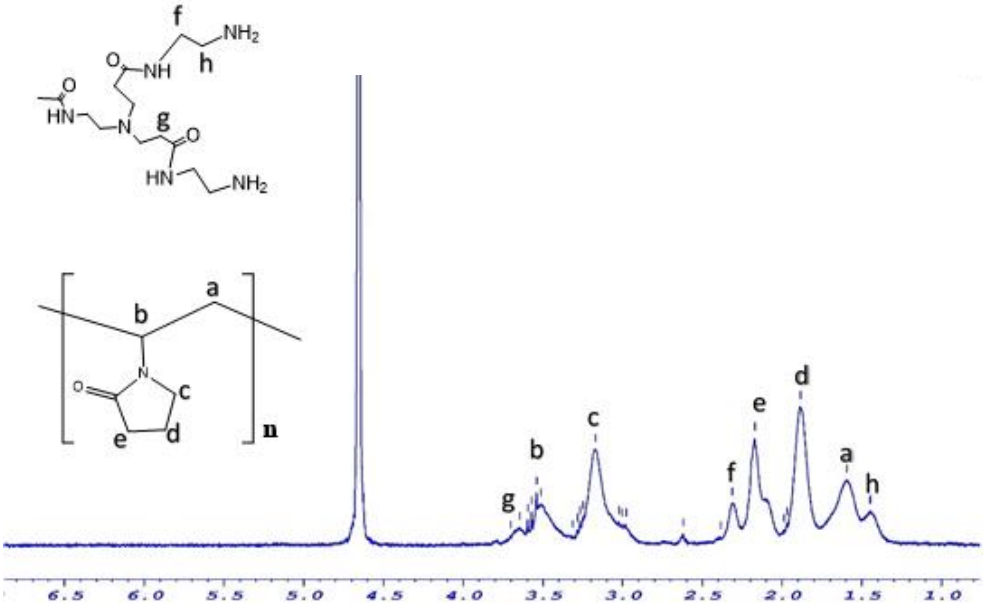

Figure 5.4: ^{1}HNMR spectral of the AC-D/PVP composite

carbon atom close to the pyrrolidine nitrogen. The proton on the polymer backbone second carbon atom which is quite shielded shows at 1.5 – 1.6 ppm. This peak may also be ascribed to the second carbon to the N atom in the pyrrolidine group. The peak around 3.2 – 3.4 ppm belongs to the proton on the pyrrolidine carbon next to the nitrogen atom. The peak within 1.8 – 2.0 ppm is for the proton on the pyrrolidine carbon next to C=O group. The protons on the two C atoms (N-C-C-N) of the ethylenediamine group in the dendrimer overlap with that of the proton on the carbon next to the nitrogen atom of pyrrolidine at 3.2 ppm. The protons on the two carbons of methacrylate group of the dendrimer appear at 2.6 ppm. The result of the ^{1}HNMR further complements the success of the composite formation as observed in the FTIR spectra.

5.4.2 The TGA results

The ability of shale inhibitors not suffering significant degradation during drilling operation is key to their design. [45], [213], [214] Based on this important target, the prepared AC-D/PVP was examined for its thermal stability. As presented in Figure 5.5, the material reflects great thermal property. It undergoes a gradual loss of weight as the temperature increases. The steep falling from the room temperature to around 150 ^{o}C which further continues with a slight reduction in weight accounts for 15.23% loss is due to the liberation of the residual moisture in the material. [173] The slit diminishing nature of the curve at around 200 ^{o}C could be attributed to further shrinking of the composite due to additional loss of intercalated vapor. The major degradation of the pyrrolidone component of the materials occurs at 450 ^{o}C with a sharp fall of the thermal analysis graph involving depolymerization and breakdown of the polyvinylpyrrolidone and the dendrimer content of the composite. This led to the loss of about 81.56% quantity of the substance under

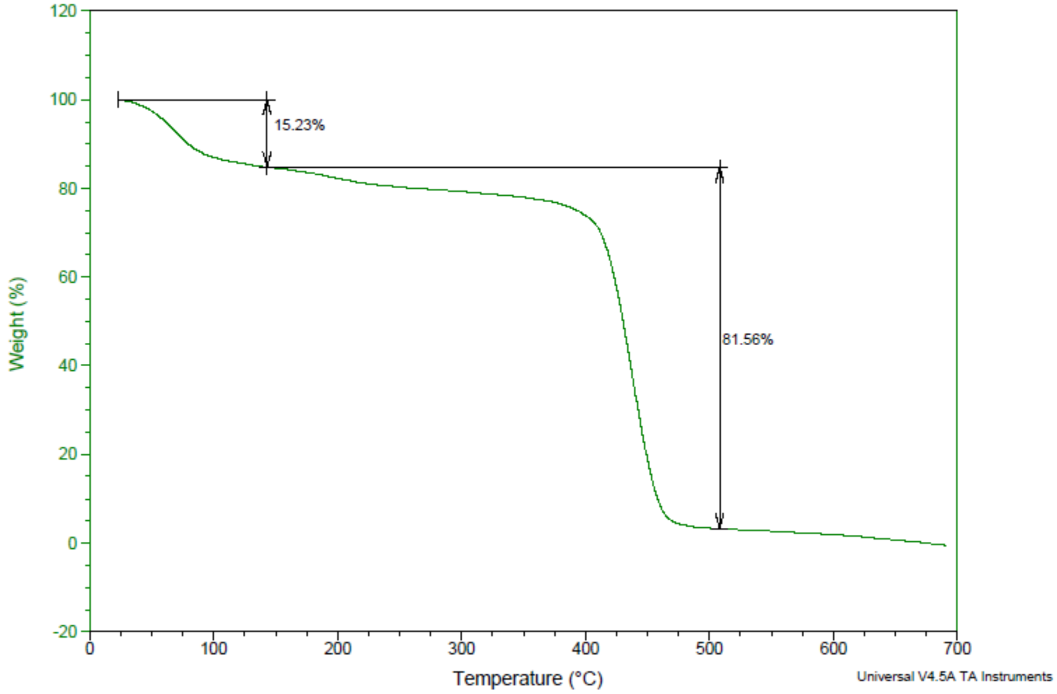

Figure 5.5: Thermal stability analysis of AC-D/PVP.

study up to 525 ^{o}C upon which the weight of material remains constant associating with the carbon residue of the AC.

5.5 Inhibition experiments

5.5.1 Anti-swelling ability of AC-D/PVP

The anti-selling capacity of 2 wt% AC-D/PVP was examined and its activity was compared to 10 wt% of potassium chloride (KCl) and water. Potassium chloride has been the conventional inhibitor with distinguish performance commonly use in drilling industry for oil and gas well. [215], [216] Figure 5.6a shows the percentage anti-swelling strength of solution AC-D/PVP and KCl on sodium bentonite (Na-Bt). The response of Na-Bt in the solutions was compared to its behavior in water. The value recorded for pure water is around 33.7%. Shales are known to suffer swelling due to their affinity for water in water-based drilling fluids based on the montmorillonite composition. [1], [14], [49], [217] Montmorillonite is the major content of Na-Bt accounting for about 80% of its weight. This makes Na-Bt undergoes rapid swelling and dispersion when it got in contact with water. The 10 wt% KCl solution gave 55.4% anti-swelling ratio while the 2 wt% solution of the AC-D/PVP with approximately 90.1% displayed a greater inhibiting characteristic. Therefore, the incorporation of 2 wt% of AC-D/PVP and even lesser concentration when incorporated in water-based drilling mud could effectively address the problem of shale hydration and borehole instability. This is because shale has far less montmorillonite content than Na-Bt. This tested concentration of the composite could be used efficiently for drilling a highly sensitive shale.

5.5.2 Shale recovery

Shale dispersion test is critical in assessing the proficiency of inhibitors to hinder shale swelling and dissipation when in contact with water component of water-based fluid. [218] Shale cuttings suffered significant fluffing in ordinary water compared to the solutions of 10 wt% KCl and the 2 wt% AC-D/PVP (Figure 5.6b). About 35.1% of the cuttings were recovered at the end of the evaluation in water due to the sensitivity of shale to water. The highest recovery was recorded in the solution of the 2 wt% AC-D/PVP amounting to 92.2% which is a great achievement comparing to previous studies of some other materials graphene, polymeric and nonpolymeric shale inhibiting materials. [51], [116], [120], [138], [142] The 10 wt% KCl solution exhibited an intermediate recovery value of around 63%. The notable high shale recovery of cuttings in the 2 wt% solution of AC-D/PVP indicates that it will not only minimize water invasion into shale formation but ultimately preserves its integrity from dispersion in the fluid formulation.

5.5.3 Immersion test

The physical observation showing the response of Na-Bt to inhibitor solution as well as water and KCl was undertaken via the immersion study. It is one of the important techniques designed to explore potential inhibitor in drilling activity. [72], [121] The image of the of the Na-Bt pellet appearance immediately it was immersed in KCl and AC-D/PVP solution as well as after 24 h. The pellet undergone substantial swelling and dispersion within 24 h which demonstrates the rapid reaction of water with the bentonite montmorillonite. The bentonite pellet did not experience swelling

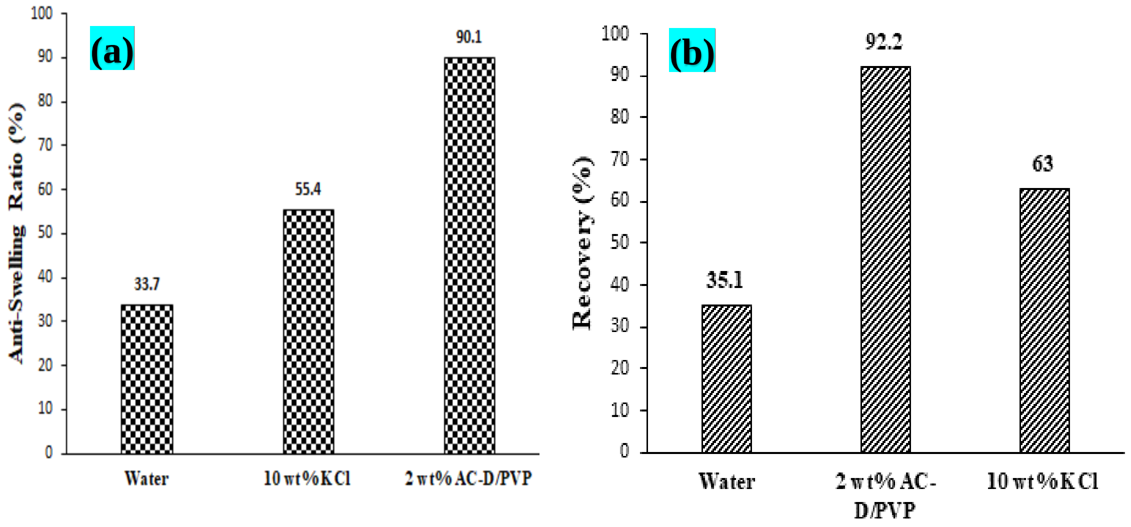

Figure 5.6: (a) Anti-swelling ratio and (b) Shale recovery test result in water, 2 wt% ACD/PVP and 10 wt% KCl.

but dispersed into the solution due to the replacement of the sodium ions (Na^+) in the Na-Bt with the potassium ion (K^+) in the solution which helps in bring the clay silica sheets together. The pellet shape is still intact after 24 h in the solution of 2 wt% AC-D/PVP. Instead of swelling and/or dispersion as observed in water and KCl solution, it felt facial contraction leading to the compact of the pellet structure.

5.5.4 The AC-D/PVP mechanism of action

In order to explain the mechanism of action of AC-D/PVP, the SEM imaging of the Na-Bt exposed to the material solution was carried out. The SEM image of the Na-Bt pellet and the pellet in contact with the AC-D/PVP solution are depicted in Figure 5.7a and b. The surface of untreated pellet looks rough with a lot of openings due to the clay silica discs comparted to form the pellet (Figure 5.7a). Upon the interaction of the AC-D/PVP with the clay surface, a contraction in the clay structure as well as formation of polymer film on the surface of the Na-Bt was observed (Figure 5.7b). The small size and the surface energy of activated carbon (AC) particles entity of AC-D/PVP make it capable to plug small interstitial spacing in the clay and it could assist in holding the PVP polymer firmly on the clay surface. [199] The dendrimer group on the AC may be responsible for the contraction of the clay structure due to its ability to form hydrogen bonding with clay particle when they are in contact via the amide hydrogen and nitrogen atoms. [74], [219], [220] The dendrimer could also form hydrogen bond with the oxygen and nitrogen atoms on the pyrrolidine group of the polymer which could lead to the intensify of the shrinking of the clay and adherence of the polymer film to its surface. The slight hydrophobic nature of the pyrrolidone rings of the polymer and the hydrodynamic volume of the polymer itself and the dendrimer could result to a large volume of hydrogen bond which also enhance the inhibition of clay swelling as well. [45], [207], [221]. The prepared AC-D/PVP has the viability to find applicable in the real usage as a shale inhibitor in water-based drilling fluid due to its vigor to form an intense hydrogen bonding, formation of protective film and physical plugging of the clay pore throat as shown in Figure 5.7c.

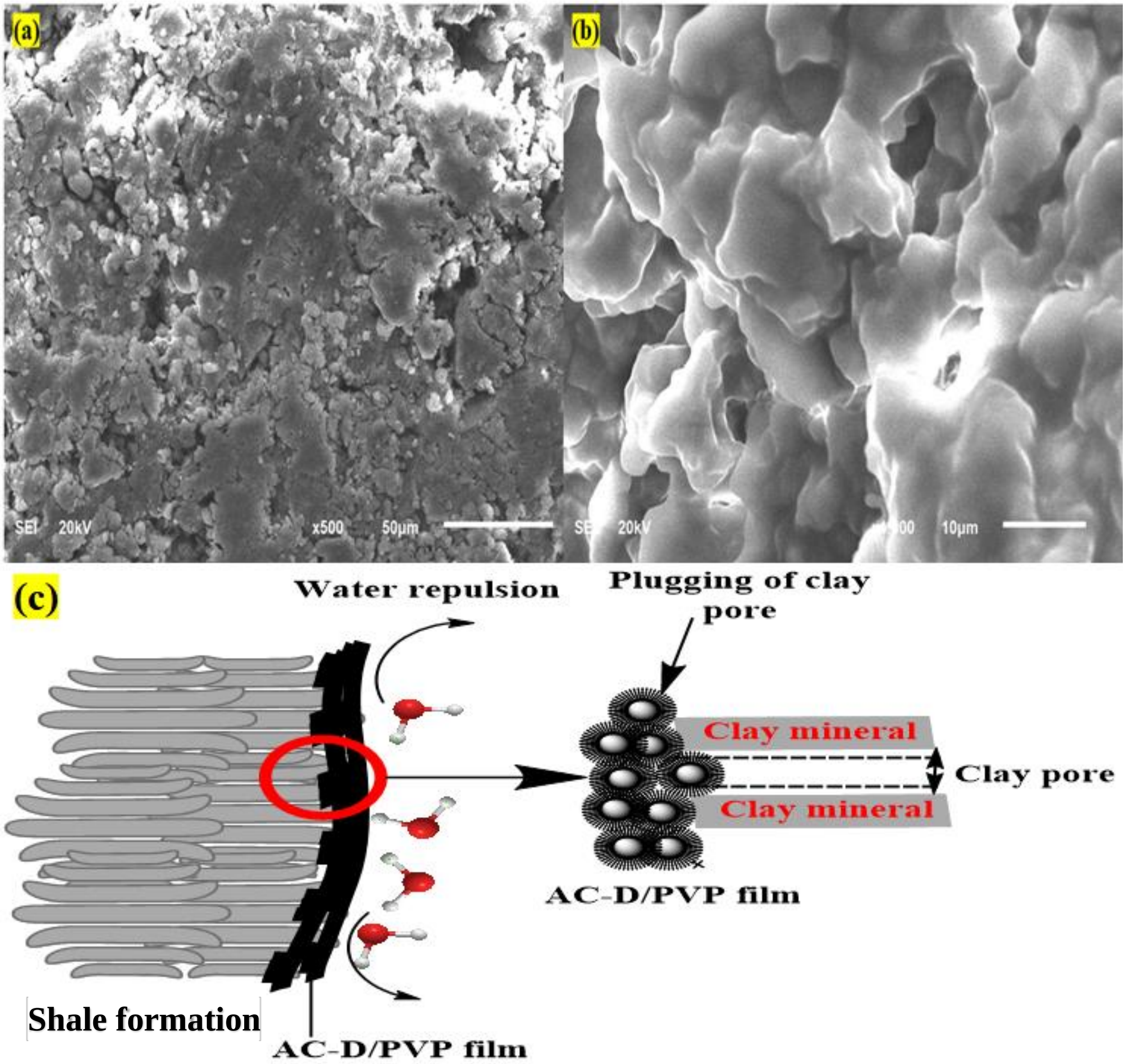

Figure 5.7: The SEM image of (a) plain Na-Bt, (b) Na-Bt in contact with 2 wt% AC-D/PVP after 24 h (c) inhibition mechanism

6. CHAPTER 6

CONCLUSION

The as-prepared C-g-AA-NH_2 tested as shale hydration inhibitor in this study exhibited a brilliant performance compared to the conventional KCl generally being used in drilling mud. The material actively enhances shale recovery upon a hot rolling test. It was able to achieve this ability as a result of its potential to plug interlayer spacing/pore throat in the shale sample. The low molecular weight of the grafted polymer component will make it more thixotropic to be able to form less viscos film coatings and adequate filter cake on the surface of shale to prevent water intrusion. In this manner, it could be compatible with other additives to achieve suitable apparent viscosity and filtration volume required in drilling challenging shale formations.

The potential of activated carbon (AC) composite of AA-AAm-C-Amyl and AA-AAm-OD-C-Amyl with varying hydrophobicity were considered. Both materials exhibited outstanding performance to ameliorate shale hydration and infiltration with AA-AAm-C-Amyl having the best efficiency to quenching the influx of water into formation. The composites showed a high anti-swelling parameter and shale dispersion recovery. About 95.2% and 93.7% of anti-swelling ratio were recorded for AA-AAm-C-Amyl and AA-AAm-OD-C-Amyl respectively compared to that of 55.4% for 10 wt% KCl. The percentage shale recovery was 97.0% for AA-AAm-C-Amyl, 95.2% for AA-AAm-OD-C-Amyl, 63.0% for 10 wt% KCl and 35.1% for pure water. The SEM imaging assessment of the Na-Bt after it got in contact with composite solutions revealed the formation of thin film of hydrophobic layer cluster of AC/polymer nanocomposite that can prevent WBM free-water interactions. In addition, the presence of C-Amyl in the synthesized materials could facilitates plugging of nanopores and cracks in a typical shale formation drilling. Overall, AA-AAm-C-Amyl and AA-AAm-OD-C-Amyl composites are suitable to act as viscosifier as well as shale inhibitor by significant controlling of the filtration loss into shale formations.

The AC-D/PVP composite material showed a remarkable tendency toward alleviation of shale instability during drilling operation using a WBM. It has a superb anti-swelling and shale dispersion inhibition properties of 90.1% and 92.2% respectively which are far better in comparison with the conventional KCl being used in oil and gas industry. The immersion test result and SEM imaging study unveiled the mechanism of inhibitive trait of the material ascribing to the plugging of clay pores as well as the formation of polymer sealing film on it surface by adsorption due to establishment of hydrogen bonding between the formulation and the clay mineral surface. Similarly, the high hydrodynamic volume of dendrimer and the polymer resulting to a large volume of hydrogen bonding further contributes to it tenacity to inhibit the hydration of clay. Polyvinylpyrrolidone of the prepared matrix has a property of moderate viscosity which is crucial to the application of polymer as a component of drilling fluid by not significantly affect the rheological parameters of the mud. All the composites have inclination to withstand high temperatures in real oil well drilling due to their thermal stability up to and beyond 200^{o}C. Therefore, they could substitute the conventional inhibitors.

References

[1] G. M. Bol, S.-W. Wong, C. J. Davidson, and D. C. Woodland, "Borehole Stability in Shales," *SPE Drill. Complet.*, vol. 9, no. 02, pp. 87–94, Jun. 1994, doi: 10.2118/24975-PA.

[2] K. Morton, B. Bomar, M. Schiller, J. Gallet, S. Azar, W. Dye, K. Daugereau, N. Hansen, M. Otto, R. Leaper, and L. Shoults, "Selection and evaluation criteria for high-performance drilling fluids," presented at the Proceedings - SPE Annual Technical Conference and Exhibition, 2005, pp. 2671–2683.

[3] C. Hawkes, P. McLelallan, B. Maurer, and C. Ruan, "Wellbore instability in shales: A review of fundamental principles and GRI-funded research," *GRI-9900252 Rep.*, pp. 1–62, 2000.

[4] R. Gholami, H. Elochukwu, N. Fakhari, and M. Sarmadivaleh, "A review on borehole instability in active shale formations: Interactions, mechanisms and inhibitors," *Earth-Sci. Rev.*, vol. 177, pp. 2–13, 2018, doi: 10.1016/j.earscirev.2017.11.002.

[5] M. S. Asadi, K. Rahman, B. Hughes, G. E. Company, Q. D. T. Ho Chi, and V. Ha, "'OTC-28421-MS Mitigating Wellbore Stability Challenges of Extended-Reach Drilling in Overpressure and Naturally Fractured Formations Field of Study,' No. Lcm," 2018.

[6] M. Khodja, J. P. Canselier, F. Bergaya, K. Fourar, M. Khodja, N. Cohaut, and A. Benmounah, "Shale problems and water-based drilling fluid optimisation in the Hassi Messaoud Algerian oil field," *Appl. Clay Sci.*, vol. 49, no. 4, pp. 383–393, 2010., doi: 10.1016/j.clay.2010.06.008.

[7] A. Yuxiu, J. Guancheng, Q. Yourong, H. Xianbin, and S. He, "Journal of Natural Gas Science and Engineering High-performance shale plugging agent based on chemically modi fi ed graphene," *J. Nat. Gas Sci. Eng.*, vol. 32, pp. 347–355, 2016, doi: 10.1016/j.jngse.2016.04.048.

[8] M. J. Wilson and L. Wilson, "Clay mineralogy and shale instability: an alternative conceptual analysis," *Clay Miner.*, vol. 49, no. 2, pp. 127–145, Apr. 2014, doi: 10.1180/claymin.2014.049.2.01.

[9] Y. An and P. Yu, "A strong inhibition of polyethyleneimine as shale inhibitor in drilling fluid," *J. of Pet. Sci. and Eng.*, vol. 161, pp. 1–8, 2018., doi: 10.1016/j.petrol.2017.11.029.

[10] M. Lal, "Shale stability: Drilling fluid interaction and shale strength," presented at the Society of Petroleum Engineers - SPE Asia Pacific Oil and Gas Conference and Exhibition 1999, APOGCE 1999, 1999.

[11] A. Aftab, A. R. Ismail, and Z. H. Ibupoto, “Enhancing the rheological properties and shale inhibition behavior of water-based mud using nanosilica , multi-walled carbon nanotube , and graphene nanoplatelet,” *Egypt. J. Pet.*, vol. 26, no. 2, pp. 291–299, 2017, doi: 10.1016/j.ejpe.2016.05.004.

[12] A. Rana, M. K. Arfaj, and T. A. Saleh, “Advanced developments in shale inhibitors for oil production with low environmental footprints – A review,” *Fuel*, vol. 247, pp. 237–249, Jul. 2019, doi: 10.1016/j.fuel.2019.03.006.

[13] R. L. Anderson, I. Ratcliffe, H. C. Greenwell, P. A. Williams, S. Cliffe, and P. V. Coveney, “Clay swelling - A challenge in the oilfield,” *Earth-Sci. Rev.*, vol. 98, no. 3–4, pp. 201–216, 2010, doi: 10.1016/j.earscirev.2009.11.003.

[14] A. Díaz-Pérez, I. Cortés-Monroy, and J. C. Roegiers, “The role of water/clay interaction in the shale characterization,” *J. Pet. Sci. Eng.*, vol. 58, no. 1–2, pp. 83–98, 2007, doi: 10.1016/j.petrol.2006.11.011.

[15] E. van Oort, “On the physical and chemical stability of shales,” *J. Pet. Sci. Eng.*, vol. 38, no. 3–4, pp. 213–235, 2003, doi: 10.1016/S0920-4105(03)00034-2.

[16] S. J. Fritz, “Ideality of clay membranes in osmotic processes: a review.,” *Clays Clay Miner.*, vol. 34, no. 2, pp. 214–223, 1986, doi: 10.1346/CCMN.1986.0340212.

[17] L. A. Alcázar-Vara and I. R. Cortés-Monroy, “Drilling Fluids for Deepwater Fields: An Overview,” in *Recent Insights in Petroleum Science and Engineering*, M. Zoveidavianpoor, Ed. InTech, 2018.

[18] S. Zhang, J. J. Sheng, and Z. Shen, “Effect of hydration on fractures and permeabilities in Mancos, Eagleford, Barnette and Marcellus shale cores under compressive stress conditions,” *J. Pet. Sci. Eng.*, vol. 156, pp. 917–926, 2017, doi: 10.1016/j.petrol.2017.06.043.

[19] H. Zhong, Z. Qiu, D. Zhang, Z. Tang, W. Huang, and W. Wang, “Inhibiting shale hydration and dispersion with amine-terminated polyamidoamine dendrimers,” *J. Nat. Gas Sci. Eng.*, 2016 Jan 1;28:52-60, doi: 10.1016/j.jngse.2015.11.029.

[20] T. J. Tambach, E. J. M. Hensen, and B. Smit, “Molecular simulations of swelling clay minerals,” *J. Phys. Chem. B*, vol. 108, no. 23, pp. 7586–7596, 2004, doi: 10.1021/jp049799h.

[21] R. F. T. Lomba, M. E. Chenevert, and M. M. Sharma, “The ion-selective membrane behavior of natives shales,” *J. Pet. Sci. Eng.*, vol. 25, no. 1–2, pp. 9–23, 2000, doi: 10.1016/S0920-4105(99)00028-5.

[22] B. M. Lombardi, R. M. Torres Sanchez, P. Eloy, and M. Genet, “Interaction of thiabendazole and benzimidazole with montmorillonite,” *Appl. Clay Sci.*, vol. 33, no. 1, pp. 59–65, 2006, doi: 10.1016/j.clay.2006.03.010.

[23] A. Dzialowski, A. Hale, and S. Mahajan, "Lubricity and wear of shale: effects of drilling fluids and mechanical parameters," presented at the Drilling Conference - Proceedings, 1993, pp. 501–511.

[24] M. E. Zeynali, "Mechanical and physico-chemical aspects of wellbore stability during drilling operations," *J. Pet. Sci. Eng.*, vol. 82–83, pp. 120–124, 2012, doi: 10.1016/j.petrol.2012.01.006.

[25] D. B. Braun and M. R. Rosen, "Rheology Modifiers Handbook: Practical Use and Application," *Rheol. Modif. Handb. Pract. Use Appl.*, 2000.

[26] Kardoost Co., "Gilsonite in Drilling Mud," *Gilsonite in Drilling Mud*. [Online]. Available: http://gilsonitesale.com/gilsonite-in-drilling-mud/.

[27] M. Alsaba, R. Nygaard, and O. Contreras, "Review of Lost Circulation Materials and Treatments with an Updated Classification," *AADE Natl. Tech. Conf. Exhib.*, pp. 15–16, 2014.

[28] A. Amer, H. Dearing, R. Jones, and M. Sergiacomo, "Drilling through salt formations: A drilling fluids review," presented at the Society of Petroleum Engineers - SPE Deepwater Drilling and Completions Conference, 2016.

[29] E. Stamatakis, C. J. Thaemlitz, G. Coffin, and W. Reid, "New generation of shale inhibitors for water-based muds," presented at the Drilling Conference - Proceedings, 1995, pp. 623–631.

[30] R. Caenn, H. C. H. Darley, and G. R. Gray, *Composition and Properties of Drilling and Completion Fluids*. 2011. DOI: 10.1016/C2009-0-64504-9

[31] X. Shu, L. Wan, and M. Duan, "Persistent inhibition performance of amine polymers to inhibit clay swelling," *Journal of Polymer Engineering*, vol. 38, no. 4, pp. 323–331, 2018.

[32] A. Patel, E. Stamatakis, S. Young, and J. Friedheim, "Advances in inhibitive water-based drilling fluids - Can they replace oil-based muds?," presented at the Proceedings - SPE International Symposium on Oilfield Chemistry, 2007, pp. 614–621.

[33] G. Zhuang, Z. Zhang, S. Peng, J. Gao, and M. Jaber, "Enhancing the rheological properties and thermal stability of oil-based drilling fluids by synergetic use of organo-montmorillonite and organo-sepiolite," *Appl. Clay Sci.*, vol. 161, pp. 505–512, 2018, doi: 10.1016/j.clay.2018.05.018.

[34] S. Shivhare and E. Kuru, "A study of the pore-blocking ability and formation damage characteristics of oil-based colloidal gas aphron drilling fluids," *J. Pet. Sci. Eng.*, vol. 122, pp. 257–265, 2014, doi: 10.1016/j.petrol.2014.07.018.

[35] Y. An, G. Jiang, Y. Ren, L. Zhang, Y. Qi, and Q. Ge, “An environmental friendly and biodegradable shale inhibitor based on chitosan quaternary ammonium salt,” *J. of Pet. Sci. and Eng.*, vol. 135, pp. 253–260, 2015, doi: 10.1016/j.petrol.2015.09.005.

[36] L. Yang, G. Jiang, Y. Shi, and X. Yang, “Application of Ionic Liquid and Polymeric Ionic Liquid as Shale Hydration Inhibitors,” *Energy & Fuels*, vol. 31, no. 4, pp. 4308–4317, Apr. 2017., doi: 10.1021/acs.energyfuels.7b00272.

[37] J. Guancheng, Q. Yourong, A. Yuxiu, H. Xianbin, and R. Yanjun, “Applied Clay Science Polyethyleneimine as shale inhibitor in drilling fl uid,” vol. 128, pp. 70–77, 2016, doi: 10.1016/j.clay.2016.04.013.

[38] L. Yang, G. Jiang, Y. Shi, and X. Yang, “Application of Ionic Liquid and Polymeric Ionic Liquid as Shale Hydration Inhibitors,” *Energy Fuels*, vol. 31, no. 4, pp. 4308–4317, Apr. 2017, doi: 10.1021/acs.energyfuels.7b00272.

[39] W. Ni, Q. Li, G. Chen, L. Lili, J. Zhang, and L. Zhang, “Preparation and Application of a Glucose Graft Copolyammonium as Shale Inhibitor 1,” vol. 89, no. 8, pp. 1354–1359, 2016, doi: 10.1134/S107042721608022X.

[40] C. Cerai, G. Tacio, E. Roditi, R. Sandra, and V. Nascimento, “Applied Clay Science Partially hydrophobized hyperbranched polyglycerols as non-ionic reactive shale inhibitors for water-based drilling fluids." *Appl. Clay Sci.* (2016): 1-11, doi: 10.1016/j.clay.2016.05.025.

[41] J. Abdo, H. AL-Sharji, and E. Hassan, “Effects of nano-sepiolite on rheological properties and filtration loss of water-based drilling fluids,” *Surf. Interface Anal.*, vol. 48, no. 7, pp. 522–526, 2016, doi: 10.1002/sia.5997.

[42] N. Al-Malki, P. Pourafshary, H. Al-Hadrami, and J. Abdo, “Controlling bentonite-based drilling mud properties using sepiolite nanoparticles,” *Pet. Explor. Dev.*, vol. 43, no. 4, pp. 717–723, 2016., doi: 10.1016/S1876-3804(16)30084-2.

[43] O. Duman and S. Tunç, “Electrokinetic and rheological properties of Na-bentonite in some electrolyte solutions,” *Microporous Mesoporous Mater.*, vol. 117, no. 1–2, pp. 331–338, 2009, doi: 10.1016/j.micromeso.2008.07.007.

[44] M. M. Barry, Y. Jung, J.-K. Lee, T. X. Phuoc, and M. K. Chyu, “Fluid filtration and rheological properties of nanoparticle additive and intercalated clay hybrid bentonite drilling fluids,” *J. Pet. Sci. Eng.*, vol. 127, pp. 338–346, 2015, doi: 10.1016/j.petrol.2015.01.012.

[45] J. Su, Q. Chu, and M. Ren, “Properties of high temperature resistance and salt tolerance drilling fluids incorporating acrylamide/2-Acrylamido-2-Methyl-1-Propane sulfonic acid/N-Vinylpyrrolidone/dimethyl diallyl ammonium chloride quadripolymer as fluid loss additives,” *J. Polym. Eng.*, vol. 34, no. 2, pp. 153–159, 2014, doi: 10.1515/polyeng-2013-0270.

[46] F. T. G. Dias, R. R. Souza, and E. F. Lucas, “Influence of modified starches composition on their performance as fluid loss additives in invert-emulsion drilling fluids,” *Fuel*, vol. 140, pp. 711–716, 2015, doi: 10.1016/j.fuel.2014.09.074.

[47] R. D. C. Balaban, E. L. F. Vidal, and M. R. Borges, “Design of experiments to evaluate clay swelling inhibition by different combinations of organic compounds and inorganic salts for application in water base drilling fluids,” *Appl. Clay Sci.*, vol. 105–106, pp. 124–130, 2015, doi: 10.1016/j.clay.2014.12.029.

[48] D. E. O’Brien and M. E. Chenevert, “Stabilizing sensitive shales with inhibited, potassium-based drilling fluids.,” *JPT J. Pet. Technol.*, vol. 25, pp. 1089–1100, 1973.

[49] H. M. Ahmed, M. S. Kamal, and M. Al-Harthi, “Polymeric and low molecular weight shale inhibitors: A review,” *Fuel*, vol. 251, pp. 187–217, Sep. 2019, doi: 10.1016/j.fuel.2019.04.038.

[50] H. Maulana, O. Murphy, A. Ghosh, H.-A. Baker, G. E. Company, M. R. Paimin, and M. Abiabhar, “OTC-28249-MS optimizing pore pressure prediction and wellbore stability in drilling ultra deepwater exploration well,” *Offshore Technol. Conf. Asia*, pp. 1–18, 2018.

[51] X. Huang, H. Shen, J. Sun, K. Lv, J. Liu, X. Dong, and S. Luo, “Nanoscale Laponite as a Potential Shale Inhibitor in Water-Based Drilling Fluid for Stabilization of Wellbore Stability and Mechanism Study,” *ACS Appl. Mater. Interfaces*, vol. 10, no. 39, pp. 33252–33259, Oct. 2018, doi: 10.1021/acsami.8b11419.

[52] G. T. Teixeira, R. F. T. Lomba, S. A. Petrobras, V. A. Meléndez, E. C. Ribeiro, A. D. S. Francisco, and R. S. V. Nascimento, “New material for wellbore strengthening and fluid losses mitigation in deepwater drilling scenario,” presented at the Society of Petroleum Engineers - SPE Deepwater Drilling and Completions Conference 2014, 2014, pp. 128–139.

[53] G. Chen, M. E. Chenevert, M. M. Sharma, and M. Yu, “A study of wellbore stability in shales including poroelastic, chemical, and thermal effects,” *J. Pet. Sci. Eng.*, vol. 38, no. 3–4, pp. 167–176, 2003, doi: 10.1016/S0920-4105(03)00030-5.

[54] E. S. Boek, P. V. Coveney, and N. T. Skipper, “Monte Carlo Molecular Modeling Studies of Hydrated Li-, Na-, and K-Smectites: Understanding the Role of Potassium as a Clay Swelling Inhibitor,” *J. Am. Chem. Soc.*, vol. 117, no. 50, pp. 12608–12617, 1995, doi: 10.1021/ja00155a025.

[55] L. S. Sundar, K. V. Sharma, M. T. Naik, and M. K. Singh, “Empirical and theoretical correlations on viscosity of nanofluids: A review,” *Renew. Sustain. Energy Rev.*, vol. 25, pp. 670–686, 2013, doi: 10.1016/j.rser.2013.04.003.

[56] X. Zhao, Z. Qiu, B. Sun, S. Liu, X. Xing, and M. Wang, “Formation damage mechanisms associated with drilling and completion fluids for deepwater reservoirs,” *J. Pet. Sci. Eng.*, vol. 173, pp. 112–121, Feb. 2019, doi: 10.1016/j.petrol.2018.09.098.

[57] D. Kania, R. Yunus, R. Omar, S. Abdul Rashid, and B. Mohamad Jan, “A review of biolubricants in drilling fluids: Recent research, performance, and applications,” *J. Pet. Sci. Eng.*, vol. 135, pp. 177–184, 2015, doi: 10.1016/j.petrol.2015.09.021.

[58] M. F. Brigatti, E. Galán, and B. K. G. Theng, *Structure and Mineralogy of Clay Minerals*, vol. 5. pp. 21, 2013.

[59] B. Karpiński and M. Szkodo, “Clay Minerals – Mineralogy and Phenomenon of Clay Swelling in Oil & Gas Industry,” *Adv. Mater. Sci.*, vol. 15, no. 1, pp. 37–55, Mar. 2015, doi: 10.1515/adms-2015-0006.

[60] M. Duc, F. Gaboriaud, and F. Thomas, “Sensitivity of the acid-base properties of clays to the methods of preparation and measurement: 1. Literature review,” *J. Colloid Interface Sci.*, vol. 289, no. 1, pp. 139–147, 2005, doi: 10.1016/j.jcis.2005.03.060.

[61] Mineralogical Society of Great Britain & Ireland and The Clay Minerals Society, “Images of Clay,” *Images of Clay*. [Online]. Available: https://www.minersoc.org/images-of-clay.html.

[62] S. Laribi, J.-M. Fleureau, J.-L. Grossiord, and N. Kbir-Ariguib, “Effect of pH on the rheological behavior of pure and interstratified smectite clays,” *Clays Clay Miner.*, vol. 54, no. 1, pp. 29–37, 2006, doi: 10.1346/CCMN.2006.0540104.

[63] Zhong HY, Huang WA, Qiu ZS, Cao J, Xie BQ, Wang FW, Zheng W. Inhibition Comparison Between Polyether Diamine and Formate Salts as Shale Inhibitor in Water-Based Drilling Fluid. *Energy Sources, Part A: Recovery, Utilization, and Environmental Effects*. 2015 Sep 17;37(18):1971-8, doi: 10.1080/15567036.2011.654315.

[64] J. Deng, D. Guo, J. Zhou, and S. Liu, “Mechanics-chemistry coupling calculation model of borehole stress in shale formation and its numerical solving method,” *Yanshilixue Yu Gongcheng XuebaoChinese J. Rock Mech. Eng.*, vol. 22, no. SUPPL., pp. 2250–2253, 2003.

[65] J. Hess, “Pipe Sticking Prediction Using LWD Real-Time Measurements,” *SPE J.*, pp. 1–15, 2016, doi: 10.2118/178828-MS.

[66] C. H. Yew, M. E. Chenevert, C. L. Wang, and S. O. Oslsanya, “Wellbore stress distribution produced by moisture adsorption,” *SPE Drill. Eng.*, vol. 5, no. 4, pp. 311–316, 1990, doi: 10.2118/19536-PA.

[67] F. K. Mody, U. A. Tare, C. P. Tan, C. J. Drummond, and B. Wu, “Development of Novel Membrane Efficient Water-Based Drilling Fluids through Fundamental Understanding of Osmotic Membrane Generation in Shales,” presented at the Proceedings - SPE Annual Technical Conference and Exhibition, 2002, pp. 1031–1046.

[68] X. Ao, Y. Lu, J. Tang, Y. Chen, and H. Li, “Investigation on the physics structure and chemical properties of the shale treated by supercritical CO2,” *J. CO2 Util.*, vol. 20, pp. 274–281, 2017, doi: 10.1016/j.jcou.2017.05.028.

[69] R. Gholami, H. Elochukwu, N. Fakhari, and M. Sarmadivaleh, “A review on borehole instability in active shale formations: Interactions, mechanisms and inhibitors,” *Earth-Sci. Rev.*, vol. 177, pp. 2–13, 2018, doi: 10.1016/j.earscirev.2017.11.002.

[70] J. Liu and J. Sun, “Borehole wall collapse and control in shale gas well drilling,” *Drill. Fluid Complet. Fluid*, vol. 33, no. 3, pp. 25–29, 2016, doi: 10.3696/j.issn.1001-5620.2016.03.005.

[71] K. Liu and M. Ostadhassan, “Microstructural and geomechanical analysis of Bakken shale at nanoscale,” *J. Pet. Sci. Eng.*, vol. 153, pp. 133–144, 2017, doi: 10.1016/j.petrol.2017.03.039.

[72] P. E. Clark, “Drilling mud rheology and the API recommended measurements,” presented at the Proceedings - SPE Production Operations Symposium, 1995, pp. 933–941.

[73] J. Xu, T. Gu, W. Shen, X. Wang, Y. Ma, L. Peng, and X. Li, “Influence simulation of inorganic salts on montmorillonite elastic mechanical parameters and experimental study,” *Zhongguo Shiyou Daxue Xuebao Ziran Kexue BanJournal China Univ. Pet. Ed. Nat. Sci.*, vol. 40, no. 2, pp. 83–90, 2016, doi: 10.3969/j.issn.1673-5005.2016.02.010.

[74] X. Bai, X. Zhang, V. Koutsos, Z. Fu, T. Ning, and Y. Luo, “Preparation and evaluation of amine terminated polyether shale inhibitor for water-based drilling fluid,” *SN Appl Sci*, vol. 1, no. 1, p. 94, 2019.

[75] P. Barati, K. Shahbazi, M. Kamari, and A. Aghajafari, “Shale hydration inhibition characteristics and mechanism of a new amin-based additive in water-based drilling fluids,” *Petroleum*, 2017 Dec 1;3(4):476-82, doi: 10.1016/j.petlm.2017.05.003.

[76] L. Bailey, C. Sawdon, M. Brady, and S. Cliffe, “New insight into the mechanisms of shale inhibition using water based silicate drilling fluids,” presented at the Proceedings of the IADC/SPE Asia Pacific Drilling Technology Conference, APDT, 1998, pp. 897–902.

[77] M. S. Aston and G. P. Elliott, “Water-based glycol drilling muds: Shale inhibition mechanisms,” presented at the European Petroleum Conference - Proceedings, 1994, pp. 107–113.

[78] S. Bell, “Using molecular modeling to understand the mechanism for adhesion of shale-stabilizing polymers to clay surfaces,” presented at the Proceedings - SPE Annual Technical Conference and Exhibition, 2005, pp. 1167–1171.

[79] X. Huang, J. Sun, K. Lv, J. Liu, H. Shen, and F. Zhang, "Application of core-shell structural acrylic resin/nano-SiO2 composite in water based drilling fluid to plug shale pores," *J. Nat. Gas Sci. Eng.*, vol. 55, pp. 418–425, 2018, doi: 10.1016/j.jngse.2018.05.023.

[80] M. Belmokhtar, P. Delage, S. Ghabezloo, and N. Conil, "Active porosity in swelling shales: Insight from the Callovo-Oxfordian claystone," *Geotech. Lett.*, vol. 8, no. 3, pp. 226–230, 2018, doi: 10.1680/jgele.18.00010.

[81] N. Chakraborty, Z. T. Karpyn, S. Liu, and H. Yoon, "Permeability evolution of shale during spontaneous imbibition," *J. Nat. Gas Sci. Eng.*, vol. 38, pp. 590–596, 2017, doi: 10.1016/j.jngse.2016.12.031.

[82] W. Huang, Q. Lan, Z. Qiu, Y. Zhang, H. Zhong, and G. Feng, "Colloidal Properties and Clay Inhibition of Sodium Silicate in Solution and Montmorillonite Suspension," *Silicon*, vol. 8, no. 1, pp. 111–122, 2016, doi: 10.1007/s12633-015-9351-2.

[83] S. Ponmani, R. Nagarajan, and J. S. Sangwai, "Effect of nanofluids of cuo and zno in polyethylene glycol and polyvinylpyrrolidone on the thermal, electrical, and filtration-loss properties of water-based drilling fluids," *SPE J.*, vol. 21, no. 2, pp. 405–415, 2016, doi: 10.2118/178919-PA.

[84] X. Guerrero, M. Guerrero, and B. Warren, "Use of amine/PHPA system to drill high reactive shales in the orito field in Colombia," presented at the Society of Petroleum Engineers - 1st International Oil Conference and Exhibition in Mexico 2006, IOCEM 2006, 2006, pp. 639–645.

[85] C. E. C. De Souza, A. S. Lima, and R. S. V. Nascimento, "Hydrophobically modified poly(ethylene glycol) as reactive clays inhibitor additive in water-based drilling fluids," *J. Appl. Polym. Sci.*, vol. 117, no. 2, pp. 857–864, 2010, doi: 10.1002/app.31318.

[86] L. J. Hall, J. P. Deville, C. M. Santos, O. J. Rojas, and C. S. Araujo, "Nanocellulose and biopolymer blends for high-performance water-based drilling fluids," presented at the Society of Petroleum Engineers - IADC/SPE Drilling Conference and Exhibition, DC 2018, 2018, vol. 2018-March.

[87] M. Zoveidavianpoor and A. Samsuri, "The use of nano-sized Tapioca starch as a natural water-soluble polymer for filtration control in water-based drilling muds," *J. Nat. Gas Sci. Eng.*, vol. 34, pp. 832–840, 2016, doi: 10.1016/j.jngse.2016.07.048.

[88] H. Yu, Hu W, Guo G, Huang L, Li L, Gu X, Zhang Z, Zhang J, Chen G. Investigation of melamine derived quaternary as ammonium salt potential shale inhibitor. *InIOP Conference Series: Earth and Environmental Science* 2017 Jun (Vol. 69, No. 1, p. 012065). *IOP Publishing*, doi: 10.1088/1755-1315/69/1/012065.

[89] Z. Jie, L. Lili, C. Gang, T. Ying, Z. Jingrui, and T. Deyao, “Synthesis and performance evaluation of quaternary ammonium salt as potential shale inhibitor,” *J. Chem. Soc. Pak.*, vol. 37, no. 5, pp. 961–966, 2015.

[90] Z. Luo, L. Wang, P. Yu, and Z. Chen, “Applied Clay Science Experimental study on the application of an ionic liquid as a shale inhibitor and inhibitive mechanism,” *Appl. Clay Sci.*, vol. 150, no. June, pp. 267–274, 2017, doi: 10.1016/j.clay.2017.09.038.

[91] X. Zhang, Z. Qiu, H. Zhong, Z. Tang, J. Xu, and D. Zhang, “Experimental Study on a New Ultrahigh Temperature Shale Inhibitor,” *Drill. Fluid Complet. Fluid*, vol. 34, no. 1, pp. 9–15, 2017, doi: 10.3969/j.issn.1001-5620.2017.01.002.

[92] H. Mao, Z. Qiu, Z. Shen, and W. Huang, “Hydrophobic associated polymer based silica nanoparticles composite with core–shell structure as a filtrate reducer for drilling fluid at utra-high temperature,” *J. Pet. Sci. Eng.*, vol. 129, pp. 1–14, May 2015, doi: 10.1016/j.petrol.2015.03.003.

[93] G. Jiang and X. Zhang, “A new inhibitor of P (AM-DMDAAC)/PVA intermacromolecular complex for shale in drilling fluids,” vol. 45584, pp. 1–8, 2018, doi: 10.1002/app.45584.

[94] G. Li, J. Zhang, H. Zhao, Y. Hou, and S. Drilling, “SPE 156997 Nanotechnology to Improve Sealing Ability of Drilling Fluids for Shale with Micro-cracks During Drilling,” pp. 1–7, 2012.

[95] F. Al Fouzan and M. A. Dafalla, “Study of cracks and fissures phenomenon in Central Saudi Arabia by applying geotechnical and geophysical techniques,” *Arab. J. Geosci.*, vol. 7, no. 3, pp. 1157–1164, 2014, doi: 10.1007/s12517-013-0884-7.

[96] H. Zhong, Z. Qiu, Z. Tang, X. Zhang, J. Xu, and W. Huang, “Study of 4 , 4 0 - methylenebis-cyclohexanamine as a high temperature-resistant shale inhibitor,” *J. Mater. Sci.*, vol. 51, no. 16, pp. 7585–7597, 2016, doi: 10.1007/s10853-016-0037-y.

[97] H. Zhong, Z. Qiu, Z. Tang, X. Zhang, D. Zhang, and W. Huang, “Minimization shale hydration with the combination of hydroxyl-terminated PAMAM dendrimers and KCl,” *J. Mater. Sci.*, vol. 51, no. 18, pp. 8484–8501, 2016, doi: 10.1007/s10853-016-0108-0.

[98] F. Ma, X. Pu, and B. Wang, “RSC Advances Preparation and evaluation of polyampholyte inhibitor DAM,” *RSC Adv.*, vol. 7, pp. 49320–49328, 2017, doi: 10.1039/C7RA08385H.

[99] X. Bai, H. Wang, Y. Luo, X. Zheng, X. Zhang, S. Zhou, and X. Pu, “The structure and application of amine-terminated hyperbranched polymer shale inhibitor for water-based drilling fluid,” vol. 45466, pp. 1–9, 2017, doi: 10.1002/app.45466.

[100] X. Li, G. Jiang, L. Yang, and S. Peng, “Study of gelatin as biodegradable shale hydration inhibitor,” *Colloids and Surfaces A: Physicochemical and Engineering Aspects*, vol. 539, pp. 192–200, 2018, doi: 10.1016/j.colsurfa.2017.12.020.

[101] L. Yang, G. Jiang, Y. Shi, and X. Yang, “Application of Ionic Liquid and Polymeric Ionic Liquid as Shale Hydration Inhibitors,” *Energy & Fuels*, vol. 31, no. 4, pp. 4308–4317, 2017, doi: 10.1021/acs.energyfuels.7b00272.

[102] S. R. Shadizadeh, A. Moslemizadeh, and A. S. Dezaki, “Applied Clay Science A novel nonionic surfactant for inhibiting shale hydration,” *Appl. Clay Sci.*, vol. 118, pp. 74–86, 2015, doi: 10.1016/j.clay.2015.09.006.

[103] A. Moslemizadeh, S. Khezerloo-ye Aghdam, K. Shahbazi, and S. Zendehboudi, “A triterpenoid saponin as an environmental friendly and biodegradable clay swelling inhibitor,” *Journal of Molecular Liquids*, vol. 247, pp. 269–280, 2017, doi: 10.1016/j.molliq.2017.10.003.

[104] Y. Zhao, C. Wang, H. Cao, Y. Chen, and W. Shen, “Influencing mechanism and modelling study of pore pressure and temperature on shale permeability,” *Meitan XuebaoJournal China Coal Soc.*, vol. 43, no. 6, pp. 1754–1760, 2018, doi: 10.13225/j.cnki.jccs.2017.1404.

[105] A. R. Ismail, N. M. Rashid, M. Z. Jaafar, W. R. W. Sulaiman, and N. A. Buang, “Effect of nanomaterial on the rheology of drilling fluids,” *J Appl Sci*, vol. 14, no. 11, pp. 1192–1197, 2014.

[106] A. H. Salih, T. A. Elshehabi, and H. I. Bilgesu, “Impact of nanomaterials on the rheological and filtration properties of water-based drilling fluids,” presented at the SPE Eastern Regional Meeting, 2016, vol. 2016, doi: 10.2118/184067-MS.

[107] Y. An, G. Jiang, Y. Qi, Q. Ge, L. Zhang, and Y. Ren, “Synthesis of nano-plugging agent based on AM/AMPS/NVP terpolymer,” *J. Pet. Sci. Eng.*, vol. 135, pp. 505–514, Nov. 2015, doi: 10.1016/j.petrol.2015.10.014.

[108] S. Akhtarmanesh, M. J. A. Shahrabi, and A. Atashnezhad, “Journal of Petroleum Science and Engineering Improvement of wellbore stability in shale using nanoparticles,” *J. Pet. Sci. Eng.*, vol. 112, pp. 290–295, 2013, doi: 10.1016/j.petrol.2013.11.017.

[109] X. Yang, Y. Yue, J. Cai, Y. Liu, and X. Wu, “Experimental Study and Stabilization Mechanisms of Silica Nanoparticles Based Brine Mud with High Temperature Resistance for Horizontal Shale Gas Wells,” vol. 2, 2015.

[110] J. Cai, “Decreasing Water Invasion into Atoka Shale Using Nonmodified Silica Nanoparticles,” p. 10, 2012.

[111] J. Zhang, Long Li, Shuangwei Wang, Jianhua Wang, Henglin Yang, Zhiliang Zhao, Jinzhi Zhu, and Zhen Zhang. "Novel micro and nano particle-based drilling fluids:

Pioneering approach to overcome the borehole instability problem in shale formations." In *SPE Asia Pacific Unconventional Resources Conference and Exhibition*. *SPE*, 2015.

[112] M. F. Zakaria, M. Husein, and G. Hareland, "SPE 156992 Novel Nanoparticle-Based Drilling Fluid with Improved Characteristics," no. 2009, 2012.

[113] K. P. Hoelscher, G. De Stefano, M. Riley, and S. Young, "Application of Nanotechnology in Drilling Fluids," in *SPE International Oilfield Nanotechnology Conference and Exhibition*, Noordwijk, The Netherlands, 2012, doi: 10.2118/157031-MS.

[114] S. Akhtarmanesh, M. J. A. Shahrabi, and A. Atashnezhad, "Improvement of wellbore stability in shale using nanoparticles," *J. Pet. Sci. Eng.*, vol. 112, pp. 290–295, 2013, doi: 10.1016/j.petrol.2013.11.017.

[115] Y. Kang, J. She, C. Lin, and L. You, "Brittleness weakening mechanisms of shale soaked by drilling & completion fluid," *Lixue XuebaoChinese J. Theor. Appl. Mech.*, vol. 48, no. 3, pp. 730–738, 2016, doi: 10.6052/0459-1879-15-286.

[116] C. Y. Ho, S. Yusup, C. V. Soon, and M. T. Arpin, "Rheological Behaviour of Graphene Nano-sheets in Hydrogenated Oil-based Drilling Fluid," presented at the Procedia Engineering, 2016, vol. 148, pp. 49–56, doi: 10.1016/j.proeng.2016.06.490.

[117] A. Aftab, A. R. Ismail, and Z. H. Ibupoto, "Enhancing the rheological properties and shale inhibition behavior of water-based mud using nanosilica, multi-walled carbon nanotube, and graphene nanoplatelet," *Egypt. J. Pet.*, vol. 26, no. 2, pp. 291–299, 2017, doi: 10.1016/j.ejpe.2016.05.004.

[118] F. Liu, G.-C. Jiang, K. Wang, and J. Wang, "Laponite nanoparticle as a multi-functional additive in water-based drilling fluids," *J. Mater. Sci.*, vol. 52, no. 20, pp. 12266–12278, Oct. 2017, doi: 10.1007/s10853-017-1375-0.

[119] N. A. Agudelo, L. D. Perez, and B. L. Lopez, "A novel method for the synthesis of polystyrene-graft-silica particles using random copolymers based on styrene and triethoxyvinylsilane," *Appl. Surf. Sci.*, vol. 257, no. 20, pp. 8581–8586, 2011, doi: 10.1016/j.apsusc.2011.05.021.

[120] J.-G. Xu, Z. Qiu, X. Zhao, and W. Huang, "Hydrophobic modified polymer based silica nanocomposite for improving shale stability in water-based drilling fluids," *J. Pet. Sci. Eng.*, vol. 153, pp. 325–330, 2017, doi: 10.1016/j.petrol.2017.04.013.

[121] American Petroleum Institute, *Recomm. Pract. Stand. Proced. Lab. Test. Drill. Fluids*, 1990.

[122] Y. An and P. Yu, "A strong inhibition of polyethyleneimine as shale inhibitor in drilling fluid," *J. Pet. Sci. Eng.*, vol. 161, pp. 1–8, 2018, doi: 10.1016/j.petrol.2017.11.029.

[123] Y. An, G. Jiang, Y. Ren, L. Zhang, Y. Qi, and Q. Ge, “An environmental friendly and biodegradable shale inhibitor based on chitosan quaternary ammonium salt,” *J. Pet. Sci. Eng.*, vol. 135, pp. 253–260, 2015, doi: 10.1016/j.petrol.2015.09.005.

[124] W.-J. Ni, Q. Li, G. Chen, L. Lili, J. Zhang, L. Zhang, J. Yan, and C. Cheng, “Preparation and application of a glucose graft copolyammonium as shale inhibitor,” *Russ. J. Appl. Chem.*, vol. 89, no. 8, pp. 1354–1359, 2016, doi: 10.1134/S107042721608022X.

[125] K. C. Taylor, R. A. Burke, H. A. Nasr-El-Din, and L. L. Schramm, “Development of a row injection analysis method for the determination of acrylamide copolymers in oilfield brines,” *SPE Int. Symp. Oilfield Chem.*, pp. 675–690, 1995.

[126] R. K. Clark, R. F. Scheuerman, H. Rath, and H. G. Van Laar, “Polyacrylamide/potassium-chloride mud for drilling water-sensitive shales.,” *JPT J. Pet. Technol.*, vol. 28, pp. 719–727, 1976, doi: 10.2118/5514-PA.

[127] H. Zhong, Z. Qiu, Z. Tang, X. Zhang, J. Xu, and W. Huang, “Study of 4, 4′-methylenebis-cyclohexanamine as a high temperature-resistant shale inhibitor,” *J. Mater. Sci.*, vol. 51, no. 16, pp. 7585–7597, 2016, doi: 10.1007/s10853-016-0037-y.

[128] J. Guancheng, Q. Yourong, A. Yuxiu, H. Xianbin, and R. Yanjun, “Polyethyleneimine as shale inhibitor in drilling fluid,” *Appl. Clay Sci.*, vol. 127–128, pp. 70–77, 2016, doi: 10.1016/j.clay.2016.04.013.

[129] X. Bai, H. Wang, Y. Luo, X. Zheng, X. Zhang, S. Zhou, and X. Pu, “The structure and application of amine-terminated hyperbranched polymer shale inhibitor for water-based drilling fluid,” *J. Appl. Polym. Sci.*, vol. 134, no. 46, p. 45466, 2017, doi: 10.1002/app.45466.

[130] Z. Luo, L. Wang, P. Yu, and Z. Chen, “Experimental study on the application of an ionic liquid as a shale inhibitor and inhibitive mechanism,” *Appl. Clay Sci.*, vol. 150, pp. 267–274, 2017, doi: 10.1016/j.clay.2017.09.038.

[131] S. R. Shadizadeh, A. Moslemizadeh, and A. S. Dezaki, “A novel nonionic surfactant for inhibiting shale hydration,” *Appl. Clay Sci.*, vol. 118, pp. 74–86, 2015, doi: 10.1016/j.clay.2015.09.006.

[132] A. Moslemizadeh, S. Khezerloo-ye Aghdam, K. Shahbazi, H. Khezerloo-ye Aghdam, and F. Alboghobeish, “Assessment of swelling inhibitive effect of CTAB adsorption on montmorillonite in aqueous phase,” *Appl. Clay Sci.*, vol. 127–128, pp. 111–122, 2016, doi: 10.1016/j.clay.2016.04.014.

[133] A. Moslemizadeh, K. Samadzadeh Hafshejani, K. Shahbazi, M. Zaravi Dezfuli, and S. Zendehboudi, “A biosurfactant for inhibiting clay hydration in aqueous solutions: Applications to petroleum industry,” *Can. J. Chem. Eng.*, vol. 97, no. 1, pp. 384–394, 2019, doi: 10.1002/cjce.23172.

[134] W. N. Aggrey, N. Y. Asiedu, C. D. Adenutsi, and P. Anumah, "A novel non-ionic surfactant extract derived from Chromolaena odarata as shale inhibitor in water based drilling mud," *Heliyon*, *5*(5), p.e01697, 2019, doi: 10.1016/j.heliyon.2019.e01697.

[135] M. Ghasemi, A. Moslemizadeh, K. Shahbazi, O. Mohammadzadeh, S. Zendehboudi, and S. Jafari, "Primary evaluation of a natural surfactant for inhibiting clay swelling," *J. Pet. Sci. Eng.*, pp. 878–891, 2019, doi: 10.1016/j.petrol.2019.02.073.

[136] H. Zhong, Z. Qiu, W. Huang, D. Zhang, and D. Sun, "Properties of PAMAM dendrimers in inhibiting shale hydration and dispersion," *Zhongnan Daxue Xuebao Ziran Kexue BanJournal Cent. South Univ. Sci. Technol.*, vol. 47, no. 12, pp. 4132–4140, 2016, doi: 10.11817/j.issn.1672-7207.2016.12.023.

[137] G. Jiang, X. Zhang, T. Dong, Y. Xuan, L. Wang, and Q. Jiang, "A new inhibitor of P(AM-DMDAAC)/PVA intermacromolecular complex for shale in drilling fluids," *J. Appl. Polym. Sci.*, vol. 135, no. 1 :45584., 2018, doi: 10.1002/app.45584.

[138] D. V. Kosynkin, G. Ceriotti, K. C. Wilson, J. R. Lomeda, J. T. Scorsone, A. D. Patel, J. E. Friedheim, and J. M. Tour, "Graphene oxide as a high-performance fluid-loss-control additive in water-based drilling fluids," *ACS Appl. Mater. Interfaces*, vol. 4, no. 1, pp. 222–227, 2012, doi: 10.1021/am2012799.

[139] M. M. Sharma, R. Zhang, M. E. Chenevert, L. Ji, Q. Guo, and J. Friedheim, "A new family of nanoparticle based drilling fluids," presented at the Proceedings - SPE Annual Technical Conference and Exhibition, 2012, vol. 5, pp. 4095–4107.

[140] A. Sameni, P. Pourafshary, M. Ghanbarzadeh, and S. Ayatollahi, "Effect of nanoparticles on clay swelling and migration," *Egypt. J. Pet.*, vol. 24, no. 4, pp. 429–437, 2015, doi: 10.1016/j.ejpe.2015.10.006.

[141] G. Li, J. Zhang, H. Zhao, and Y. Hou, "Nanotechnology to improve sealing ability of drilling fluids for shale with micro-cracks during drilling," presented at the Society of Petroleum Engineers - SPE International Oilfield Nanotechnology Conference 2012, 2012, pp. 254–260.

[142] Z. Qiu, J. Xu, P. Yang, X. Zhao, T. Mou, H. Zhong, and W. Huang, "Effect of Amphiphilic Polymer/Nano-Silica Composite on Shale Stability for Water-Based Muds," *Appl. Sci.*, vol. 8, no. 10, p. 1839, 2018, doi: 10.3390/app8101839.

[143] D. Guo, C. Lou, Z. Huang, N. Muhammad, Z. Qiming, S. Wu, and Y. Zhu, "Fabrication of graphene oxide polymer composite particles with grafted poly(amidoamine) dendrimers and their application in ion chromatography," *New J. Chem.*, vol. 42, no. 11, pp. 8653–8660, 2018, doi: 10.1039/c8nj00754c.

[144] A. Yuxiu, J. Guancheng, Q. Yourong, H. Xianbin, and S. He, “High-performance shale plugging agent based on chemically modified graphene,” *J. Nat. Gas Sci. Eng.*, vol. 32, pp. 347–355, 2016, doi: 10.1016/j.jngse.2016.04.048.

[145] N. M. Taha and S. Lee, “Nano Graphene Application Improving Drilling Fluids Performance,” *Int. Pet. Technol. Conf.*, 2015.

[146] Y. Kang, J. She, H. Zhang, L. You, and M. Song, “Strengthening shale wellbore with silica nanoparticles drilling fluid,” *Petroleum*, vol. 2, no. 2, pp. 189–195, 2016, doi: 10.1016/j.petlm.2016.03.005.

[147] K. P. Hoelscher, G. De Stefano, M. Riley, and S. Young, “Application of nanotechnology in drilling fluids,” *Appl. Nanotechnol. Drill. Fluids*, pp. 1–7, 2012.

[148] P. J. Boul, B. R. Reddy, J. Zhang, and C. Thaemlitz, “Functionalized nanosilicas as shale inhibitors in water-based drilling fluids,” *SPE Drill. Complet.*, vol. 32, no. 2, pp. 121–130, 2017.

[149] Y. X. An, G. C. Jiang, Y. R. Qi, and Q. Y. Ge, “Plugging Agent of Shale Base on Nano Flexible Polymer,” *Appl. Mech. Mater.*, vol. 835, pp. 15–19, 2016, doi: 10.4028/www.scientific.net/AMM.835.15.

[150] X. Liu, K. Liu, S. Gou, L. Liang, C. Luo, and Q. Guo, “Water-Soluble Acrylamide Sulfonate Copolymer for Inhibiting Shale Hydration,” *Ind. Eng. Chem. Res.*, vol. 53, no. 8, pp. 2903–2910, Feb. 2014, doi: 10.1021/ie403956d.

[151] G. Jiang, X. Zhang, T. Dong, Y. Xuan, L. Wang, and Q. Jiang, “A new inhibitor of P(AM-DMDAAC)/PVA intermacromolecular complex for shale in drilling fluids,” *J. Appl. Polym. Sci.*, vol. 135, no. 1, 2018, doi: 10.1002/app.45584.

[152] X. Zhao, Z. Qiu, Y. Zhang, H. Zhong, W. Huang, and Z. Tang, “Zwitterionic polymer P(AM-DMC-AMPS) as a low-molecular-weight encapsulator in deepwater drilling fluid,” *Appl. Sci. Switz.*, vol. 7, no. 6 :594, 2017, doi: 10.3390/app7060594.

[153] L. Zhang, Z. Kou, H. Wang, Y. Zhao, M. Dejam, J. Guo, and J. Du, “Performance analysis for a model of a multi-wing hydraulically fractured vertical well in a coalbed methane gas reservoir,” *J. Pet. Sci. Eng.*, vol. 166, pp. 104–120, 2018, doi: 10.1016/j.petrol.2018.03.038.

[154] M. Dejam, H. Hassanzadeh, and Z. Chen, “Semi-analytical solution for pressure transient analysis of a hydraulically fractured vertical well in a bounded dual-porosity reservoir,” *J. Hydrol.*, vol. 565, pp. 289–301, 2018, doi: 10.1016/j.jhydrol.2018.08.020.

[155] Z. Sun, J. Shi, K. Wu, B. Xu, T. Zhang, Y. Chang, and X. Li, “Transport capacity of gas confined in nanoporous ultra-tight gas reservoirs with real gas effect and water storage mechanisms coupling,” *Int. J. Heat Mass Transf.*, vol. 126, pp. 1007–1018, 2018, doi: 10.1016/j.ijheatmasstransfer.2018.05.078.

[156] T. Ma and P. Chen, “A wellbore stability analysis model with chemical-mechanical coupling for shale gas reservoirs,” *J. Nat. Gas Sci. Eng.*, vol. 26, pp. 72–98, Sep. 2015, doi: 10.1016/j.jngse.2015.05.028.

[157] Z. Jin and A. Firoozabadi, “Phase behavior and flow in shale nanopores from molecular simulations,” *Fluid Phase Equilibria*, vol. 430, pp. 156–168, 2016, doi: 10.1016/j.fluid.2016.09.011.

[158] F. Ma, X. Pu, B. Wang, J. Li, and C. Cao, “Preparation and evaluation of polyampholyte inhibitor DAM,” *RSC Adv.*, vol. 7, no. 78, pp. 49320–49328, 2017, doi: 10.1039/c7ra08385h.

[159] J. Song, Y. Yuan, S. Gu, X. Yang, Y. Yue, J. Cai, and G. Jiang, “2D Numerical Simulation of Improving Wellbore Stability in Shale Using Nanoparticles Based Drilling Fluid,” *Energies*, vol. 10, no. 5, p. 651, 2017, doi: 10.3390/en10050651.

[160] M. Liang, Z. Wang, L. Gao, C. Li, and H. Li, “Evolution of pore structure in gas shale related to structural deformation,” *Fuel*, vol. 197, pp. 310–319, 2017, doi: 10.1016/j.fuel.2017.02.035.

[161] X. Tang, Z. Jiang, S. Jiang, L. Cheng, and Y. Zhang, “Characteristics and origin of in-situ gas desorption of the Cambrian Shuijingtuo Formation shale gas reservoir in the Sichuan Basin, China,” *Fuel*, vol. 187, pp. 285–295, 2017, doi: 10.1016/j.fuel.2016.09.072.

[162] K. Song, Q. Wu, M. Li, S. Ren, L. Dong, X. Zhang, T. Lei, and Y. Kojima, “Water-based bentonite drilling fluids modified by novel biopolymer for minimizing fluid loss and formation damage,” *Colloids Surf. Physicochem. Eng. Asp.*, vol. 507, pp. 58–66, 2016, doi: 10.1016/j.colsurfa.2016.07.092.

[163] B. Xie and X. Liu, “Thermo-thickening behavior of LCST-based copolymer viscosifier for water-based drilling fluids,” *J. Pet. Sci. Eng.*, vol. 154, pp. 244–251, 2017, doi: 10.1016/j.petrol.2017.04.037.

[164] R. Jain, V. Mahto, and V. P. Sharma, “Evaluation of polyacrylamide-grafted-polyethylene glycol/silica nanocomposite as potential additive in water based drilling mud for reactive shale formation,” *J. Nat. Gas Sci. Eng.*, vol. 26, pp. 526–537, Sep. 2015, doi: 10.1016/j.jngse.2015.06.051.

[165] R. Y. Lochhead, “The Role of Polymers in Cosmetics: Recent Trends,” in *Cosmetic Nanotechnology*, vol. 961, S. E. Morgan, K. O. Havelka, and R. Y. Lochhead, Eds. Washington, DC: American Chemical Society, 2007, pp. 3–56.

[166] V. Mahto, P. Srikanth, and B. V. Krishna, “Development of non-damaging and inhibitive water based oil well drilling fluids,” *Pet. Sci. Technol.*, vol. 31, no. 7, pp. 721–726, 2013, doi: 10.1080/10916466.2010.531353.

[167] J. Xu, Z. Qiu, W. Huang, and X. Zhao, “Preparation and performance properties of polymer latex SDNL in water-based drilling fluids for drilling troublesome shale formations,” *J. Nat. Gas Sci. Eng.*, vol. 37, pp. 462–470, 2017, doi: 10.1016/j.jngse.2016.11.064.

[168] Y. Zhengqin, Y. Zhongbin, H. Lei, B. Yun, L. Lili, Z. Jie, Q. Chentun, and C. Gang, “Preparation and Application of a New Crosslinked Polyammonium as a Shale Inhibitor,” *J. Appl. Biomater. Funct. Mater.*, vol. 16, no. 1_suppl, pp. 119–124, 2018, doi: 10.1177/2280800017753054.

[169] Z. Vryzas and V. C. Kelessidis, “Nano-based drilling fluids: A review,” *Energies*, vol. 10, no. 4 :540, 2017, doi: 10.3390/en10040540.

[170] H. C. Lau, M. Yu, and Q. P. Nguyen, “Nanotechnology for oilfield applications: Challenges and impact,” *J. Pet. Sci. Eng.*, vol. 157, pp. 1160–1169, 2017, doi: 10.1016/j.petrol.2017.07.062.

[171] J.-G. Xu, Z.-S. Qiu, X. Zhao, H.-Y. Zhong, G.-R. Li, and W.-A. Huang, “Synthesis and characterization of shale stabilizer based on polyethylene glycol grafted nano-silica composite in water-based drilling fluids,” *J. Pet. Sci. Eng.*, vol. 163, pp. 371–377, 2018, doi: 10.1016/j.petrol.2018.01.007.

[172] J.-Y. Liu, Z.-S. Qiu, and W. Huang, “Novel latex particles and aluminum complexes as potential shale stabilizers in water-based drilling fluids,” *J. Pet. Sci. Eng.*, vol. 135, pp. 433–441, 2015, doi: 10.1016/j.petrol.2015.10.003.

[173] J. K. M. William, S. Ponmani, R. Samuel, R. Nagarajan, and J. S. Sangwai, “Effect of CuO and ZnO nanofluids in xanthan gum on thermal, electrical and high pressure rheology of water-based drilling fluids,” *J. Pet. Sci. Eng.*, vol. 117, pp. 15–27, 2014, doi: 10.1016/j.petrol.2014.03.005.

[174] D. Bhatia, D. Datta, A. Joshi, S. Gupta, and Y. Gote, “Adsorption Study for the Separation of Isonicotinic Acid from Aqueous Solution Using Activated Carbon/Fe3O4 Composites,” *J. Chem. Eng. Data*, vol. 63, no. 2, pp. 436–445, 2018, doi: 10.1021/acs.jced.7b00881.

[175] J. Rivera-Utrilla, M. Sánchez-Polo, V. Gómez-Serrano, P. M. Álvarez, M. C. M. Alvim-Ferraz, and J. M. Dias, “Activated carbon modifications to enhance its water treatment applications. An overview,” *J. Hazard. Mater.*, vol. 187, no. 1–3, pp. 1–23, 2011, doi: 10.1016/j.jhazmat.2011.01.033.

[176] D. Mohan and C. U. Pittman Jr., “Arsenic removal from water/wastewater using adsorbents-A critical review,” *J. Hazard. Mater.*, vol. 142, no. 1–2, pp. 1–53, 2007, doi: 10.1016/j.jhazmat.2007.01.006.

[177] E. Schröder, K. Thomauske, C. Weber, A. Hornung, and V. Tumiatti, “Experiments on the generation of activated carbon from biomass,” *Pyrolysis 2006 Pap. Present.*

17th Int. Symp. Anal. Appl. Pyrolysis Bp. Hung. 22-26 May 2006, vol. 79, no. 1, pp. 106–111, 2007, doi: 10.1016/j.jaap.2006.10.015.

[178] D. Prahas, Y. Kartika, N. Indraswati, and S. Ismadji, “Activated carbon from jackfruit peel waste by H3PO4 chemical activation: Pore structure and surface chemistry characterization,” *Chem. Eng. J.*, vol. 140, no. 1–3, pp. 32–42, 2008, doi: 10.1016/j.cej.2007.08.032.

[179] D. Mohan and C. U. Pittman Jr., “Activated carbons and low cost adsorbents for remediation of tri- and hexavalent chromium from water,” *J. Hazard. Mater.*, vol. 137, no. 2, pp. 762–811, 2006, doi: 10.1016/j.jhazmat.2006.06.060.

[180] N. A. Rashidi, S. Yusup, A. Borhan, and L. H. Loong, “Experimental and modelling studies of carbon dioxide adsorption by porous biomass derived activated carbon,” *Clean Technol. Environ. Policy*, vol. 16, no. 7, pp. 1353–1361, 2014, doi: 10.1007/s10098-014-0788-6.

[181] S. Deng, B. Hu, T. Chen, B. Wang, J. Huang, Y. Wang, and G. Yu, “Activated carbons prepared from peanut shell and sunflower seed shell for high CO2 adsorption,” *Adsorption*, vol. 21, no. 1–2, pp. 125–133, 2015, doi: 10.1007/s10450-015-9655-y.

[182] A. Heidari, H. Younesi, A. Rashidi, and A. A. Ghoreyshi, “Evaluation of CO2 adsorption with eucalyptus wood based activated carbon modified by ammonia solution through heat treatment,” *Chem. Eng. J.*, vol. 254, pp. 503–513, 2014, doi: 10.1016/j.cej.2014.06.004.

[183] S. K. R. Kuppireddy, K. Rashid, A. Al Shoaibi, and C. Srinivasakannan, “Production and characterization of porous carbon from date palm seeds by chemical activation with h3po4: process optimization for maximizing adsorption of methylene blue,” *Chem. Eng. Commun.*, vol. 201, no. 8, pp. 1021–1040, 2014, doi: 10.1080/00986445.2013.797896.

[184] H.-C. Lee, N. Byamba-Ochir, W.-G. Shim, M. S. Balathanigaimani, and H. Moon, “High-performance super capacitors based on activated anthracite with controlled porosity,” *J. Power Sources*, vol. 275, pp. 668–674, 2015, doi: 10.1016/j.jpowsour.2014.11.072.

[185] M. A. Lillo-Ródenas, D. Cazorla-Amorós, and A. Linares-Solano, “Understanding chemical reactions between carbons and NaOH and KOH: An insight into the chemical activation mechanism,” *Carbon*, vol. 41, no. 2, pp. 267–275, 2003, doi: 10.1016/S0008-6223(02)00279-8.

[186] P. Azadi, O. R. Inderwildi, R. Farnood, and D. A. King, “Liquid fuels, hydrogen and chemicals from lignin: A critical review,” *Renew. Sustain. Energy Rev.*, vol. 21, pp. 506–523, 2013, doi: 10.1016/j.rser.2012.12.022.

[187] M. P. Pandey and C. S. Kim, "Lignin Depolymerization and Conversion: A Review of Thermochemical Methods," *Chem. Eng. Technol.*, vol. 34, no. 1, pp. 29–41, 2011, doi: 10.1002/ceat.201000270.

[188] B. Kueh, M. Kapsi, C. M. Veziri, C. Athanasekou, G. Pilatos, K. S. K. Reddy, A. Raj, and G. N. Karanikolos, "Asphaltene-Derived Activated Carbon and Carbon Nanotube Membranes for CO2 Separation," *Energy Fuels*, vol. 32, no. 11, pp. 11718–11730, Nov. 2018, doi: 10.1021/acs.energyfuels.8b02913.

[189] D. Li, T. Ma, R. Zhang, Y. Tian, and Y. Qiao, "Preparation of porous carbons with high low-pressure CO2 uptake by KOH activation of rice husk char," *Fuel*, vol. C, no. 139, pp. 68–70, 2015, doi: 10.1016/j.fuel.2014.08.027.

[190] R. C. Bansal and M. Goyal, *Activated Carbon Adsorption*, 0 ed. CRC Press, 2005.

[191] W. Hao, F. Björnerbäck, Y. Trushkina, M. Oregui Bengoechea, G. Salazar-Alvarez, T. Barth, and N. Hedin, "High-Performance Magnetic Activated Carbon from Solid Waste from Lignin Conversion Processes. 1. Their Use As Adsorbents for CO2," *ACS Sustain. Chem. Eng.*, vol. 5, no. 4, pp. 3087–3095, 2017, doi: 10.1021/acssuschemeng.6b02795.

[192] J. Donald Carruthers, M. A. Petruska, E. A. Sturm, and S. M. Wilson, "Molecular sieve carbons for CO2 capture," *Microporous Mesoporous Mater.*, vol. 154, pp. 62–67, May 2012, doi: 10.1016/j.micromeso.2011.07.016.

[193] V. Presser, J. McDonough, S.-H. Yeon, and Y. Gogotsi, "Effect of pore size on carbon dioxide sorption by carbide derived carbon," *Energy Environ. Sci.*, vol. 4, no. 8, pp. 3059–3066, Aug. 2011, doi: 10.1039/C1EE01176F.

[194] A. Labropoulos, C. Veziri, M. Kapsi, G. Pilatos, V. Likodimos, M. Tsapatsis, N. K. Kanellopoulos, G. E. Romanos, and G. N. Karanikolos, "Carbon Nanotube Selective Membranes with Subnanometer, Vertically Aligned Pores, and Enhanced Gas Transport Properties," *Chem. Mater.*, vol. 27, no. 24, pp. 8198–8210, 2015, doi: 10.1021/acs.chemmater.5b01946.

[195] S. Kim, J. R. Jinschek, H. Chen, D. S. Sholl, and E. Marand, "Scalable Fabrication of Carbon Nanotube/Polymer Nanocomposite Membranes for High Flux Gas Transport," *Nano Lett.*, vol. 7, no. 9, pp. 2806–2811, Sep. 2007, doi: 10.1021/nl071414u.

[196] M. Yu, H. H. Funke, J. L. Falconer, and R. D. Noble, "High density, vertically-aligned carbon nanotube membranes," *Nano Lett.*, vol. 9, no. 1, pp. 225–229, Jan. 2009, doi: 10.1021/nl802816h.

[197] G. Pilatos, E. C. Vermisoglou, G. E. Romanos, G. N. Karanikolos, N. Boukos, V. Likodimos, and N. K. Kanellopoulos, "A Closer Look Inside Nanotubes: Pore Structure Evaluation of Anodized Alumina Templated Carbon Nanotube Membranes

Through Adsorption and Permeability Studies,” *Adv. Funct. Mater.*, vol. 20, no. 15, pp. 2500–2510, 2010, doi: 10.1002/adfm.200901429.

[198] S. N. Duncum and C. A. Sawdon, “Wellbore fluid comprising sulfonated copolymers with pendant alkyl groups,” US7919437B2, 2011.

[199] O. S. Chan, W. H. Cheung, and G. McKay, “Preparation and characterisation of demineralised tyre derived activated carbon,” *Carbon*, vol. 14, no. 49, pp. 4674–4687, 2011, doi: 10.1016/j.carbon.2011.06.065.

[200] L. Ji and T. Geehan, “‘Shale Failure Around Hydraulic Fractures in Water Fracturing of Gas Shale’ 2040,” pp. 5–7, 2013.

[201] L. A. Alcázar-Vara and I. R. Cortés-Monroy, “Drilling Fluids for Deepwater Fields: An Overview,” *Recent Insights Pet. Sci. Eng.*, pp. 71-86, Dec. 2017, doi: 10.5772/intechopen.70093.

[202] D. B. Bennion, F. B. Thomas, D. W. Bennion, and R. F. Bietz, “Mechanisms of Formation Damage and Permeability Impairment Associated With the Drilling, Completion and Production of Low API Gravity Oil Reservoirs,” in *SPE International Heavy Oil Symposium*, Calgary, Alberta, Canada, 1995, doi: 10.2118/30320-MS.

[203] A. Desmecht, T. Steenhaut, F. Pennetreau, S. Hermans, and O. Riant, “Synthesis and Catalytic Applications of Multi-Walled Carbon Nanotube–Polyamidoamine Dendrimer Hybrids,” *Chem. - Eur. J.*, vol. 24, no. 49, pp. 12992–13001, 2018, doi: 10.1002/chem.201802301.

[204] F. Giacalone, V. Campisciano, C. Calabrese, V. La Parola, Z. Syrgiannis, M. Prato, and M. Gruttadauria, “Single-Walled Carbon Nanotube-Polyamidoamine Dendrimer Hybrids for Heterogeneous Catalysis,” *ACS Nano*, vol. 10, no. 4, pp. 4627–4636, 2016, doi: 10.1021/acsnano.6b00936.

[205] Y. Fan, G. Wu, F. Su, K. Li, L. Xu, X. Han, and Y. Yan, “Lipase oriented-immobilized on dendrimer-coated magnetic multi-walled carbon nanotubes toward catalyzing biodiesel production from waste vegetable oil,” *Fuel*, vol. 178, pp. 172–178, 2016, doi: 10.1016/j.fuel.2016.03.071.

[206] S. N. S. Alconcel, A. S. Baas, and H. D. Maynard, “FDA-approved poly(ethylene glycol)–protein conjugate drugs,” *Polym. Chem.*, vol. 2, no. 7, pp. 1442–1448, Jun. 2011, doi: 10.1039/C1PY00034A.

[207] S. Aroua, E. G. V. Tiu, M. Ayer, T. Ishikawa, and Y. Yamakoshi, “RAFT synthesis of poly(vinylpyrrolidone) amine and preparation of a water-soluble C_{60}-PVP conjugate,” *Polym. Chem.*, vol. 6, no. 14, pp. 2616–2619, 2015, doi: 10.1039/C4PY01333F.

[208] F. Fischer and S. Bauer, “Polyvinylpyrrolidon. Ein Tausendsassa in der Chemie,” *Chem. Unserer Zeit*, vol. 43, no. 6, pp. 376–383, 2009, doi: 10.1002/ciuz.200900492.

[209] D. W. Lim, Y. I. Yeom, and T. G. Park, “Poly(DMAEMA-NVP)-b-PEG-galactose as Gene Delivery Vector for Hepatocytes,” *Bioconjug. Chem.*, vol. 11, no. 5, pp. 688–695, Sep. 2000, doi: 10.1021/bc000014u.

[210] D. A. Tomalia, B. Huang, D. R. Swanson, H. M. Brothers, and J. W. Klimash, “Structure control within poly(amidoamine) dendrimers: size, shape and regio-chemical mimicry of globular proteins,” *Recent Dev. Dendrimer Chem.*, vol. 59, no. 22, pp. 3799–3813, May 2003, doi: 10.1016/S0040-4020(03)00430-7.

[211] D. Guo, N. Muhammad, C. Lou, D. Shou, and Y. Zhu, “Synthesis of dendrimer functionalized adsorbents for rapid removal of glyphosate from aqueous solution,” *New J. Chem.*, vol. 43, no. 1, pp. 121–129, 2019, doi: 10.1039/c8nj04433c.

[212] Y. Kobayashi, A. Kosuge, and M. Konno, “Fabrication of high concentration barium titanate/polyvinylpyrrolidone nano-composite thin films and their dielectric properties,” *Appl. Surf. Sci.*, vol. 255, no. 5, Part 2, pp. 2723–2729, Dec. 2008, doi: 10.1016/j.apsusc.2008.08.006.

[213] X. Wang, X. Yang, and L. Wang, “Advances in researching and applying filtrate reducers with resistance to high temperature at home and abroad,” *Sino-Glob. Energy*, vol. 14, no. 4, pp. 37–42, 2009.

[214] Y. M. Wu, D. J. Sun, B. Q. Zhang, and C. G. Zhang, “Properties of high-temperature drilling fluids incorporating disodium itaconate/acrylamide/sodium 2-acrylamido-2-methylpropanesulfonate terpolymers as fluid-loss reducers,” *J. Appl. Polym. Sci.*, vol. 83, no. 14, pp. 3068–3075, 2002, doi: 10.1002/app.2335.

[215] K. Sehly, H.-L. Chiew, H. Li, A. Song, Y.-K. Leong, and W. Huang, “Stability and ageing behaviour and the formulation of potassium-based drilling muds,” *Appl. Clay Sci.*, vol. 104, pp. 309–317, 2015, doi: 10.1016/j.clay.2014.12.013.

[216] H. Y. Zhong, Z. S. Qiu, W. A. Huang, J. Cao, F. W. Wang, and X. B. Zhang, “An inhibition properties comparison of potassium chloride and polyoxypropylene diamine in water-based drilling fluid,” *Pet. Sci. Technol.*, vol. 31, no. 20, pp. 2127–2133, 2013, doi: 10.1080/10916466.2011.561265.

[217] W. He, S. L. Gomez, R. S. Leonard, and D. T. Li, “Shale-fluid interactions and drilling fluid designs,” presented at the Society of Petroleum Engineers - International Petroleum Technology Conference 2014, IPTC 2014: Unlocking Energy Through Innovation, Technology and Capability, 2014, vol. 1, pp. 349–360.

[218] J. Friedheim, Q. Guo, S. Young, and S. Gomez, “Testing and evaluation techniques for drilling fluids-shale interaction and shale stability,” *45th US Rock Mech. Geomech. Symp.*, 2011.

[219] C. Blachier, L. Michot, I. Bihannic, O. Barrès, A. Jacquet, and M. Mosquet, "Adsorption of polyamine on clay minerals," *J. Colloid Interface Sci.*, vol. 336, no. 2, pp. 599–606, 2009, doi: 10.1016/j.jcis.2009.04.021.

[220] P. Barati, K. Shahbazi, M. Kamari, and A. Aghajafari, "Shale hydration inhibition characteristics and mechanism of a new amine-based additive in water-based drilling fluids," *Petroleum*, vol. 3, no. 4, pp. 476–482, Dec. 2017, doi: 10.1016/j.petlm.2017.05.003.

[221] D. Mondal, M. M. R. Mollick, B. Bhowmick, D. Maity, M. K. Bain, D. Rana, A. Mukhopadhyay, K. Dana, and D. Chattopadhyay, "Effect of poly(vinyl pyrrolidone) on the morphology and physical properties of poly(vinyl alcohol)/sodium montmorillonite nanocomposite films," *Prog. Nat. Sci. Mater. Int.*, vol. 23, no. 6, pp. 579–587, 2013, doi: 10.1016/j.pnsc.2013.11.009.

Appendices

Appendix A: Sample Preparation Procedure for SEM Imaging Experiment

- ✓ Small quantity of the sample was dispersed in 10 ml ethanol.
- ✓ Few drops of the mixture were then drop-casted on clean SEM stub and expose to airdried and this was followed by another layer.
- ✓ The dried sample was then imaged under SEM-EDX instrument.

Appendix B: TGA Analysis

- ✓ The instrument was tailed to zero after cleaning of the α-Al_2O_3 crucible. About 5-20 mg dried sample was transferred into the bowl and the furnace was closed.
- ✓ The degradation of the material was finally monitored based on wait difference between the sample pan and that of the reference under nitrogen (N_2) flow of 50 cm^3 min^{-1} with temperature ramping of 30 – 700 ^oC at an increase rate of 10 ^oC min^{-1}.

Vitae

Name : Mukaila Abiodun Ibrahim

Nationality : Nigerian

Date of Birth : 5/16/1988

Email : ibrahimmukailaa@gmail.com

Address : Akure, Ondo State, Nigeria

Academic Background :

2019: King Fahd University of Petroleum and Minerals (KFUPM). Dhahran, KSA.

M.Sc. Chemistry; CGPA: 3.786/4.0.

2013: Adekunle Ajasin University, Akungba-Akoko, Nigeria.

B.Sc. Industrial Chemistry; CGPA: 4.53/5.0.

Personal Skills

- self-confidence and motivation to investigate and solve complex problems
- the ability to prioritize and schedule work to meet demands set by the department, company or external customer.
- presentation skills and the ability to convey technical information to non-technical people
- a good standard of numeracy and skills in data analysis
  - IT and technology skills to work with advanced techniques
  - creativity and the ability to use initiative for independent work
  - effective teamworking skills
  - a flexible and methodical approach to work.

Technical Skills

HyperChem, ChemDraw, Gaussian 08, Analytical Chemistry, nanomaterial development and characterization, GC-MS, AAS, XRD, SEM-EDS, NMR, MS Office, etc.

Certification

Course: Future of Digitalization and the Industrial Internet of Things Application in the Oil and Gas Industry. “Certificate of Completion”
Award Body: SPE International, Kingdom of Saudi Arabia Section

Work Experience

Chemistry Department, King Fahd University Petroleum and Minerals
Dhahran 31261, Saudi Arabia

Research Assistant, September, 2018 – Present

Duties / Responsibilities:

- Use different methods in samples and nanomaterials analyses.
- Prepare experimental reagents and standards.
- Collaborative work with others.
- Use different analytical techniques including GC-MS, HPLC, IR, NMR, XRD, SEM among others.
- Analysis and interpretation of data from experiment as well as reporting and documentation of findings.
- Perform analysis of samples from diverse source to disclose their compositions qualitatively and quantitatively.
- Supervise technician and give directive on required lab procedure and method for analytical tests.
- Develop of functionalized nanomaterials and conduct their characterization for various applications.

Ondo State Ministry of Environment and Mineral Resources
Akure, Ondo State, Nigeria

Scientific Officer (Chemist), January, 2015 - August, 2018

Duties / Responsibilities: Pollution control, laboratory management, administration and enforcement of Environmental Impact Assessment (EIA) for sustainable development and periodic compliance monitoring to industries.

NYSC- AUD Comprehensive High School,
Ado, Ekiti State, Nigeria

Chemistry and Mathematics Teacher, November, 2013 - December, 2014

Glass Blowing and Chemistry Lab,
Federal University of Technology, Akure

Ondo State, Nigeria

Intern, January-March 2012

Duties / Responsibilities: Quality control and quality assurance of water; industrial effluents and other environmental samples analyses; food analysis; reagent preparation; and construction of laboratory glasswares such as test tubes, condensers among others using glass tubes.

Ondo State Water Corporation, Akure

Ondo State, Nigeria
Intern, January- March 2011

Duties / Responsibilities: Treament of raw water and process monitoring for municipal supply; quality control and quality assurance of water; preparation of laboratory reagents; and maintenace of chemical inventories.

Publications

Novel partially aminated acrylic acid grafted activated carbon nanoparticles as an inexpensive shale hydration inhibitor. (Under Review)

Amyl ester surface carbon-nanopolymer composite for sensitive shale drilling. (Under Review)

Efficient shale inhibition with activated carbon dendrimer/polyvinylpyrrolidone composite (Under Review)

Tawfik A. Saleh, **Mukaila A. Ibrahim**, Advances in functionalized Nanoparticles based drilling inhibitors for oil production, *Energy Reports*, Vol. 5, 2019, Pages 1293-1304. *https://doi.org/10.1016/j.egyr.2019.06.002*

Adelaja, O.A., **Ibrahim, M.A.**, Bello, L.A. et al. *Int. J. Energ. Water Res.* (2019), *pp 1-15. https://doi.org/10.1007/s42108-019-00020-0*

T. A. Akinnifesi, A. Olonisakin, **M. A. Ibrahim**, and A.O. Adeola (2017). *Chem. Tech. Journal Vol. 12, pp 34 - 44*

Professional Affiliations:

- Chemical Society of Nigeria (CSN)
- Member, American Chemical Society (ACS)
- Member, Saudi Arabian International Chemical Sciences Chapter of American Chemical Society (SAICSC-ACS)

Honor and Award

- King Fahd University of Petroleum and Minerals, KSA Full M.S. Scholarship Award, 2018